MECHANOTRANSDUCTION IN FIBROBLASTS

INAUGURALDISSERTATION

zur
Erlangung der Würde eines Doktors der Philosophie
vorgelegt der
Philosophisch-Naturwissenschaftlichen Fakultät
der Universität Basel

von
Michaela Brosig
aus München, Deutschland

Friedrich Miescher Institute
for Biomedical Research

Basel, 2011

Genehmigt von der Philosophisch-Naturwissenschaftlichen Fakultät
auf Antrag von:

Prof. Dr. Ruth Chiquet-Ehrismann
Prof. Dr. Matthias Chiquet
Prof. Dr. Susan Gasser
Prof. Dr. Markus Rüegg

Basel, den 23.06.2009

Prof. Dr. Eberhard Parlow
Dekan

Darin besteht das Wesen der Wissenschaft. Zuerst denkt man an das, was wahr sein könnte. Dann sieht man nach, ob es der Fall ist und im Allgemeinen ist es nicht der Fall.

-Bertrand Russel

TABLE OF CONTENTS

SUMMARY

I. SUMMARY

Response to mechanical stress is important for tissue homeostasis, tissue architecture and muscle regeneration. All cells of an organism are subject to at least one of three types of mechanical stress: compression, shear stress or tension. The exact mechanisms how a cell senses mechanical stress and how it converts mechanical into chemical signals are still unknown and the elucidation of this process is the aim of my thesis.

Defective mechanotransduction can be observed in a diverse group of diseases called laminopathies, such as Emery-Dreifuss muscular dystrophy or dilated cardiomyopathy [1-5]. LaminA and emerin, the proteins affected in these diseases, are part of a physical link that spans from the nuclear lamina to the extracellular matrix and might play a role in a cell's sensation of and response to mechanical stress. Cells lacking either protein display reduced nuclear structural integrity, changes in transcriptional regulation, and defective nuclear mechanics and mechanotransduction.

In the present study the first microarray-analysis of stretched primary mouse embryo fibroblasts revealed that cells react to biaxial strain by upregulation of a very distinct group of around 30 genes within 1 hour of stretching. No transcripts were downregulated, whereas after 6 hours of strain a large group of genes was affected by mechanical stress and showed up as well as downregulation. Among them was tenascin-C as well as some other proteins involved with extracellular matrix function. This was confirmed by QPCR and Affymetrix chip analysis in 2 immortalized mouse embryo fibroblast cell lines.

We observed that biaxial strain leads to the activation of Erk, Rho/ROCK, and NfκB pathways. However, though all three pathways were activated upon stretching, inhibition of Erk or ROCK did not decrease the early response to biaxial strain since transcripts induced after 1 hour of stretching were still upregulated in the presence of these inhibitors. Only inhibition of the NfκB pathway blocked the stretch response of selected genes after one hour of cyclic stretching. Our results suggest that activation of NfκB seem to depend on Ca^{2+}-influx that is mediated by stretch-gated ion-channels in the cell membrane.

One of the genes responding to stretching is Egr3. It is an immediate early growth response gene which is induced by mitogenic stimulation and may play a role in muscle development. Its ability to activate tenascin-C, which possesses an Egr binding site in its promoter region, was examined by promotor-SEAP-reporter assays and by western blot.

The role of the LINC complex in mechanotransduction was analyzed by expressing dominant-negative forms of sun1 and nesprin in fibroblasts as well as in myogenic progenitors. Live imaging of mouse embryo fibroblasts revealed that nuclei are rotating in response to stretching. Although some nuclei

were slowly rotating with time when monitored at rest, stretching induced nuclear spinning. Upon disruption of this direct link by overexpression of truncated dominant-negative forms of sun1 or nesprin-1, nuclei remained in their position even in stretched cells. Contrary to our expectations disruption of the LINC complex did not inhibit the stress response as determined by transcript profiling of stretched cells.

To address the question whether a functional LINC complex plays a role in muscle development, we examined the differentiation of C2C12 myogenic progenitor cells in the presence and absence of dominant-negative sun and nesprin. C2C12 cells differentiate in the presence of 5% horse serum in the medium but not when stretched for 1 hour every 24 hours [6-8]. When the direct link is disrupted cells continue to differentiate even when stretched. This indicates that sun and nesprin are necessary for the sensation of mechanical signals in differentiating C2C12 cells.

INTRODUCTION

II. INTRODUCTION

II. 1 MECHANOTRANSDUCTION

II.1.1 What is mechanotransduction?

All cells of an organism are subject to at least one of three types of mechanical stress: compression, shear stress or tension. In response to it cells adjust their shape, function and behavior in apoptosis, migration, differentiation and proliferation [9, 10]. But the exact mechanisms how a cell senses and reacts to mechanical signals are widely unknown.

The conversion of mechanical cues into chemical signals is known as mechanotransduction. Cells are in close contact to their environment via various cell adhesion molecules, tight junctions and cell surface receptors (figure 1A c, and h respectively). These molecules and complexes transmit changes in mechanical properties of the environment to the cell interior. There these signals are translated into chemical signals by activation of signaling cascades or release of intracellular Ca^{2+} by stretch-activated ion channels in the plasma membrane (figure 1A a). Several mutations in mechanosensing structures and proteins or in molecules involved in downstream signaling pathways such as Erk or Rho/ROCK have been described [11].

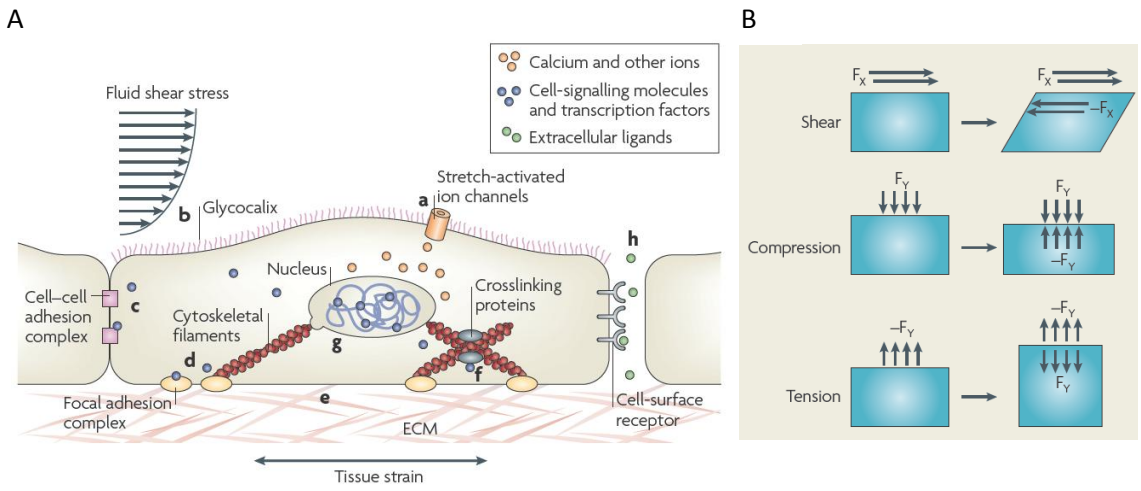

Figure 1 | **Cells are subject to various types of mechanical stress from their environment.** Several biological components have been proposed to act as cellular mechanosensors and are schematically depicted in figure 1A [12]. Most of these features can be found in many cell types whereas some might only be relevant in a subset of cells. Figure 1B shows an overview of the 3 subtypes of mechanical stress [13].

Mechanical crosstalk between integrins and the actin-cytoskeleton is a key feature of environmental sensing. However, other molecules inside and outside a cell were shown to contribute to mechanosensation as well. In endothelial cells, for example, the glycocalix (figure 1A b) can mediate mechanotransduction signaling in response to fluid shear stress. Some proteins of the extracellular matrix (figure 1A f) can unfold when being stretched and thus initiate mechanotransduction signaling outside the cell. And even the nucleus (figure 1A g) itself has been proposed to act as a mechanosensor as deformations can influence chromatin conformation.

II.1.2 Where does mechanotransduction play a role?

Often mechanotransduction research focuses on sensory cells like hair cells of the inner ear. These cells are tailored to transduce mechanical signals into biochemical signals by opening ion channels and thus represent a good model for experimental studies. However, it has been shown that mechanotransduction is involved in a broad range of cellular functions, not just in a subset of specialized cells and tissues. Response to mechanical stress is needed for cells to adapt to their physical surroundings and is important for tissue homeostasis, tissue architecture and muscle regeneration. Therefore all cells and organisms, no matter how primitive, have the ability to sense mechanical stress [14].

Among others, mechanoresponse is crucial for organ development and the maintenance of many mechanically stressed tissues such as bones, muscles, cartilage, and blood vessels [15-17]. Exposure to zero gravity or long bed rest leads to loss of bone mass and muscle atrophy [18, 19]. A reorientation of "stress fibers" in bones can be observed after fractures [16, 17]. Adaptation to mechanical forces in bones works via the lacunae-canalicular network. This network consists of small cavities within the compact bone comprised of concentric layers of bone matrix. The cavities, known as lacunae, are interspersed at regular intervals, harbor osteocytes and are connected through canaliculi. Gravity and compression generated by muscle contractions during locomotion leads to deformations of the bone, resulting in pressure gradients that drive interstitial fluid through the lacunae-canalicular network. This stimulates localized bone remodeling and optimizes physical performance of the bone through mechanotransduction signaling [16]

Cells of the cardiovasculature constantly experience 2 types of mechanical forces. The endothelial cells inside the blood vessels are subject to shear stress that results from the friction of blood against the vessels. The other type, cyclic tensile stress, results from the pulsatile blood pressure and is the major determinant of vessel stretch that affects both endothelial and smooth muscle cells. Shear stress induced by blood flow permits artery maturation by directing endothelial cells and their

filamentous cytoskeletal networks to elongate and align with the direction of flow [20, 21]. Pressure and shear stress from the flowing blood in the cardiovasculature influence the morphology and the physiology of the heart [22-25]. Changes in the flow patterns in the developing zebrafish heart have shown to lead to an abnormal third chamber, reduced looping and defective valves - symptoms common to some congenital heart diseases [26].

Mechanotransduction does not just influence the development of the heart but embryonic development in general. It has been shown that not just gradients of morphogenic factors, but also interactions such as tension and adhesion, might be important in embryonic development (for a review see [27]). Stem cell fate during differentiation depends on geometry and stiffness of the substrate on which cells are grown [28, 29]. Mesenchymal stem cells undergo lineage selection in response to elasticity of the matrix substrate. Soft matrices (similar to brain) direct stem cells into neurogenic lineage. Stiffer matrices found in muscle and newly deposited bone direct them into myogenic or osteogenic lineages [28].

II. 2 COMPONENTS OF MECHANOSENSATION

II.2.1 Signaling pathways

Several reports indicate that stretch initiates complex signal transduction cascades leading to gene transcription and functional responses, via interaction of integrins with extracellular matrix proteins, or by stimulation of G protein coupled receptors, tyrosine kinase receptors or ion channels. Intracellular pathways reported to be activated include mitogen-activated kinase pathway (MAPK), nuclear factor kappa B (NfκB) signaling and the rho/ROCK pathway [30-32]. Often not just a single pathway is activated but several ones that are overlapping and crosstalking.

The assembly of focal adhesions perpetuates downstream signaling through kinases and initiates cytoskeletal remodeling through the nucleation of an assortment of adhesion proteins and signaling molecules, including Ras, Rac and Rho [33, 34]. Ras couples force-dependent integrin signaling to mitogen activated protein kinases (MAPK) including Erk which has been illustrated in lung epithelial cells in response to mechanical strain [35]. An increase in Erk phosphorylation has also been reported in endothelial cells in response to cyclic strain [36]. Stress-activated Erk cooperates with Src and focal adhesion kinase (FAK) to induce cell proliferation or sustain cell survival in keratinocytes and osteocytes [37-41]. Src family kinases have also shown to be phosphorylated by stretch-induced conformational changes in the adaptor protein p130Cas (also known as BCAR1). These changes expose a hidden phosphorylation site that thus becomes a target of Src family kinases [42].

This site is also recognized by other proteins that in turn activate small GTPases like Rho [43]. Rho and its target kinase ROCK have been shown to be activated by mechanical strain through changes in actin dynamics [44, 45]. Local external changes in the rigidity of the extracellular matrix are sensed as increased or decreased tension and communicated intracellularly. The communication network that signals the state of the extracellular physical environment acts through the actin cytoskeleton to modulate Rho GTPase activity [46, 47].

A third way described to be activated by mechanical stress is the classical nuclear factor-kappa B (NfκB) pathway. Kumar et al. [48] showed that in skeletal muscles from normal and mdx mice, a model for Duchenne muscular dystrophy (DMD), NfκB activity was increased by the application of uniaxial mechanical stretch in a time-dependent manner. The increased activation of NfκB was associated with a concomitant increase in I-kappa B (IκB) kinase activity and the degradation of IκBα protein.

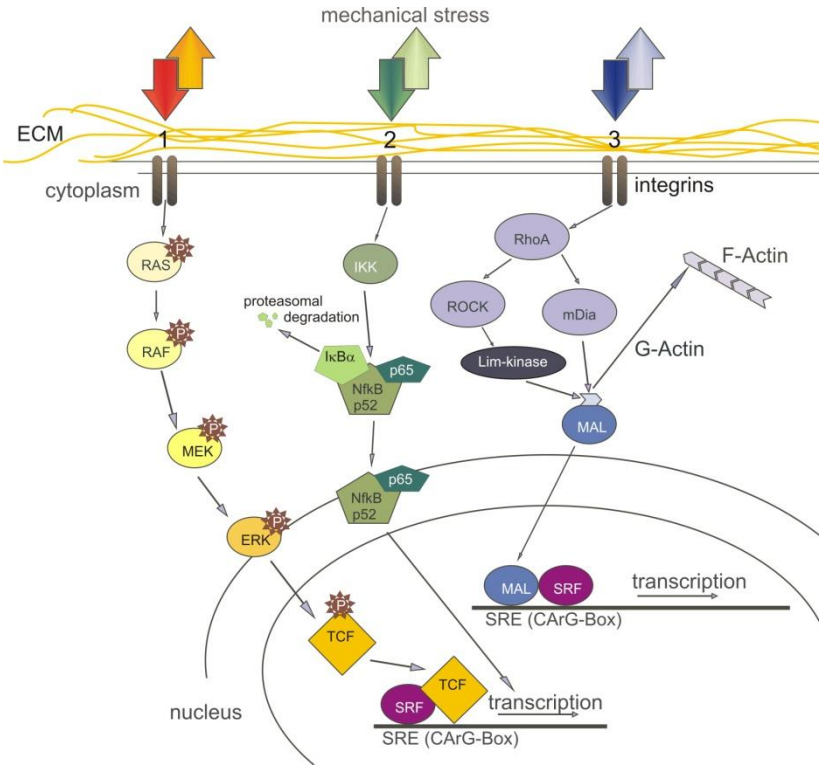

Figure 2 | **The three main pathways involved in mechanotransduction. 1** One pathway previously described in connection with mechanotransduction, is the Erk pathway via Ras and Raf that leads to the translocation of phosphorylated Erk to the nucleus and successive binding of TCF and SRF to the SRE. **2** A second pathway described to be activated by shear stress is the NfκB pathway. **3** Mechanical stress is sensed by integrins and transduced to the nucleus via Rho/ROCK and MAL. Upon activation, MAL dissociates from G-actin and translocates to the nucleus where it can together with SRF bind to the serum response element (SRE) of genes.

II.2.2 Calcium signaling

The cell membrane presents a major target of the external forces that act upon a cell. Mechanosensitive ion channels in the membrane can contribute to mechanotransduction. The idea of mechanically gated ion channels arose originally from studies of mechanosensory cells. They play a role in mammalian hearing and balance which are results from electrochemical response to sound waves, pressure and gravity. Mechanical forces cause small displacements in the stereocilia of hair cells in the inner ear. This causes tension in the tip links which connect tips of neighboring stereocilia and pulls open stretch-sensitive ion channels. This process leads to a rapid influx of calcium and other ions and subsequent activation of biochemical signaling pathways [49, 50].

Mechanosensitive channels have also been discovered in embryonic chick skeletal muscles [51] and frog muscle [52]. Since then they have also been found in many other cell types [53-55]. Significantly, cells that transduce mechanical stimuli into electrical signals are the most common sensory receptors in vertebrates.

II.2.3 The LINC complex

A cell is not just a visco-elastic cytoplasm surrounded by an elastic cell membrane. It also harbors a network consisting of cytoskeletal structures that are stable enough to resist mechanical stress and at the same time undergo constant dynamic remodeling. According to Ingber's tensegrity (tension – integrity) or prestressed inhomogeneous solid model (figure 3) actin stress fibres that polymerize at the focal adhesions can act as visco-elastic cables [56-60]. These respond to the extracellular mechanical environment with myosin-induced cell contractility and anchor the cell to and pull on ECM fibrils, creating intracellular tension [61-63]. This leads to a prestressing of the cell, which is necessary to enable cells to sense changes in the mechanical properties of the surrounding [32, 57, 58, 64-66]. Mechanotransduction of externally applied forces is lost if myosin-based contractility is inhibited or if the ECM is not rigid enough [30] [67], [68]. Thus cell-generated forces and forces from a cell's environment must act together as a mechanosensor to generate a response. A cell can only sense shear or strain when it is properly attached to its substratum. This attachment is mediated by focal adhesions. A cytoskeletally generated force leads to stress in the focal adhesions because equal and opposite reactive force arises in the ECM. If cells are attached to a less rigid matrix, for example, when cells attach to ECM-protein coated microbeads, cytoskeletal tension and stress at the adhesions do not develop and focal adhesions fail to mature [68]. Conversely externally applied forces through the ECM result in stress at focal adhesions only when the actin cytoskeleton provides an opposite, reactive force that balances the applied force [65], [69]. This force is generated by the actin-cytoskeleton, either by passive deformation or by changes in myosin motor-activity. This also explains why inhibition of myosin-generated contractility inhibits stress response.

The tensegrity model furthermore implies that integrins are linked to the nucleus through the cytoskeleton. Thus an applied force is transmitted to the DNA through the cytoskeleton by nuclear lamins and nuclear envelope receptor complexes. Such a connection might then directly modulate gene expression by inducing conformational changes in chromatin either by altering the nature of the protein complexes at the telomeres of chromosomes or by changing the activity of DNA remodeling enzymes [59, 60, 70, 71].

Proof for the tensegrity model comes from linking magnetic beads directly to integrins at the cell surface. Pulling on the beads leads to physical deformation of the cell and immediate force-dependent changes in internal structures and the cytoskeleton. It induces actin filament reorientation and realignment along the newly applied field lines [66, 72-74].

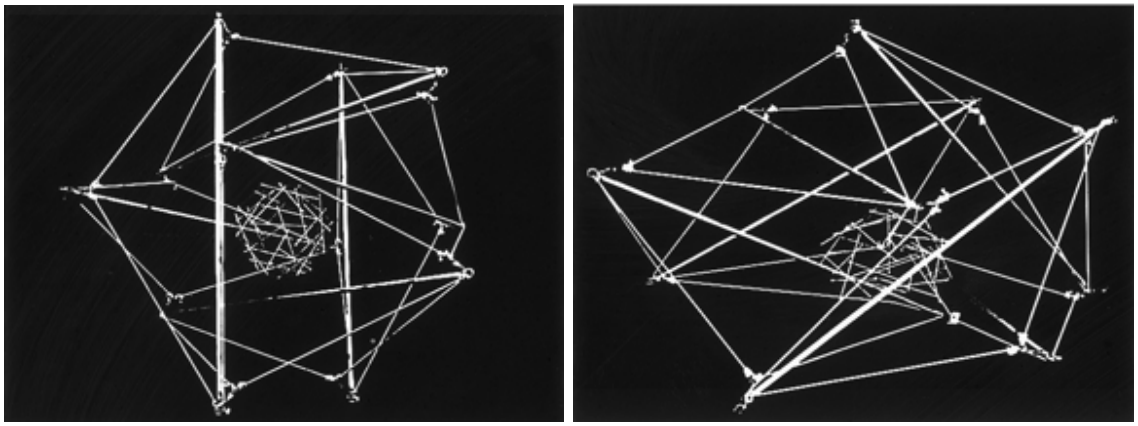

Figure 3 | **Tensegrity model according to Donald Ingber** [58]. A cell is attached to a substratum or matrix by focal adhesions. These are connected to a network consisting of cytoskeletal structures that are stable enough to resist mechanical stress and at the same time undergo constant dynamic remodeling. This way a cell can tense its load-bearing cytoskeletal elements and stiffen them relative to the surrounding viscous cytoplasm. This leads to a prestressing of the cell, which is necessary to enable cells to sense changes of the surrounding mechanical properties.

In addition to the actin fibres that are linked to the integrins via talin other proteins are involved in linking the ECM to the nucleus. As described by Melissa Crisp [75] sun and nesprin are among the components of such a direct link, the so called LINC complex (see figure 5). The family of nesprins comprises three proteins, nesprin-1, 2 and 3. There are many splicing isoforms of nesprin 1 and 2 which result in proteins of various sizes. The small isoform of nesprin-1 localizes to the inner nuclear membrane and binds to laminA and emerin [76, 77]. The longest isoforms are around 800kDa and are among the largest proteins in a cell. They possess an N-terminal actin binding domain (ABD) and a C-terminal Klarsicht homology (KASH) domain that spans the outer nuclear membrane [78-81].
Figure 4 gives a more detailed overview over the various isoforms of nesprin-1 and 2. Recently a third member of the family, nesprin-3, has been discovered. It is also anchored at the nuclear membrane, but instead of actin it binds to plectin and thereby connects the intermediate filaments to the nucleus [82].

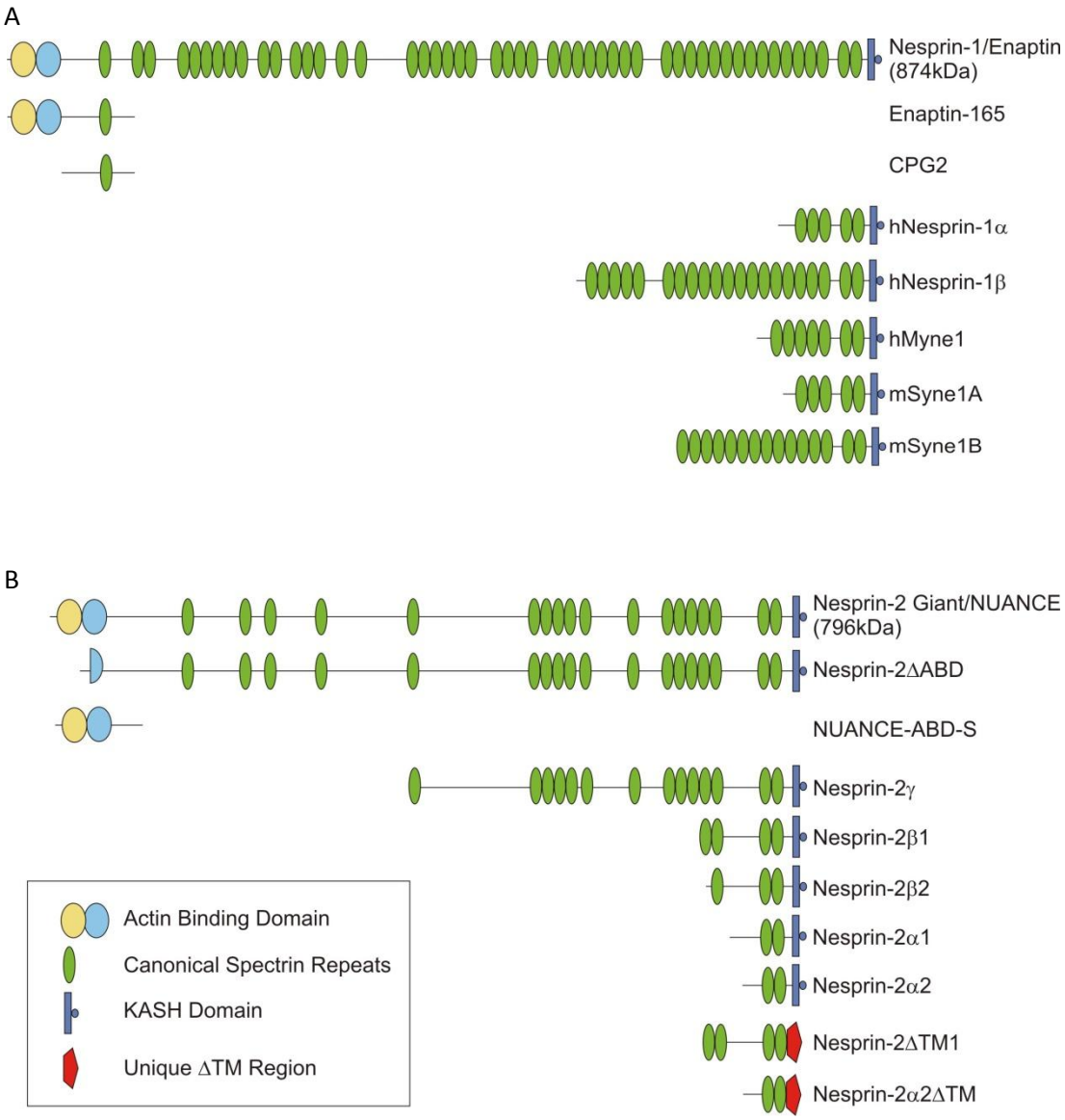

Figure 4 | **Isoforms of nesprin 1 and human nesprin 2** (derived from [79] and [83] respectively). Both nesprins have long isoforms that possess an N-terminal actin binding domain (ABD) and a C-terminal KASH domain. Thus they can anchor the nucleus to the actin cytoskeleton.

At the perinuclear space nesprins can, via their KASH domain, interact with sun. Sun is a homodimer with its luminal C-terminal domain inside the perinuclear space. This so called sun domain allows binding to KASH-domain proteins like the nesprins. Sun is anchored to the inner nuclear membrane with its transmembrane domains and interacts with chromatin either directly or via laminA and emerin [84].

Lamins are structural components of the nuclear lamina, a protein network underlying the inner nuclear membrane. The nuclear lamina determines nuclear shape and size as mutations in A-type lamins have shown [85]. Lamins also play an important role in organizing and recruiting other proteins such as emerin to the nuclear lamina [86] [87]. There are 2 types of lamins in mammalian cells: A-type lamins (lamin A+C) that are encoded by a single gene, lmna, and B-type lamins (lamin B1 and B2/B3), that are encoded by separate genes. A-type lamins are developmentally regulated and only expressed in differentiated cells whereas B-type lamins are constitutively expressed in all cells [85, 88-93]. Mutations in the A-type lamins result in changes in the supramolecular structure of lamins [94].

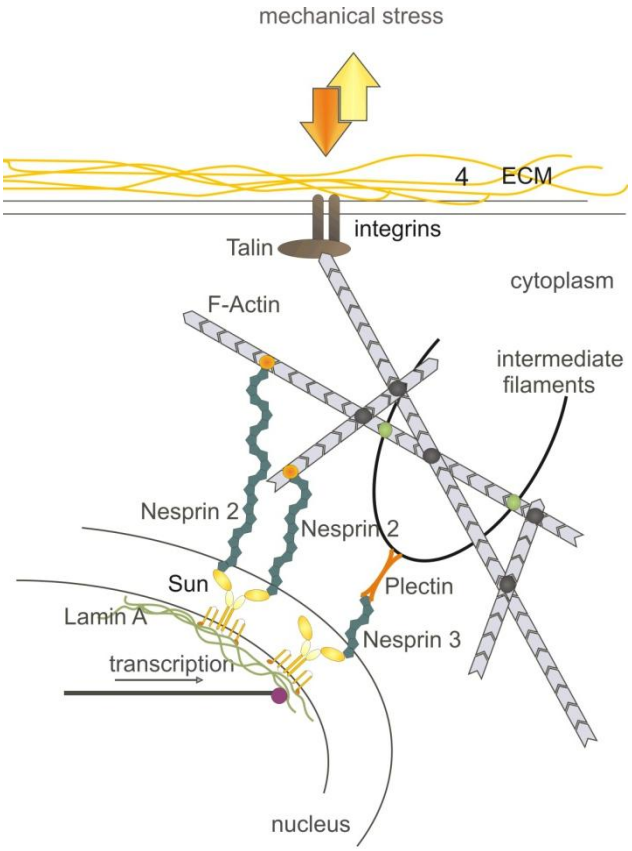

Figure 5 | Model for transducing mechanical signals to the nucleus via the LINC complex. This suggests that nesprin binds to the actin cytoskeleton on one side and the nuclear membrane on the other. There it either interacts directly with sun1 or with a protein mediating this interaction. Sun1 interacts with laminA which can then influence gene transcription.

As mentioned before a connection between components of the LINC complex and changes in chromatin structure in response to mechanical cues could dynamically alter gene expression in response to exogenous force. Ingber [14] and Kim [95] showed interactions between force, Rho

signaling, cell shape and histone acetylation. Adhesion induces changes in human mammary epithelial cell shape. This is associated with altered actin organization, RhoGTPase activity, actomyosin contractility and modified global patterns of chromatin histone acetylation [96].

Taken all these facts into account, such a direct link could facilitate much faster force propagation from the environment to the cell nucleus than biochemical signaling cascades do.

II. 3 DISEASES

II.3.1 Diseases in general

Defects in mechanotransduction, such as mutation or misregulation of proteins that disturb cellular or extracellular mechanics, are implicated in the development of various diseases. Among those diseases are muscular dystrophies, cardiomyopathy, cancer progression and metastasis, and loss of hearing. A common denominator of many mechanobiology diseases is a disruption in the force transmission between the ECM, the cytoskeleton and the interior of the nucleus. Almost all cells rely on mechanotransduction signaling for normal function. Therefore defective mechanotransduction can result in or at least contribute to the pathogenesis of various human diseases.

II.3.2 Cancer

Even cells of mechanically static tissues, such as brain or breast, are exposed to isometric force or tension generated locally at the nanoscale level by cell-cell or cell-ECM interactions. The force generated depends on the stiffness of the substratum. This stiffness varies a lot among the different tissues (see figure 6) and is very specific for a certain organ. It has been shown that these specific properties are an important factor for the differentiation of stem cells into tissue-specific cell types (for a review see: [27]). These properties also influence cell function through actomyosin contractility and actin dynamics and modulate together with biochemical cues cell and tissue behavior and tissue homeostasis. Loss of tissue homeostasis and changes in tissue properties are a hallmark of disease. Multiple pathologies including cancer are characterized by compromised tensional homeostasis [11]. Thus tumors are often detected as a palpable stiffening of the tissue, and approaches such as magnetic resonance imaging (MRI) and sono-elastography have been developed to exploit this observation to enhance cancer detection.

Matrix stiffening occurs by an increase in protein concentration, increase in matrix crosslinking, parallel orientation of matrix fibrils (bundeling), and MMP-cleavage or glycosylation [11]. Fibroblasts respond to mechanical stress by secreting various ECM proteins like tenascin and collagen. As a result of this, the matrix surrounding a tumor changes its mechanical properties. This in turn alters cell growth or cell migration [30, 97-99]. Normal mammary epithelial cells generate greater force and occupy more surface area on a stiff matrix (5.000Pa) than similar cells interacting with soft matrix of 140Pa [11].

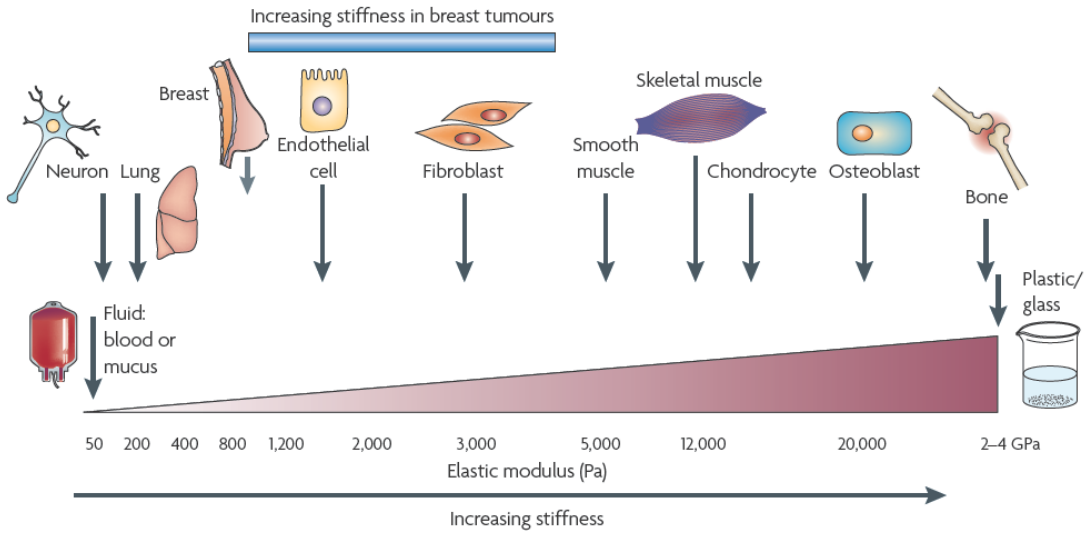

Figure 6 | Substrate stiffness is a characteristic that varies a lot among different tissues. Cells adapt their behavior, function and shape according to it [13].

Sudden changes in ECM mechanics, ECM remodeling and resultant disturbance in cytoskeletal tension and mechanotransduction signaling are important factors that can contribute to malignant transformation, tumorigenesis and tumor formation in addition to genetic mutations [11, 100-104]. As a consequence the cytoskeleton reorganizes. Higher ECM stiffness can result in the disruption of normal epithelial cell polarity, as well as alterations in the tensional forces, morphological changes of tumor cells and the development of an invasive phenotype. Thus cancer cells lose their dependency on anchorage and cell-surface tension as they become able to invade other tissues [105].

One of the main regulators of cytoskeletal tension is the Rho family of GTPases. Matrix stiffness and cytoskeletal tension functionally cooperate in a mechano-circuit that modulates phenotypic transformations in tumors by coupling the mechanosensing role of integrins in relaying external physical cues to Rho and Erk signaling pathways [106, 107]. This results in elevated Rho/ROCK-dependent cytoskeletal tension and amplifies the formation and stabilization of focal adhesion assembly. It further increases cell-generated force and focal adhesion assembly accompanied by FAK signaling, ROCK mediated disruption of adherens junctions and enhanced growth-factor-dependent Erk activation. All of this drives tumor cell proliferation and disruption of polarity and abrogates lumen formation and remodeling of mammary tissue architecture. Disruption of Rho or Erk signaling was shown to reduce cytoskeletal tension to normal levels and thereby repress the malignant phenotype [101, 107, 108].

II.3.3 Defects in cardiac and skeletal muscle

The heart can adapt to prolonged changes in the mechanical workload with an increase in cardiac myocyte size and modification of the surrounding ECM (cardiac remodeling). Defects in regulating the adaptation process lead to pathological and physiological hypertrophy [19]. More than 400 mutations have been identified in patients with cardiomyopathy, affecting 9 separate sarcomeric genes including actin, α-tropomyosin, troponin, titin, and β-myosin heavy chain [109]. Cardiac myocytes can respond directly to mechanical deformation or stretch through several internal mechanosensors like integrins, integrin linked kinase (ILK), sarcomeric proteins and cell surface receptors. Mechanosensors might include stretch-sensitive ion-channels at the cell membrane. Subsequently multiple overlapping signaling cascades, like Rho/ROCK, MAPK, phospholipase C, calcium/calcineurin and even microRNAs are activated when muscle cells are stretched [19]. Activation of these pathways triggers hypertrophic gene expression and causes an increase in myocyte length.

Disruption of the cytoskeletal-ECM coupling renders cells more susceptible to membrane damage and causes aberrant activation of MAPK (Erk) signaling in response to stretch [110]. In the skeletal muscle forces that are generated in the sarcomeres are transmitted to the ECM through a specialized protein complex that consists of dystrophin and dystrophin-associated proteins in the membrane. Mutations in important sarcomere components, like the cytoskeletal proteins desmin, titin and myosin have been reported to result in disorganized sarcomeres and disturbed cellular mechanics. As a result of these mutations cells show impaired force generation and altered (passive) cytoskeletal stiffness accompanied by impaired relaxation dynamics of myocytes [111].

Muscular dystrophies are a group of genetic muscle diseases that is characterized by progressive skeletal muscle weakness and death of muscle cells and tissues [112]. The most common type is Duchenne muscular dystrophy (DMD) where mutations in the dystrophin gene disrupt the force transmission between the cytoskeleton and the ECM. While Duchenne patients do not express dystrophin, patients suffering from Becker muscular dystrophy express a truncated dystrophin and thus display a milder phenotype [113]. Dystrophin is part of the dystrophin-glycoprotein complex that is responsible for joining the cytoskeleton of myofibers to the ECM [114]. Loss of dystrophin destabilizes this structural complex and hence the integrity of the muscle [115]. Stress-induced rupture of the plasma membrane in dystrophin-deficient muscle fibers leads to an influx of extracellular calcium. This results in abnormal muscle contraction, a physical damage of the cytoskeleton and a consecutive loss of muscle cells [116-118].

Mutations in laminin-α, integrin α7 (a laminin-receptor), collagen VI, or α-dystroglycan are the cause for another group of neuromuscular disorders, the congenital muscular dystrophies. As reviewed by

Jimenez-Mallebrera [119] many proteins affected in this clinically and genetically heterogeneous group of diseases are involved in the interaction between the muscle cell and the ECM.

Muscular dystrophies can also arise from mutations in the nuclear envelope proteins emerin and laminA/C [3, 5]. This type of muscular dystrophy is called Emery-Dreyfuss muscular dystrophy (EMDM) and has recently also been described for patients carrying mutations in nesprin 1 [4, 120-124]. Cells from laminA/C knock-out mice display decreased nuclear stiffness, increased nuclear fragility and impaired activation of mechanosensitive genes [2, 3]. Cells derived from emerin deficient mice have normal nuclear mechanics but increased apoptosis in response to stretching. Attenuated expression of Iex1 (also known as Ier3), an anti-apoptotic gene, might contribute to increased sensitivity.

It is not clear whether defects in mechanotransduction signaling arise as a direct consequence of altered nuclear stiffness or whether they mainly reflect broader defects in specific signaling pathways (for example, in NfκB) that are modulated by nuclear Lamins.

II.3.4 Laminopathies

The previously decribed Emery-Dreifuss muscular dystrophy belongs to a group of very diverse diseases called laminopathies. It includes muscular dystrophies, progeria (premature ageing), and cardiomyopathies as well as lipodystrophy and neuropathy. Their common characteristics are mutations in the nuclear lamins. Cells deficient in A-type lamins have decreased viability, reduced expression of mechanosensitive genes and altered nuclear mechanics in response to mechanical stress. They also display an attenuated NfκB response upon mechanical stimulation [5]. A lack of B1-type lamins does not show these effects [2]. However, also mutations in nesprin have now been found in patients suffering from Emery-Dreifuss muscular dystrophy, a disease previously only described in the context of mutations in emerin and laminA. Unc84 and ANC1 (C.elegans homologs of sun1 and nesprin respectively) mutants in C.elegans have defects in nuclear positioning and nuclear anchorage [80, 125], [126].

Among the diseases described in the context of mutations in the lmna gene is Hutchinson-Gilford progeria syndrome (HGPS), a progeroid disorder. Patients appear normal at birth but fail to grow shortly thereafter and die at their early teens due to arteriosclerosis, an extensive loss of vascular smooth muscle cells and an unusual susceptibility to haemodynamic stress [127, 128]. Mechanotransduction in vascular cells in response to fluid shear stress and strain from vessel expansion is a crucial protective mechanism against arteriosclerosis. This mechanism can mediate apoptosis, proliferation and ECM secretion in healthy vascular smooth muscle cells. Fibroblasts from

mice and patients with HGPS show decreased viability when subject to stretching and lack a strain-induced proliferation response [129].

Other laminopathies affect the fat tissue or neurons. In Dunnigan's familial partial lipodystrophy the white fat is lost or redistributed. Patients suffering from Charcot-Marie-Tooth neuropathy show reduced axon density, demyelinated axons and later on a wasting of their peripheral muscles.

How mutations in a single gene can give rise to such a variety of phenotypes is unclear. Mutant A-type lamins affect the structural integrity of the nucleus, either through the altered structural properties of laminA, as reviewed by Yosef Gruenbaum [94], or through missing interactions with the nuclear envelope and associated proteins [130]. These changes lead to an increased nuclear fragility and a greater susceptibility to physiological stress and might contribute to the pathologies affecting tissues that are subject to mechanical stress, such as muscles [3-5, 19].

The effects seen on nuclear structure might also have direct consequences on gene expression. Disruption of the nuclear lamina affects chromatin organization and transcriptional regulation of gene expression in specific ways. Proteins associated with the nuclear envelope (NE) interact either directly or indirectly with chromatin and thus influence chromatin organization, transcription and binding to DNA. Silencing often correlates with a relocation of the silenced gene to the nuclear periphery [72, 131-133].

Redistribution of emerin has been seen in mice as a consequence of the loss of functional laminA. However these changes have not been seen in laminA mutations causing Dunnigan's familial partial lipodystrophy (FPLD). The majority of the mutations leading to FPLD are found at the surface of the C-terminal globular domain whereas the muscle phenotype mutations are inside this domain. Mutations inside the globular domain are more likely to affect the structure of laminA thus leading to an instable nucleus. Mutations on the outside may rather affect the interaction of laminA with other proteins such as the sterol response element binding protein 1 (SREBP1) which is a transcription factor involved in adipogenesis [130, 134-137].

There is no evidence for just one of the two hypotheses suggesting that both structural weakness and altered chromatin accessability contribute to the diversity among the laminopathy phenotypes.

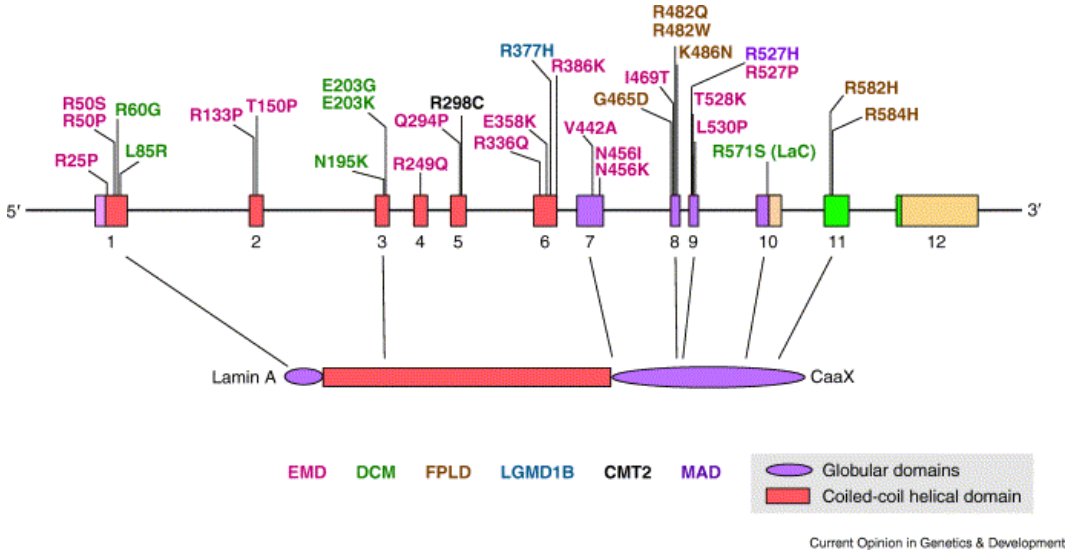

Figure 7 | **Known mutations in laminA/C causing laminopathies.** To date there are about 20 mutations kown in lamin A/C leading to the various diseases comprised in the group of laminopathies [138].

II.3.5 Mechanotransduction in the eye

The eye is also affected by disturbed mechanotransduction. Increased mechanical stress could contribute to the pathogenesis of glaucoma and axial myopia [139] where stress arises from intraocular pressure. Human sclera fibroblasts, primary cells implicated in sclera remodeling that accompanies elongation during the development of myopia, express many genes that are modulated by mechanical strain application. Among these genes are some encoding for ECM proteins, for example, tenascin-C. Others are protein kinases, cell growth and differentiation factors (FGF and bone morphogenic proteins) and transcription factors (JunB) [140].

II.4 TENASCINC AND MECHANICAL STRESS

II.4.1 Tenascins

The tenascins are a highly conserved family of large oligomeric glycoproteins [141] that comprises 4 tenascins in vertebrates, tenascin-C, tenascin-R, tenascin-W, and tenascin–X (avian tenascin–Y) whereas there are none in C.elegans [141]. They are present in many connective tissues throughout the body [142]. However, each tenascin has a unique expression pattern. Tenascin-W is expressed in the developing skeleton and periostium in the adult, as well as in the kidney, certain muscles [143] and in breast tumors [98]. Tenascin-R is exclusively expressed in the central nervous system, tenascin-X in muscles. It is secreted by fibroblasts present in the epi-, peri-, and endomysium. Tenascin-C is highly expressed during embryogenesis and is absent or largely reduced in developed organs. In the adult it can only be found in infections, inflammation, wound healing and tumorigenesis [144, 145]. In addition it is expressed in tissues that are subject to mechanical strain.

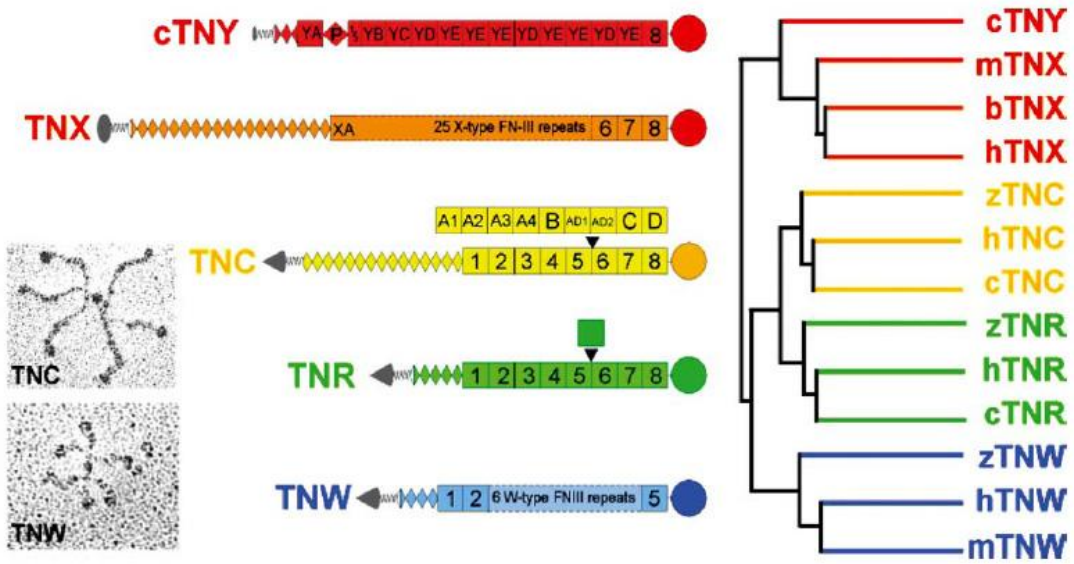

Figure 8 | **Schematic representation of the tenascin family proteins**. All tenascins share an amino-terminal oligomerization domain followed by consecutively arranged heptad repeats, EGF-like domains, fibronectin type III repeats and a fibrinogen globe [141].

Tenascin-C and tenascin-R knockout mice show abnormalities in the nervous system including decreased axonal conduction velocities and motor coordination deficits as well as impaired hippocampal synaptic plasticity. However their full function is not very well understood.

The four tenascins all possess the same structural motifs that are aligned in the same order in each family member (figure 8 A). At the N-terminus they all possess heptad repeats followed by epidermal growth factor (EGF)-like repeats, and fibronectin type III (FN III) domains. The C-terminus is a globular domain shared with fibrinogens. The number of these subdomains however differs among the 4 family members. In addition tenascin-C and tenascin–R are subject to alternative splicing that leads to the insertion of variable amounts of fibronectin type III repeats and gives rise to a multitude of isoforms. The long extended molecules oligomerize (see figure 8 B) with their N-terminal domains and form trimers (tenascin-R) or hexamers (tenascin-C) [142, 146].

Tenascins interact with specific cell surface receptors ($\alpha 2\beta 1$ integrin, $\alpha v\beta 3$, $\alpha 9\beta 1$, syndecan, annexinII) and other ECM proteins like FN or perlecan [141, 142].

II.4.2 Tenascin-C induction by mechanical stress

Tenascin-C was the first family member to be discovered as an extracellular matrix protein that was enriched in the stroma of gliomas and as myotendinous antigen [147-149]. Due to alternative splicing 9 additional FNIII repeats can be included in tenascin-C resulting in a great number and diversity of isoforms (figure 8 A). While tenascin-C is mainly absent in the adult organism, basic levels can be found in tissues that are subject to strain, such as tendons and ligaments, predominantly at the myotendinous junctions.

Cyclic mechanical stress in fibroblasts leads to the induction of various ECM-components, among them tenascin-C. In in vivo experiments mechanical stress (10% of the body weight) was applied to one wing of young chickens. This led to stretching of the anterior latissimus dorsi (ALD) holding muscle. Within a few hours tenascin-C was induced ectopically in the endomysium throughout the ALD muscle [150]. TN-C levels stayed elevated after 7 days of loading. This was also seen on the mRNA level by Northern blotting where there was an increase in TN-C mRNA already after 4 hours of stretching. These results were confirmed by in situ hybridization that also identified the endomysial fibroblasts as the source of TN-C. The response was only transient and the protein level decreased again 5 days after removal of the load. Induction of tenascin-C by mechanical stress has also been shown in vitro [18, 138, 150]. Furthermore TN-C was released into the medium after 6 hours of cyclic strain. Induction is not mediated by factors released into the medium as incubation of cells with conditioned medium from stretched cells did not induce TN-C expression. Interestingly, prestress of the cell is a prerequisite for the activation of TN-C and inhibition of Rho-dependent kinase desensitizes fibroblasts to mechanical signals and blocks the induction of TN-C [31].

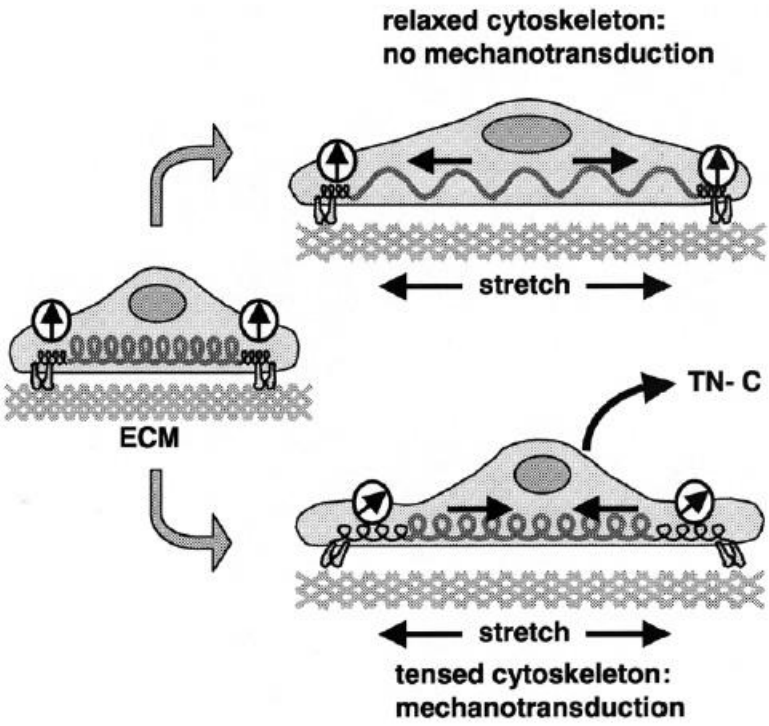

Figure 9 | **Model of cellular prestress.** Prestressing is crucial for a cell's sensation of mechanical strain and consequent up regulation of tenascin C [32].

II. 5 AIM OF THE WORK

The aim of this thesis is to investigate the importance of the so-called LINC complex, a direct link from the extracellular matrix to the nucleus, in mechanosensation, gene regulation and cell differentiation. The focus lies on the early gene regulatory mechanisms that are activated upon exposure of fibroblasts and myogenic progenitor cells to biaxial strain. Many components of a cell's response to mechanical cues have already been identified, but many are still unknown, especially mechanosensors.

As research in mechanotransduction is still a relatively new field of research there are many open questions to address for example how adhesion receptors that lack enzymatic activity trigger downstream signaling cascades. How do the various signaling cascades that have previously been described to be activated by one or several types of mechanical stimulation interact with each other? How are the diverse molecular interactions at the adhesion sites regulated? And how do the physical features of the adhesive surface activate specific signaling pathways? Other interesting questions address the molecular sensitivity of the adhesive interactions and the spatial, temporal and compositional resolutions of adhesion-mediated signaling.

We have decided to focus on the early stress response within 1h of biaxial cyclic strain and the activation of signaling pathways regulating this early stress response. The main emphasis of this thesis was to investigate the role of the LINC complex in response to biaxial and uniaxial strain and cell differentiation. We investigated the immediate cellular response biochemically and by live imaging and followed cytoskeletal changes induced by biaxial and uniaxial strain.

RESULTS

III. RESULTS

III.1 PUBLISHED DATA

The International Journal of Biochemistry & Cell Biology 42 (2010) 1717–1728

Contents lists available at ScienceDirect

The International Journal of Biochemistry & Cell Biology

journal homepage: www.elsevier.com/locate/biocel

Interfering with the connection between the nucleus and the cytoskeleton affects nuclear rotation, mechanotransduction and myogenesis

Michaela Brosig[a], Jacqueline Ferralli[a], Laurent Gelman[a], Matthias Chiquet[b], Ruth Chiquet-Ehrismann[a,*]

[a] Friedrich Miescher Institute for Biomedical Research, Novartis Research Foundation, Maulbeerstrasse 66, CH-4058 Basel, Switzerland
[b] University of Berne, Department of Orthodontics and Dentofacial Orthopedics, University of Berne, Freiburgstrasse 7, CH-3010 Bern, Switzerland

ARTICLE INFO

Article history:
Received 7 May 2010
Received in revised form 1 July 2010
Accepted 3 July 2010
Available online 17 July 2010

Keywords:
Mechanotransduction
Myogenesis
LINC complex
Stretch
Gene expression

ABSTRACT

Mechanical stress controls a broad range of cellular functions. The cytoskeleton is physically connected to the extracellular matrix via integrin receptors, and to the nuclear lamina by the LINC complex that spans both nuclear membranes. We asked here how disruption of this direct link from the cytoskeleton to nuclear chromatin affects mechanotransduction. Fibroblasts grown on flexible silicone membranes reacted to cyclic stretch by nuclear rotation. This rotation was abolished by inhibition of actomyosin contraction as well as by overexpression of dominant-negative versions of nesprin or sun proteins that form the LINC complex. In an in vitro model of muscle differentiation, cyclic strain inhibits differentiation and induces proliferation of C2C12 myoblasts. Interference with the LINC complex in these cells abrogated their stretch-induced proliferation, while stretch increased p38 MAPK and NFkB phosphorylation and the transcript levels of myogenic transcription factors MyoD and myogenin. We found that the physical link from the cytoskeleton to the nuclear lamina is crucial for correct mechanotransduction, and that disruption of the LINC complex perturbs the mechanical control of cell differentiation.

1. Introduction

Response and adaptation to mechanical stress is important for a broad range of cellular functions including development, tissue homeostasis, tissue architecture and muscle regeneration. Cell differentiation not only depends on the expression of certain growth factors but also on the mechanical properties of the microenvironment (Butcher et al., 2009). Therefore cells need to sense mechanical cues, transduce them into biochemical signals and respond to them appropriately. This has become an active area of research (for recent reviews see Ingber, 2006a, b; Patwari and Lee, 2008; Jaalouk and Lammerding, 2009; Wozniak and Chen, 2009).

There are several types of cell surface proteins that are able to sense mechanical forces and translate them into biochemical signals and the most immediate consequence of stretch is the opening of stretch-sensitive ion channels (for a review see Kung, 2005). Furthermore, the extracellular matrix (ECM) is linked to the cytoskeleton by integrin and/or dystroglycan receptors, and these linkages enable cells to respond to external mechanical stimuli by activation of signaling pathways that often lead to cytoskeletal contraction (Jones et al., 2005; Geiger et al., 2009; Wozniak and Chen, 2009). In the cell interior the actin cytoskeleton as well as intermediate filaments are connected to the nuclear lamina through members of the nesprin family of proteins anchored in the outer nuclear membrane (Starr and Han, 2002; Zhang et al., 2002; Padmakumar et al., 2004; Wilhelmsen et al., 2005). The nesprins, through their KASH domain, are bound to proteins of the sun family that span the inner nuclear membrane. This provides the link to lamin A/C of the nuclear lamina (Haque et al., 2006; Wilhelmsen et al., 2006). This bridge across the nuclear membranes linking the nucleus with the cytoplasm has been coined the LINC complex (Crisp et al., 2006). With the identification of the LINC complex, a physical connection between the ECM and the nuclear lamina (and thus the chromatin) is now firmly established. The existence of a connection between the ECM and the inside of the nucleus was already proposed in 1982 by Mina Bissell (Bissell et al., 1982), and elegant experiments by Maniotis et al. (1997) demonstrated the existence of this connection by pulling on integrins from the outside of cells causing distortion of nuclei along the axis of the applied tension field.

The structural continuity between the ECM and the nuclear lamina is particularly crucial for muscle cell function. Mutations in any protein that is part of this connection can cause muscular dystrophies or other myopathies (for review see Jaalouk and Lammerding, 2009). Muscular dystrophies can even arise from mutations in the nuclear envelope proteins emerin and lamin A/C. This type of disease is called Emery–Dreifuss muscular dystrophy (EDMD) and has recently also been described for patients carrying mutations in

* Corresponding author. Tel.: +41 61 697 24 94; fax: +41 61 697 39 76.
E-mail address: ruth.chiquet@fmi.ch (R. Chiquet-Ehrismann).

1357-2725/$ – see front matter © 2010 Elsevier Ltd. All rights reserved.
doi:10.1016/j.biocel.2010.07.001

nesprins (Zhang et al., 2007a). Since the LINC complex is implicated in mechanical stabilization of the nuclear envelope and since fibroblasts from EDMD patients exhibit nuclear morphology defects (Zhang et al., 2007a), we decided to investigate the effect of disruption of the LINC complex on mechanotransduction in fibroblasts as well as muscle cells. We performed live imaging of cells under cyclic strain with or without a functional LINC complex. Our results show that the LINC complex is an important factor contributing to mechanotransduction in normal cells, and that disruption of the LINC bridge perturbs many aspects of cellular physiology including nuclear movements and muscle differentiation.

2. Materials and methods

2.1. Live imaging of cells under strain

After assembly of the devices (Fig. 1 and Supplement 1 for the specifications of the equibiaxial cell stretching device) the silicone membrane forming the bottom of the wells is coated with 100 μg/ml fibronectin as described previously (Chiquet et al., 2004) for 1 h at 20 °C. Due to the tight seal between the Teflon rim and the silicone membrane, cells can be seeded into the wells in 2 ml medium without leakage. Devices (without pump) are put in a CO_2-incubator overnight to allow attachment and spreading of 7×10^4 cells per well. The stretching device was placed under a microscope (Axiovert200 M; Carl Zeiss) equipped with a fluorescent light source (TILL polychromator V; Agilent), as well as CO_2 and temperature control that allows live cell imaging and time-lapse experiments. The setup is controlled by the Metamorph software (Molecular Devices). Prior to microscopy the medium was exchanged to DMEM + 5% bovine serum, 30 mM HEPES without phenolred. In each live imaging experiment, cells were first monitored for at least 1 h at rest. Then, using the pneumatic mechanism, the membrane with attached cells was stretched by 15% over the Teflon cylinder, and relaxed again.

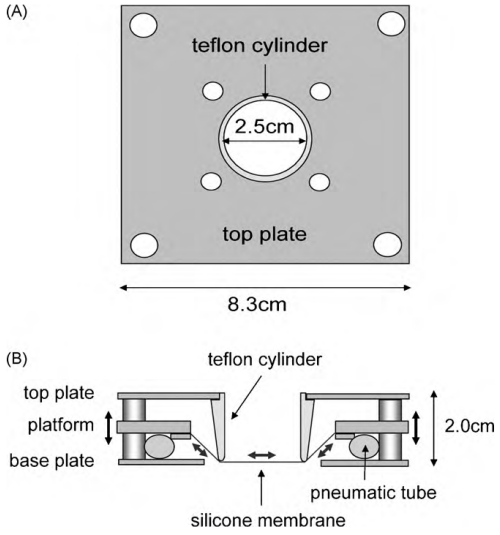

Fig. 1. Equibiaxial cell stretching device for life imaging. (A) The view from above depicts the top plate of the device with the inserted Teflon cylinder that forms the culture well. (B) The side view shows the mechanism. The frame consists of a bottom and a top plate connected by vertical steel rods at the four corners. A platform in between can be moved up and down along the rods by means of pneumatic tubing. A silicone membrane is fitted across the central opening of the platform, and spans across the lower rim of the Teflon cylinder. Cells are plated on the fibronectin-coated silicone membrane. Lifting of the platform leads to equibiaxial stretching of the membrane with attached cells. The device is placed on the stage of an inverted microscope and cells are viewed from the bottom (for a detailed description, see Section 2.1 and Supplement 1).

To analyze nuclear rotation of NIH3T3 (ATCC; CRL-1658) or C2C12 (ATCC; CRL-1772) cells were plated in these devices on fibronectin-coated silicone membranes and left to adjust to microscopy conditions for 1 h and then monitored for 1 h at rest, taking phase contrast pictures every 10 min. After that cells were stretched every 2 min and pictures were acquired at the relaxed as well as the stretched state for 5–10 cycles of stretching. Rotation angles of nuclei were measured by putting a line through two clearly visible nucleoli of every cell in each field analyzed and the change of the angle of this line to a fixed horizontal line was measured after every stretch and relaxation using the ImageJ software. No nuclear rotation was observed during the 1 h at rest prior to stretching. There was no loss of cells in the course of these experiments and no cells were excluded from the analysis. Similar methods of assessing nuclear rotation based on nucleolar positions have been used in other studies (Ji et al., 2007; Levy and Holzbaur, 2008; Gerashchenko et al., 2009). In some cases the following inhibitors were included during the adjustment period before stretching: Y-27632 (10 μM Calbiochem), nocodazole (1 μM; Sigma Aldrich) and colchicine (1 μM; Sigma Aldrich).

2.2. RNA isolation, RT and QPCR

RNA was isolated using QiaShredder (Qiagen) and the RNeasy kit (Qiagen) according to the manufacturer's protocol. RNA was eluted with 30 μl H_2O per column for RT and QPCR. For quantitative PCR, reverse transcription of the isolated RNA was performed with the ThermoScript™ RT-PCR System (Invitrogen) according to the supplied protocol using 1 μg RNA in a 20 μl setup with oligo dT primers. The generated cDNA was then used for quantitative real-time PCR using Platinum® SYBR® Green qPCR SuperMix-UDG with ROX (Invitrogen) on an Abi7000 (Applied Biosystems). The primers used for qPCR are listed in Supplement 2. Values were normalized to GAPDH and fold changes calculated using the efficiency ΔΔct method (Pfaffl, 2001). Each experiment was performed in triplicates and was repeated at least three times.

2.3. Protein extracts and Western blot analyses

Cells were washed once with PBS on ice. 200 μl RIPA buffer (150 μM NaCl, 1%NP-40, 0.25% DOC, 50 μM Tris pH 7.4, 1 mM EDTA) per well was added to cells in a 6-well dish on ice. Cells were scraped off and frozen immediately at −80 °C. Samples were prepared by mixing 20 μl of RIPA extract with 7 μl loading buffer + β-mercaptoethanol and heating at 95 °C for 5 min. Proteins were resolved by SDS-page and transferred to immobilon-P membranes (Millipore). Proteins of interest were visualized using specific antibodies against NfkB p65 (#4764, Cell Signaling), p-NfkB p65 (#3036, Cell Signaling), p44/42 MAP kinase (#9102, Cell Signaling), p-p44/42 Map Kinase (#9101, Cell Signaling), p38 MAPK (#9212, Cell Signaling) and p-p38MAPK (#9215, Cell Signaling) and super signal (Pierce) chemiluminescence reagents according to the manufacturer's recommendations.

2.4. Retroviral transduction

For the production of retrovirus for dominant-negative Sun1 and Nesprin-2 the following constructs were cloned. For Nesprin-2 the same sequences as in the construct GFP-Cterm1 described in Zhen et al. (2002) and for Sun1 the same sequence as GFP-Sun1-TM-C described in Padmakumar et al. (2005) were amplified from a mouse whole embryo cDNA library and cloned as N-terminal eGFP

fusions into the first MCS of pQCXIX (Clontech). As control eGFP was also cloned into the first MCS of the same vector. This resulted in the constructs referred to pQCeGFPNes (DN Nes), pQCeGFPSun (DN Sun), or pQCeGFP (eGFP control) in the present manuscript. EcoPack™ 293 cells (Clontech) were transfected with pQCeGFPSun, pQCeGFPNes or pQCeGFP using the Mirus TransIT® Transfection reagent MIR 2700 (Mirus). Cells were incubated for 48 h before the virus containing medium was collected, filtered and applied to NIH 3T3 cells plated at 50–70% confluence the day before. NIH3T3 cells were incubated with the virus for 24 h before the medium was exchanged according to the following experimental requirements indicated.

2.5. Immunofluorescence staining

Cells were washed once with PBS then fixed with 4%PFA in PBS for 15 min at room temperature. After washing twice in PBS cells were permeabilized for 5 min with 0.1% Triton X-100 (Fluka) in PBS. Cells were washed twice for 10 min with PBS before antibody application. The following antibodies were used: anti-Nesprin-1 (ab5250 from Abcam) and anti-α-tubulin (clone YL1/2; Millipore). If cells on Silicone membranes were analyzed membranes were cut and removed from the wells for incubations with anti-NfkB p65 (#4764, Cell Signaling), over night at 4 °C. Cells were washed 3 × 10 min with PBS. Secondary antibodies conjugated to Alexa 488 or Alexa 568 were purchased from Molecular Probes and incubated together with Hoechst (Sigma) and Phalloidin Alexa 568 (Molecular Probes) for 1 h at room temperature at dark. After washing 3 × 10 min with PBS the membranes were mounted on slides and covered with cover slips using Prolong Gold (Molecular Probes). Images were acquired on an Axioimager Z1 microscope (Carl Zeiss).

2.6. NFkB reporter assays

NIH3T3 or C2C12 cells were transduced with the viruses DN Sun, DN Nes or eGFP for 24 h in 6-well plates. After removal of the virus supernatants, cells were cultured in serum-containing medium for 18 h before transfection with pNFkB-SEAP (Clontech) in medium containing 0.3% serum using fugene 6 transfection reagent (Roche). Twenty-four hours later 10 ng/ml transforming growth factor-alpha (TNF-alpha; Peprotech) were added to half of the wells. After 24 h the medium was collected and secreted alkaline phosphatase was measured using the chemiluminescent alkaline phosphatase detection kit SEAP Reporter Gene Assay (Roche) according to the manufacturer's procedure. For normalization co-transfection with the firefly luciferase-containing pGL3 basic vector (Promega, Madison, WI, USA) was performed. Cells were lysed with Passive Lysis Buffer (Promega) and assayed with the LARII Luciferase Assay System (Promega). Secreted alkaline phosphatase and firefly luciferase activity were measured in a Luminometer Mithras LB 940 (Berthold technologies, Regensdorf, Switzerland).

2.7. C2C12 cell cultures

5×10^4 C2C12 cells/well were plated on 6-well cell culture dishes or fibronectin-coated BioFlex™ plates (Dunn Labortechnik GmbH). One day after seeding, the medium was replaced by differentiation medium (DMEM with 5% horse serum) or growth medium (DMEM and 10% FCS) for 5 days. In some cases C2C12 cells were transduced 1 day after plating with retroviruses for 24 h before the medium was exchanged to growth or differentiation medium. In some experiments the C2C12 cells were stretched for 1 h (biaxial strain, 10% elongation, 0.3 Hz) before mRNA was isolated. In another set of experiments cells were stretched for 1 h per day for 5 days while control cells remained at rest. Differentiation of C2C12 cells into myotubes was observed by phase contrast and imunofluorenscence microscopy and the differentiation monitored either by measuring creatine kinase levels using a CK NAC opt.kit (Randox Laboratories), by counting percentage of nuclei in multinucleated myotubes (fusion index) or by qPCR for myosin heavy chain, MyoD and myogenin expression with the primers listed in Supplement 2. Cell extracts for Western blots and mRNA isolation were prepared 16 h after the last hour of stretching.

3. Results

3.1. The device for live imaging of cyclically stretched cells

In order to observe direct effects of cyclic stretch on cells by live imaging, we constructed a device that fits under a microscope and allows strain to be applied to an elastic substrate without moving it out of focus (Fig. 1; for precise specifications see Supplement 1). The essential part of the device consists of a circular silicone membrane that seals the lower rim of a hollow Teflon cylinder. Membrane and cylinder form a culture well in which cells are plated onto the fibronectin-coated elastomer. The membrane is fixed to a platform that surrounds the Teflon well. When the platform is lifted, the membrane with attached cells is stretched equibiaxially by 15% over the rim of the cylinder. Cells in the field of view may shift laterally during stretching, but will return to exactly the same position after relaxation. Thus, cells can be imaged after each individual stretch cycle, and their responses monitored. To prove the functionality of this device an example of a time-lapse movie is available in Supplement 3. It shows two mouse embryo fibroblasts stably transfected with GFP-tagged integrin-linked kinase (ILK), an adaptor protein of focal adhesions (Maier et al., 2008). If cells need to be observed at the relaxed as well as the stretched state, the cells have to be tracked by moving the microscope stage in the *X*/*Y* axis.

3.2. Stretching of NIH3T3 fibroblasts results in immediate nuclear rotation requiring actin dynamics and an intact LINC complex

In order to analyze instant effects of cyclic strain, we used our device to observe cellular morphology in the stretched as well as the relaxed state. We were able to track NIH3T3 fibroblasts during the stretch cycle and to photograph them by phase contrast microscopy just before stretch was applied and immediately after maximal stretch was reached. Thereby we noticed an interesting phenomenon. Already after applying a single bout of 15% equibiaxial stretch to the substratum and holding the culture in the stretched position, the nuclear orientation within most of the cells changed substantially, and the nuclei rotated instantly as judged by the change in position of their nucleoli (Fig. 2A). We then took series of pictures of cells over 8 stretch/relaxation cycles both at the relaxed as well as the stretched position. One example is shown in Fig. 2B and a summary of all cells captured is given in Fig. 2C. We found that the nucleus turns in one direction during stretching, and upon relaxing the membrane, the direction of rotation reverses but not completely back to the original position. After each stretch–relaxation cycle, the nucleus comes to rest at a positive or negative angle relative to its pre-cycle position, resulting in net rotation per cycle. This can go back and forth over several cycles and is visible by the zigzag lines in the graph. There are some cases where the nucleus keeps turning in the same direction and others where the net movement reverses. The different behavior of individual nuclei is depicted in Fig. 2C. Such a behavior implied a passive as well as an active mechanism that was triggered by stretch.

The nucleus of a cell is known to be linked to the cytoskeleton through nesprin and sun proteins, representing the so-called LINC

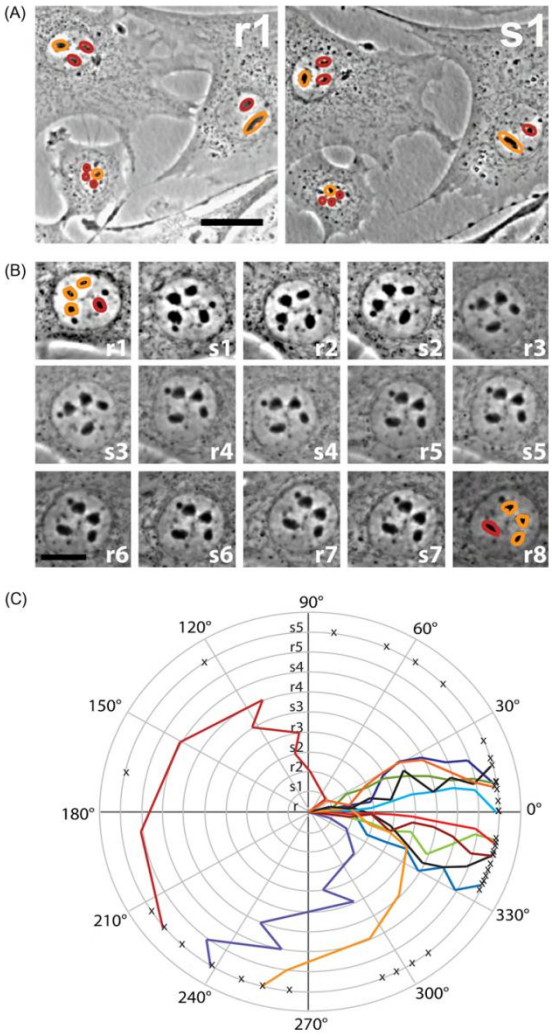

Fig. 2. Nuclei rotate in response to biaxial strain. (A) NIH3T3 cells were stretched on fibronectin-coated silicon membranes once to about 15% elongation and a picture was taken at the relaxed (r1) and at the stretched state (s1). Nucleoli are outlined in red and orange as a help to visualize the rotation of the nuclei. Bar, 25 μm. (B) An example of a single nucleus stretched over 7 cycles and photographed at each relaxed (r1–r8) and stretched (s1–s7) position. As can be seen from the nucleoli outlined in orange and red in the first and last picture this nucleus rotated clockwise by 120°. Bar, 20 μm. (C) Evaluation of a larger number of cells revealed that 83% of all nuclei are rotating more than 10° over 10 cycles of stretching. Angles of rotation were measured for 5 stretching cycles at both the relaxed and stretched position and the values are indicated on the circles starting at the centre (r) until circle s5 resulting in the colored trajectories. Crosses (x) marked in circle s5 depict the endpoints reached by all of the nuclei analyzed. Most nuclei rotate within 30° clockwise or counter clockwise as can be seen by the accumulation of crosses in this sector of the circle indicating the endpoints of all nuclei analyzed. The colored trajectories show that while some of the nuclei rotate immediately, others take several stretches before they react with extensive rotations. The rotation continues during relaxing phases as well, for some cells in the same direction as during stretching, for others in the opposite direction resulting in a zigzag line. The blue line ending at 240° represents the rotation of the nucleus shown in (B). (For interpretation of the references to colors in this figure legend, the reader is referred to the web version of this article.)

complex. We used our observation of the stretch-induced nuclear rotation to test whether overexpression of dominant-negative versions of Nesprin-2 or Sun1, which are known to disturb the LINC connection (Padmakumar et al., 2005; Crisp et al., 2006; Stewart-Hutchinson et al., 2008), would effectively detach the nucleus from the cytoskeleton. NIH3T3 cells were transduced with retroviral constructs encoding eGFP alone, eGFP-tagged dominant-negative Nesprin-2 (DN Nes) or Sun1 (DN Sun). As presented in Fig. 3A, retroviral transduction was very efficient and the eGFP-tagged proteins (but not eGFP alone) accumulated in the nuclear membranes of the cells. In order to confirm that overexpression of the DN Sun and DN Nes constructs were effective in displacing the

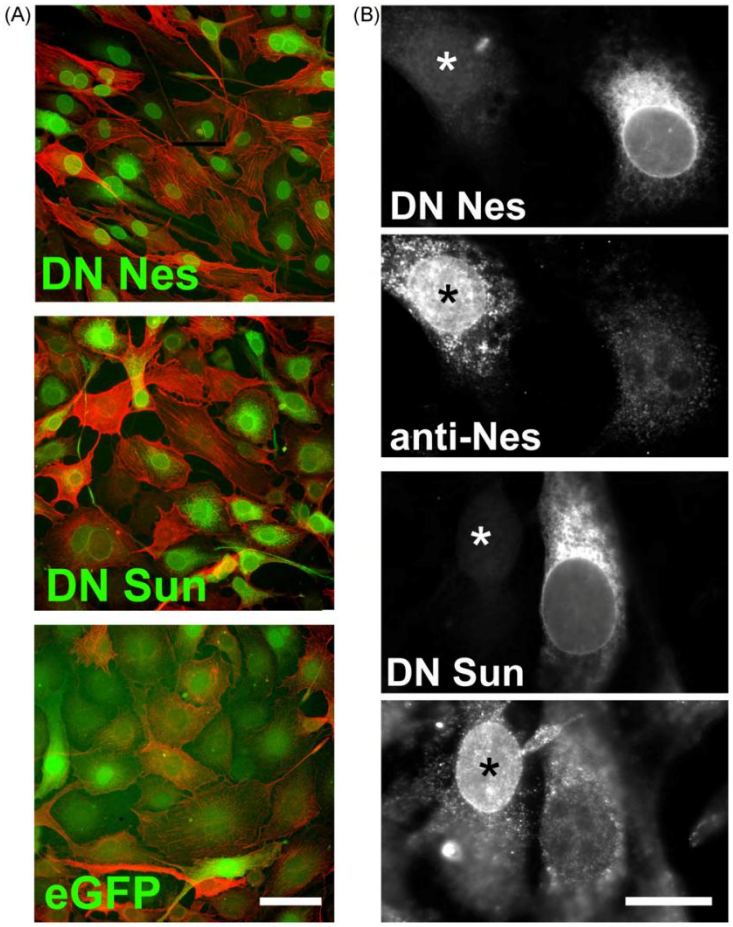

Fig. 3. Expression of DN Nes and DN Sun constructs in NIH3T3 cells. (A) NIH3T3 cells were transduced with retroviruses encoding GFP-tagged dominant-negative nesprin (DN Nes), dominant-negative Sun (DN Sun) or eGFP. The transduction efficiency was over 95% and nesprin and sun proteins accumulated in the nuclear membranes, as can be seen by the green fluorescence. The actin cytoskeleton is revealed by phalloidin staining. Bar, 50 μm. (B) DN Nes and DN Sun overexpression interferes with endogenous Nesprin-1 accumulation in the nuclear membranes: immunostaining of the endogeneous Nesprin-1 protein (anti-Nes) in untransduced cells (marked by a star) exhibit a strong nuclear envelope staining while the staining in the transduced cells, recognizable by their nuclear envelope staining from the transduced eGFP-DN constructs, is greatly reduced. Note that the anti-nesprin antibody does not only stain the nuclear envelope, but also the nesprin variants present in the nucleoplasm and in the cytoplasm, however, the nuclear envelope staining was abolished in all cells expressing the dominant-negative constructs. Bar, 25 μm. (For interpretation of the references to colors in this figure legend, the reader is referred to the web version of this article.)

endogenous proteins from the nuclear membranes, we stained the DN Nes and DN Sun transduced cells for endogenous Nesprin-1 (Fig. 3B). While non-transduced cells (marked by a star) showed a strong nuclear envelope staining by the anti-Nes antibody, the staining in the transduced cells, discernable by their green fluorescent nuclear envelope resulting from the transduced eGFP-DN constructs, was greatly reduced. When we now compared stretch-induced nuclear rotation in the eGFP-transduced cells to the DN Nes or DN Sun transduced cells, we found that overexpression of the truncated LINC proteins prevented nuclear rotation induced by cyclic strain. An example can be seen in Fig. 4A where two adjacent cells, one of which was transduced by DN Sun in green, were observed first for 1 h at rest. During this time both nuclei remained in the same position. However, after a single stretch the nucleus of the non-transduced cell turned by about 38° while the DN Sun containing nucleus remained in its position. Quantification of the cumulative angles of rotation in the course of 5 stretch and relaxation cycles in the parental NIH3T3 versus the retrovirally transduced cells revealed that interference with the LINC complex completely abolished the stretch-induced rotation (Fig. 4C).

Since nesprins connect to the cytoskeleton and the nuclei often exhibited a net rotation upon repeated stretching cycles, an involvement of actin or microtubule dynamics was considered. Treatment of the cells with the ROCK inhibitor Y27632 completely abolished nuclear rotation triggered by stretch, while treatment with microtubule-disrupting agents had not effect (Fig. 4B and C). Thus, the net nuclear rotation induced by cyclic strain required

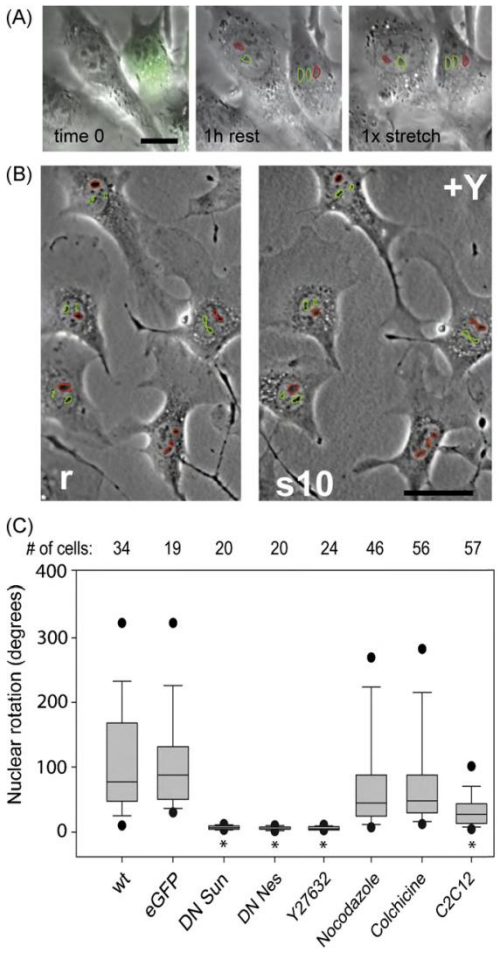

Fig. 4. Disruption of the LINC complex prevents nuclear rotation. (A) Phase contrast pictures of two adjacent cells of which one expresses DN Sun as can be seen by the GFP fluorescence overlaid in the picture at the time 0. During a 1-h period of rest (1 h rest) nucleoli of both cells remained in the same position. After a single stretch the non-transduced cell reacted by nuclear rotation, whereas the nucleus of the DN Sun transduced cell remained in the same position. The position of the nucleus of the DN Sun transduced cell also remained at the same position during several stretching cycles (not shown). Bar, 25 μm. (B) Inhibition of actomyosin contraction by Y-27632 blocks nuclear rotation as can be seen in this overview of cells before and after 10 stretching cycles. The position of all nucleoli outlined in red and green remained unchanged. Bar, 100 μm. (C) Parental NIH3T3 cells (wt) as well as NIH3T3 cells transduced with eGFP, DN Sun or DN Nes were subjected to 5 cycles of stretching and the nuclear rotation was measured as described in Fig. 2. The cumulative degrees of rotation over the period of 5 stretching cycles is plotted and reveals that the vast majority of nuclei of parental (wt) and eGFP control cells rotated by over 20°, while none of the DN Sun or DN Nes transduced cells reached 20° of rotation. Number of cells evaluated for each condition is shown on top and the results are presented with a box plot. The line within the box represents the median value which was 77.5 for wt, 88.0 for eGFP, 6.5 for DN Sun, 5.0 for DN Nes, 44.4 for nocodazole, 48.0 for colchicine, 3.4 for Y27632 and 27.3° for C2C12. The grey areas above and below the median represent 50% of all cells and the whiskers 75%. Outliers are individually plotted as black circles. Statistical analysis by ANOVA on Ranks followed by Dunn's method (multiple comparison versus a control group) showed that the rotation of nuclei of parental NIH3T3 cells (wt) was statistically significantly inhibited by the ROCK inhibitor Y-27632 as well as the DN Nes and DN Sun overexpression but not by the microtubule disrupting agents nocodazole or colchicine. The rotation of nuclei in C2C12 cells was significantly lower than in NIH3T3 cells but higher than in NIH3T3 cells perturbed by DN Nes, DN Sun or Y27632. The groups that were statistically different ($p < 0.05$) from the wt control cells are marked by an asterisk.

an intact LINC complex as well as actin dynamics, but not microtubules.

Using C2C12 myoblasts in our stretching device, we found that they also reacted to cyclic strain by nuclear rotation, although not to the same extent as NIH3T3 cells (cf. Fig. 4C). This is likely to be due to the different morphology of the spindle-shaped C2C12 as compared to the very spread and polygonal NIH3T3 cells.

3.3. Prolonged NFkB signaling in response to cyclic strain in fibroblasts with an impaired LINC complex

In a next step, we asked whether disruption of the LINC could affect cyclic strain-induced signaling pathways. NFkB is one of the transcription factors that has been shown to be activated by mechanical stress, e.g. by fluid shear stress in endothelial cells (Davis et al., 2004), osteoblasts (Chen et al., 2003) or colon cancer cells (Orr et al., 2005; Avvisato et al., 2007), or by uniaxial cyclic strain in human fibroblasts (Inoh et al., 2002; Amma et al., 2005). Therefore, we investigated whether in our model NFkB signaling was induced by cyclic strain and whether disruption of the LINC had an effect on NFkB signaling. We found that cyclic strain induced a rapid and transient translocation of NFkB into the nucleus of NIH3T3 cells. At rest NFkB was cytoplasmic and after 5 min of mechanical stimulation over 80% of all cells showed predominantly nuclear NFkB (Fig. 5A). The nuclear staining decreased gradually thereafter during the 1 h period of the stretching regimen. Nuclear translocation of NFkB was completely abolished by inhibiting NFkB signaling with sulfasalazine (not shown). We then analyzed nuclear translocation of NFkB in response to stretch in the presence or absence of a functional LINC complex, and found that nuclear accumulation of NFkB was prolonged in cells transduced with the DN Sun construct when compared to control cultures transduced by GFP only (Fig. 5B). Thus, whereas one aspect of mechanotransduction (nuclear rotation) is abolished in fibroblasts in the absence of a functional LINC complex, another (NFkB signaling) is increased.

To confirm in an independent experiment that NFkB signaling is increased in the absence of a functional LINC complex, we analyzed the transcriptional activity of NFkB upon stimulation with transforming growth factor alpha (TNF-alpha) in NIH3T3 as well as C2C12 myoblasts. Cells transduced with DN Sun, DN Nes or the eGFP control constructs were transfected with an NFkB-dependent reporter plasmid and the induction of the reporter activity by TNF-alpha was monitored (Fig. 6). The induction of NFkB activity was consistently higher (about 2-fold) in both cell types transduced with DN Sun and DN Nes in comparison to eGFP control cells.

3.4. Inhibition of C2C12 myogenic differentiation by cyclic strain requires a functional LINC complex

Judged from genetic diseases in patients with mutations in LINC complex proteins (Zhang et al., 2007a; Attali et al., 2009) and from genetic mouse models (Zhang et al.), it seems that muscle physiology is particularly sensitive to disruption of the LINC complex. It has been reported that cyclic stretching of the C2C12 mouse myogenic cell line induces cell proliferation and inhibits muscle differentiation (Kumar et al., 2004; Kook et al., 2008).

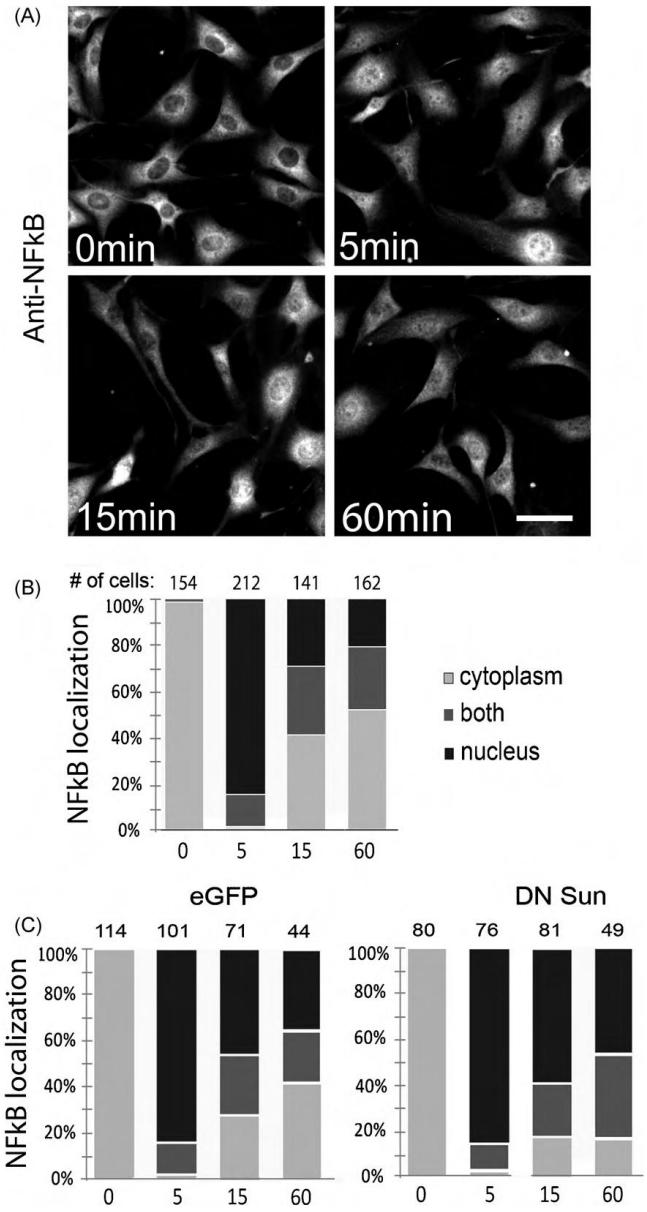

Fig. 5. Stretch-induced activation of the NfkB pathway is prolonged in the absence of an intact LINC complex. (A) Immunostaining of NFkB in NIH3T3 cells before and after 5, 15 and 60 min of continuous cyclic strain reveals that NFkB translocates into the nucleus already within 5 min of continuous cyclic strain. The translocation is transient. Bar, 100 μm. (B) Quantification of the localization of NFkB during 0–60 min of continuous cyclic strain in NIH3T3 cells shown in (A). Number of cells analyzed is given above the bars and the minutes of stretch exposure is given below each bar. (C) Localization of NFkB during 0–60 min of continuous cyclic strain of eGFP and DN Sun transduced NIH3T3 cells. Number of cells analyzed is given above the bars and the minutes of stretch exposure is given below each bar. Quantification of the nuclear localization of NFkB during 1 h of cyclic stretching revealed that in DN Sun transduced cells NFkB persisted longer in the nucleus than in the eGFP-transduced cells.

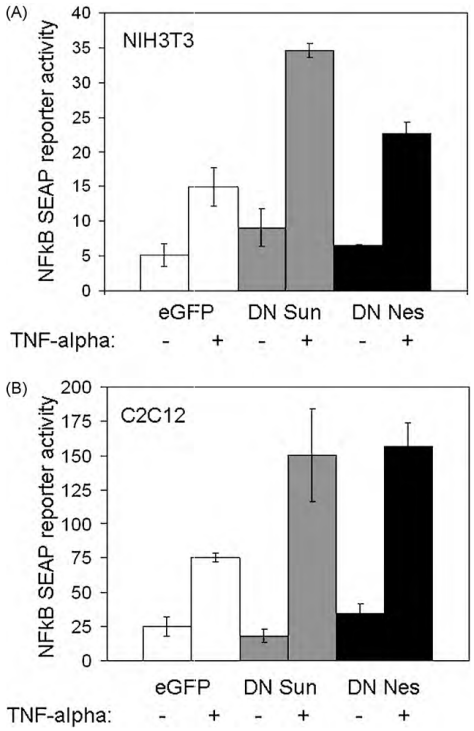

Fig. 6. Transcriptional activity of NFkB is increased in the absence of an intact LINC complex. NIH3T3 cells (A) or C2C12 cell (B) transduced with eGFP (white bars), DN Sun (grey bars) pr DN Nes (black bars) followed by transfection of a SEAP reporter construct under the control of NFkB binding sites were treated with TNF-alpha as indicated (±). TNF-alpha induced the NFkB-dependent promoter activity significantly more in the DN Sun or DN Nes transduced cells, than in the eGFP control cells. SEAP activity was normalized to a co-transfected luciferase control plasmid and the data are given as the mean and standard deviation of three experiments.

Therefore, we analyzed myogenic differentiation in the presence and absence of an intact LINC complex, and with and without mechanical stimulation. Differentiation of C2C12 cells transduced with eGFP alone was very efficient in differentiation medium (DM) where large multinucleated myotubes formed within 5 days, but not in growth medium where proliferating mononuclear cells persisted (Fig. 7A). As expected, activity of the muscle differentiation marker creatine kinase (CK) as well as the percentage of nuclei in multinucleated cells (the fusion index) was highly increased in cells cultured in DM compared to growth medium (Fig. 7C). C2C12 cells transduced with DN Nes and DN Sun fused equally well into multinucleated myotubes as the eGFP-transduced control cultures in DM, and CK was increased to the same extent (Fig. 7B and C). Thus, in the absence of mechanical stimulation, there was no noticeable difference in the myogenic differentiation of C2C12 cells.

We next investigated morphological as well as biochemical differentiation of these cultures after applying cyclic strain daily for 1 h over 5 days in DM. As expected (Kumar et al., 2004; Kook et al., 2008), this protocol of mechanical stimulation inhibited the fusion of eGFP-transduced C2C12 cells into myotubes, and the cells continued to proliferate (Fig. 8A; upper right panel). Interestingly, when we applied the same stretching regimen to C2C12 cells transduced with DN Nes or DN Sun, we found that these cultures differentiated into myotubes to the same extent as in the absence of mechanical stimulation (Fig. 8A; middle and lower right panel). It is known that p38 MAPK is a major regulator of myogenesis (Keren et al., 2006) and p38 MAPK and NFkB activity were shown to be required for myogenic differentiation of C2C12 cells (Baeza-Raja and Munoz-Canoves, 2004). Therefore, we investigated the phosphorylation levels of these signaling molecules in cell extracts of the cells cultured under the various conditions by immunoblotting and found that NFkB as well as p38 MAPK were activated in differentiating cultures, whereas Erk phosphorylation was the same under all conditions (Fig. 8B). Thus, NFkB signaling was elevated in cells that underwent daily stretch cycles only if the LINC complex was impaired and this accompanied differentiation. It seems that in the absence of an intact LINC complex, myogenic precursors are not able to translate cyclic stretch into growth stimulation and differentiation is favored.

3.5. *MyoD and myogenin transcript levels are elevated in stretched C2C12 cells with a disturbed LINC complex*

Myogenesis is known to be driven by transcription factors such as MyoD and myogenin (for reviews see Perry and Rudnick, 2000; Berkes and Tapscott, 2005). We therefore investigated the effect of cyclic strain on transcript levels of these factors as well as of the differentiation marker myosin heavy chain (MHC) in C2C12 cells, both in the presence and absence of an intact LINC. To study the immediate response of mRNA levels to cyclic strain, the transduced cells were cultured for 1 day in DM after which they were cyclically stretched for 1 h, and mRNA was subsequently isolated from these as well as from control cultures kept at rest. Quantitative PCR showed that in eGFP-transduced controls, stretching stimulated the mRNA levels of MyoD and myogenin more than 5-fold compared to cells at rest, and also MHC transcripts were elevated (Fig. 9A). Interestingly, the stretch-induced increase in these transcripts was significantly higher in the DN Nes and DN Sun than in the eGFP-transduced cultures (Fig. 9A). Thus, in C2C12 myoblasts, these myogenic factors are hyper-induced by mechanical stress in the absence of an intact LINC.

Next, we explored whether a functional LINC complex affected the steady state expression levels of MyoD, myogenin and MHC transcripts in C2C12 cultures in DM over several days with or without daily application of cyclic strain for 1 h. After the first day in DM and 16 h after the first bout of stretching, the steady state transcript levels of MyoD, myogenin and MHC were increased relative to cells kept in growth medium, but there was no significant difference between stretched or resting cultures. Independently of stretching, however, the levels of the muscle-specific transcripts were significantly higher in the DN Sun and DN Nes transduced cells than in the eGFP control cells (Fig. 9B). After 5 days in DM with daily application of cyclic strain, MyoD levels were reduced in all cultures to similarly low levels as found in undifferentiated cells in growth medium. However, at this late time point cyclic strain caused a large decrease in myogenin and MHC expression in eGFP-transduced cells in DM compared to the resting controls, in agreement with the observed suppression of myogenesis by mechanical stimulation. In contrast, in cells lacking a functional LINC complex no reduction was observed for myogenin in response to cyclic stretch, and also the MHC transcript level was much less diminished (Fig. 9B). These data indicate that in the absence of an intact LINC complex, a stretch-dependent hyper-induction of the expression of myogenic factors antagonizes the inhibition of differentiation normally caused by chronic mechanical stress.

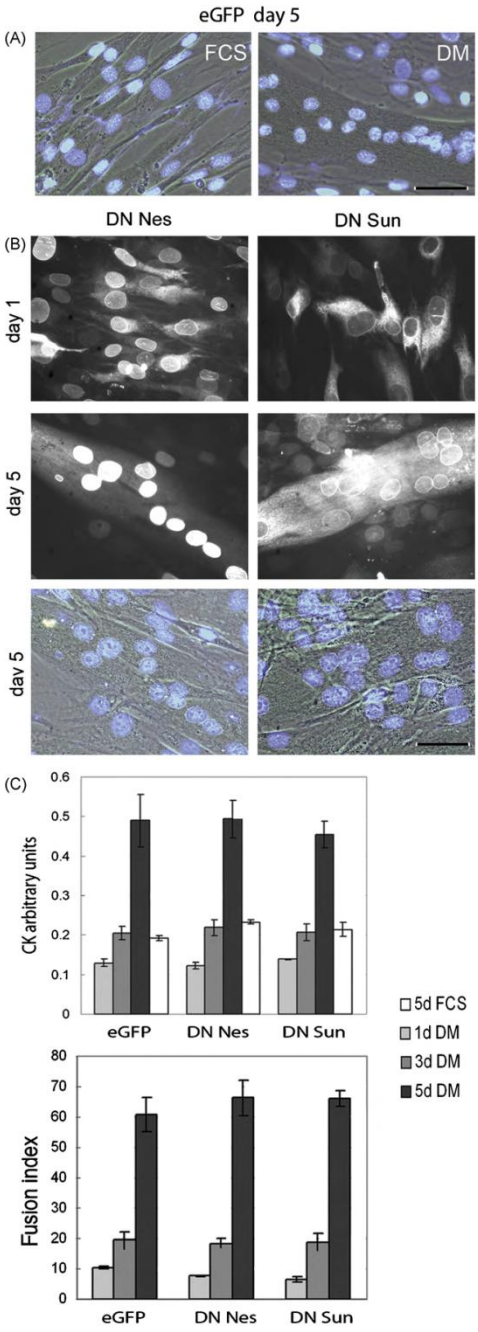

Fig. 7. Muscle differentiation of C2C12 cells in the presence of DN Nes and DN Sun. (A) C2C12 cells were transduced with the control eGFP virus and 1 day later the medium was exchanged against fresh growth medium (FCS) or differentiation medium containing horse serum (DM). Five days later pictures were taken. In DM the cells differentiated into large multinucleated myotubes and in growth medium the cells remained mononuclear. Nuclei are stained with Hoechst dye. Bar, 100 μm. (B) Transduction of the C2C12 cells with DN Nes and DN Sun revealed high transduction efficiency and the proteins accumulated in the nuclear membranes at day 1 in DM. The expression persists during the differentiation process and the proteins are present in the large multinucleated myotubes as can be seen by eGFP fluorescence in comparison to the phase contrast pictures with Hoechst dye stained nuclei. Bar, 100 μm. (C) Differentiation of C2C12 cells transduced with control eGFP, DN Nes or DN Sun proceeds equally well as determined by the increase in creatine kinase levels (upper panel) and by the fusion index determined by counting the percentage of nuclei in myotubes (lower panel). Mean values and standard deviation of three independent experiments are shown.

4. Discussion

We demonstrated in this work that cyclic equibiaxial stretch profoundly influences cell behavior on several levels, and that the LINC complex, which connects the actin cytoskeleton to the nucleus, is crucial for mechanotransduction. Firstly, nuclear rotation induced by stretching of NIH3T3 fibroblasts required an intact LINC complex. Secondly, stretch-induced inhibition of differentiation of C2C12 myoblasts required an intact LINC complex.

4.1. Mechanism of stretch-induced nuclear rotation

Using a device that allows us to view cells while being cyclically stretched, we discovered that this induces a surprising reaction in the cells: the nuclei rotate, some of them immediately and some of them after a lag period. We show that this is due to the connection of the actin cytoskeleton to the nucleus called the LINC complex. If a cell is seen as a tensegrity structure (Ingber, 2003a, b), it is to be expected that stretching of the substratum will generate forces that are propagated inside the cell, and that the cytoskeleton anchored nucleus will thus be re-oriented through cytoskeletal rearrangement. Such a model is supported by our experiments showing that a single stretch was sufficient to induce an immediate rotation of many of the nuclei. In addition, we found that nuclei did not rotate back to the original position after stretch relaxation, but instead continued to turn in one direction during repeated stretch cycles. This indicated that cyclic strain triggered an active process involving actin dynamics, a notion supported by the fact that the ROCK antagonist Y-27632 inhibited the process. Nevertheless, a direct mechanical link to the cytoskeleton is required to initiate stretch-induced re-orientation of the nucleus. This is supported by our experiments with cells that were transduced with dominant-negative nesprin or sun constructs, two crucial proteins of the LINC complex. In these cells, stretching of the substratum no longer induced nuclear rotation, presumably because the nuclear anchor to the actin cytoskeleton was lost.

4.2. Physiological implications of nuclear rotation

Nuclear rotation has been observed previously at the margin of scratch wounds in tissue culture. Before cells migrate and populate the wounded space their nuclei rotate (Levy and Holzbaur, 2008). Nuclear rotation over a culture period of several hours was also observed in cells lacking lamin B1 suggesting that lamin B1 stabilizes nuclear position (Ji et al., 2007). If nuclear orientation is linked to the direction of migration, it is conceivable that a mechanically induced nuclear rotation may have a physiological counterpart. For example, morphogenetic movements that cause tissue strains during development could induce nuclear rotations, thereby altering cell polarity and the direction of cell migration. It is clear from different transgenic mouse models that nuclear positioning and

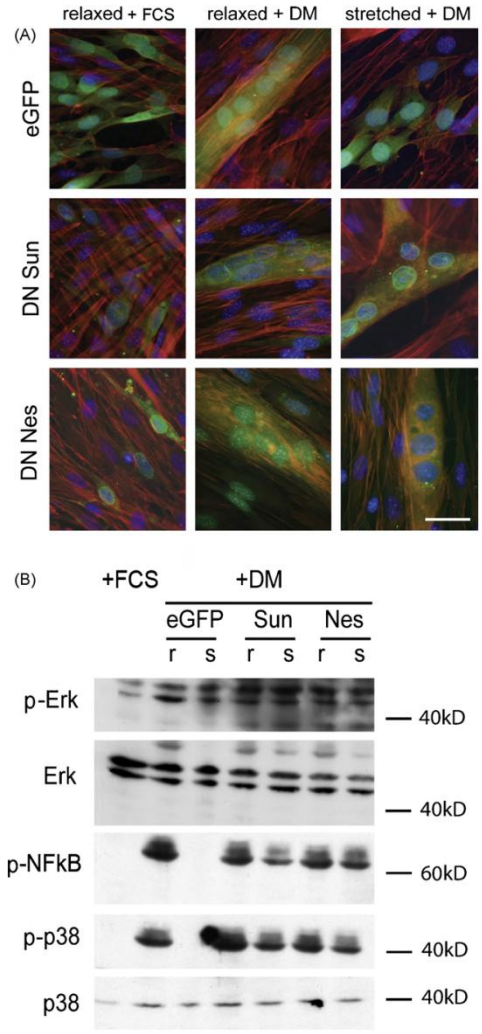

Fig. 8. In the presence of DN Nes and DN Sun differentiation of C2C12 cells is not inhibited by cyclic strain. (A) C2C12 cells were transduced with eGFP, DN Sun or DN Nes and cultured in growth medium (relaxed +FCS) or in differentiation medium (relaxed +DM) for 5 days. Parallel cultures in DM were stretched at 0.3 Hz, 10% elongation, 1 h per day over 5 days (stretched +DM). After 5 days the cultures were fixed and analyzed for eGFP fluorescence, F-actin with phalloidin and Hoechst nuclear staining. Differentiation of C2C12 myogenic progenitor cells into myotubes is inhibited in the stretched cells. However, in cells overexpressing DN Sun or DN Nes this block in differentiation is ineffective and multinucleated myotubes have formed. Bar, 100 μm. (B) Myogenic differentiation is accompanied by the activation of p38 MAPK and NFkB pathways but not by changes in Erk phosphorylation as shown by Western blot of C2C12 cells transduced with the indicated constructs and cultured for 5 days in DM with or without the daily stretching regimen. In the stretched cultures NFkB as well as p38 phosphorylation are increased in DN Sun and DN Nes transduced cells when compared to eGFP control cultures.

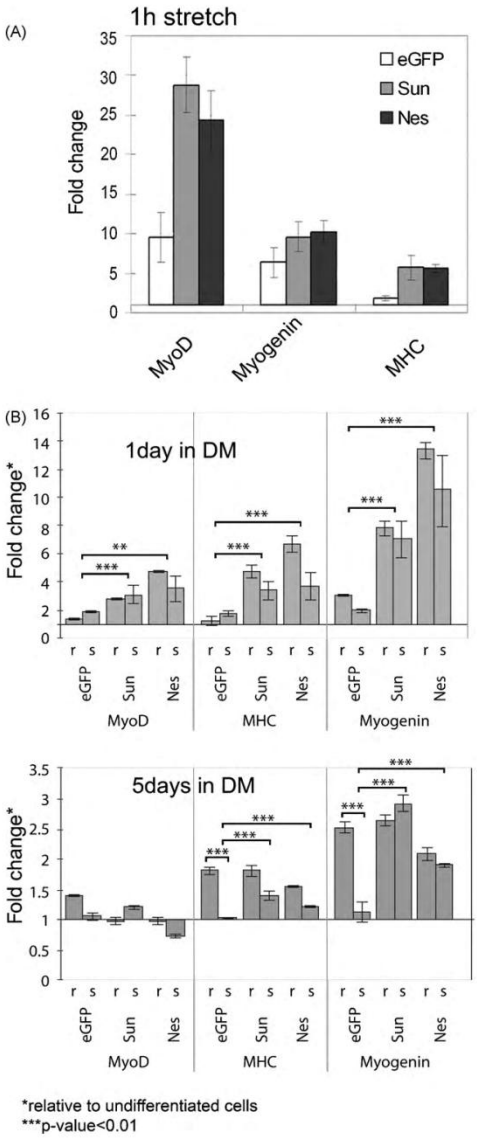

Figure 9. Elevated induction of myogenic factors in C2C12 cells deficient in the LINC complex. (A) C2C12 cells plated overnight in differentiation medium were cyclically stretched for 1 h before mRNA was isolated for qPCR. Stretching resulted in the induction of the transcript levels of MyoD and myogenin when compared to parallel cultures kept at rest. Interestingly, this induction was higher in cells transduced with DN Sun (Sun) or DN Nes (Nes) where also the levels of MHC transcripts were higher than in eGFP-transduced control cells. Fold change compared to parallel cultures at rest is shown. Average values and standard deviation of three experiments are shown. (B) Quantitative real-time PCR to detect steady state levels of MyoD, MHC and myogenin (normalized to GAPDH) in mRNA isolated from cells after 1 day in DM and 16 h after the first stretch regimen (s; upper panel) and 5 days in DM and 16 h after the fifth daily stretch regimen (s; lower panel) and in parallel cultures kept at rest (r): The results are presented as fold change relative to undifferentiated cells. Average values and standard

anchorage is disturbed in mice with deletions in the sun and nesprin genes (Zhang et al., 2007b; Lei et al., 2009; Zhang et al., 2010) and in a recent study with double knock-out mice for Sun1 and 2 as well as Nesprin-1 and -2 it was found that neurogenesis and neuronal migration was disturbed presumably due to problems in nuclear movement (Zhang et al., 2009).

4.3. Mechanical control of gene transcription?

Because of the direct connection of the ECM to the actin cytoskeleton through integrin receptors and then by the LINC complex to the nuclear lamina, we considered that mechanical stimulation of cells could trigger nuclear deformations that ultimately result in changes in chromatin accessibility for enzymes and transcription factors. This might then directly modulate gene expression by inducing conformational changes in chromatin (Bustamante et al., 2003; Ingber, 2003a, b). In an interesting study addressing this question, Maniotis et al. analyzed sequestration of AluI-sensitive sites in the chromatin of cells cultured under different conditions. Sequestration and exposure of these sites was found to be sensitive to biomechanical forces that regulate cellular and tissue architecture (Maniotis et al., 2005). Thus, a connection between components of the LINC complex and changes in chromatin structure in response to mechanical cues could dynamically alter gene expression in response to exogenous force. We found that an impaired LINC complex in muscle cells led to elevated stretch-induced transcript levels of myogenic transcription factors. This could be explained by LINC complex-dependent mechanical control of proteins involved in gene repression rather than gene activation.

Since we have found that nuclear NFkB accumulation is prolonged in DN Sun transduced cells this could represent a further mechanism for the induction of transcription in the absence of an intact LINC. Normally, NFkB is removed from the nucleus by IkBα-mediated CRM1-dependent nuclear export (Huang et al., 2000). From Drosophila genetics it is known that the nuclear pore proteins Nup214–Nup88 sequester CRM1 at the nuclear rim thereby modulating the export of NFkB and the degree of activation of NFkB downstream target genes (Xylourgidis et al., 2006). We thus postulate that an intact LINC is necessary for efficient nuclear export of NfKB. Since Sun1 was reported to be associated with nuclear pores (Lu et al., 2008) it is conceivable that LINC proteins could have an influence on CRM1 localization and a role of the LINC in nuclear export regulation is certainly an interesting function to be explored in the future.

4.4. Implications for muscle physiology and myopathies

It is known that nuclear lamins, the LINC complex, the actin cytoskeleton and cell adhesion molecules act closely together to maintain cell shape and keep adherent cells in a mechanically pre-stressed state. This is required for cells to be able to sense and adapt to external mechanical strain (for reviews see Chiquet et al., 2009; Geiger et al., 2009; Wang et al., 2009). Interestingly, mutations in any of the genes encoding proteins building the ECM-nuclear lamina connection, ranging from ECM proteins themselves to their receptors, the cytoskeleton, or the bridge through the nuclear membranes to the nuclear lamin proteins, all lead to different forms of muscular dystrophies (Wallace and McNally, 2008; Jaalouk and Lammerding, 2009). Laminopathies develop due to mutations in lamin A/C or emerin and include EDMD and Hutchinson–Gilford progeria syndrome (for reviews see (Burke and Stewart, 2002; Gruenbaum et al., 2005). Nuclear fragility and defective mechanotransduction has been described in laminopathies caused by mutations in lamin A/C (Lammerding et al., 2004). In addition, Nesprin-1 and -2 mutations have been identified in EDMD patients (Zhang et al., 2007a). Also in mice disruption of Nesprin-1 produces an EDMD-like phenotype (Puckelwartz et al., 2009). Thus, an intact LINC complex is crucial for muscle physiology. Therefore, we analyzed whether disruption of the LINC complex affects mechanotransduction and differentiation of the myogenic cell line C2C12. This model has been used in several studies and it has been shown that mechanical stimulation of C2C12 cells stimulates proliferation and inhibits differentiation (Kumar and Boriek, 2003; Grossi et al., 2007; Kook et al., 2008).

The major factors regulating myogenesis are the myogenic transcription factors such as MyoD and myogenin (for reviews see Perry and Rudnick, 2000; Berkes and Tapscott, 2005) and there have been recent reports that mechanical stimulation of C2C12 cells can induce these factors (Chandran et al., 2007; Abe et al., 2009). Thus, we considered that the regulation of MyoD or myogenin could be influenced by interfering with the LINC complex. Indeed, we could confirm that MyoD and myogenin mRNAs are rapidly induced in C2C12 cells by acute cyclic stretch. This increase was much higher in C2C12 cells transduced with DN Nes or DN Sun. After 5 days including daily stretch cycles of 1 h each, the difference between stretched and relaxed cultures became striking. Steady state levels of MHC and myogenin were greatly reduced in the stretched compared to relaxed cultures of eGFP-transduced control cells, whereas in the DN Nes and DN Sun transduced cultures this was not the case. These data indicate that in cells with a LINC defect, a stretch-dependent increase in the expression of myogenic factors might override the stimulation of proliferation normally caused by chronic mechanical stress. Now that the first EDMD patients with heterozygous missense mutations in nesprins are identified (Zhang et al., 2007a) it will be interesting to analyze whether expression of such mutant proteins have similar effects as the expression of the dominant-negative protein variants used in this study. This is not unlikely since fibroblasts from these patients have been reported to exhibit nuclear morphology defects and specific patterns of emerin and Sun2 mislocalization (Zhang et al., 2007a).

deviation of three experiments are shown. MyoD, MHC and myogenin transcript levels are already significantly increased in the presence of DN Sun and DN Nes when compared to the eGFP-transduced control cultures after the first day in DM. This was the case for both the stretched and the relaxed cultures (thus the brackets and *p*-values refer to both conditions). Four days later (5 days in DM) the difference between stretched and relaxed cultures became obvious. While in eGFP control cells all of the muscle markers are greatly reduced in the stretched cultures, in DN Sun (Sun) and DN Nes (Nes) transduced cells myogenin is almost the same as in relaxed cells and also MHC is significantly higher in the samples of the stretched cells than of the eGFP control cells. In all of the samples MyoD levels were reduced again and cluster around the levels of undifferentiated cells.

Acknowledgements

This work was supported by the Novartis Research Foundation, the SNF grant 3100A0-120235 to R.C.E. and the SNF grant 3100A0-107515 to M.C. We thank Enrico Martina for the help with statistics and Florence Brellier, Maria Asparuhova and Richard P. Tucker for critical reading of the manuscript. The authors declare that they have no conflict of interest.

Appendix A. Supplementary data

Supplementary data associated with this article can be found, in the online version, at doi:10.1016/j.biocel.2010.07.001.

References

Abe S, Rhee S, Iwanuma O, Hiroki E, Yanagisawa N, Sakiyama K, et al. Effect of mechanical stretching on expressions of muscle specific transcription fac-

tors MyoD, Myf-5, myogenin and MRF4 in proliferated myoblasts. Anat Histol Embryol 2009;38:305–10.
Amma H, Naruse K, Ishiguro N, Sokabe M. Involvement of reactive oxygen species in cyclic stretch-induced NF-kappaB activation in human fibroblast cells. Br J Pharmacol 2005;145:364–73.
Attali R, Warwar N, Israel A, Gurt I, McNally E, Puckelwartz M, et al. Mutation of SYNE-1, encoding an essential component of the nuclear lamina, is responsible for autosomal recessive arthrogryposis. Hum Mol Genet 2009;18:3462–9.
Avvisato CL, Yang X, Shah S, Hoxter B, Li W, Gaynor R, et al. Mechanical force modulates global gene expression and beta-catenin signaling in colon cancer cells. J Cell Sci 2007;120:2672–82.
Baeza-Raja B, Munoz-Canoves P. p38 MAPK-induced nuclear factor-kappaB activity is required for skeletal muscle differentiation: role of interleukin-6. Mol Biol Cell 2004;15:2013–26.
Berkes CA, Tapscott SJ. MyoD and the transcriptional control of myogenesis. Semin Cell Dev Biol 2005;16:585–95.
Bissell MJ, Hall HG, Parry G. How does the extracellular matrix direct gene expression? J Theor Biol 1982;99:31–68.
Burke B, Stewart CL. Life at the edge: the nuclear envelope and human disease. Nat Rev Mol Cell Biol 2002;3:575–85.
Bustamante C, Bryant Z, Smith SB. Ten years of tension: single-molecule DNA mechanics. Nature 2003;421:423–7.
Butcher DT, Alliston T, Weaver VM. A tense situation: forcing tumour progression. Nat Rev Cancer 2009;9:108–22.
Chandran R, Knobloch TJ, Anghelina M, Agarwal S. Biomechanical signals upregulate myogenic gene induction in the presence or absence of inflammation. Am J Physiol Cell Physiol 2007;293:C267–276.
Chen NX, Geist DJ, Genetos DC, Pavalko FM, Duncan RL. Fluid shear-induced NFkappaB translocation in osteoblasts is mediated by intracellular calcium release. Bone 2003;33:399–410.
Chiquet M, Gelman L, Lutz R, Maier S. From mechanotransduction to extracellular matrix gene expression in fibroblasts. Biochim Biophys Acta 2009;1793:911–20.
Chiquet M, Sarasa-Renedo A, Tunc-Civelek V. Induction of tenascin-C by cyclic tensile strain versus growth factors: distinct contributions by Rho/ROCK and MAPK signaling pathways. Biochim Biophys Acta 2004;1693:193–204.
Crisp M, Liu Q, Roux K, Rattner JB, Shanahan C, Burke B, et al. Coupling of the nucleus and cytoplasm: role of the LINC complex. J Cell Biol 2006;172:41–53.
Davis ME, Grumbach IM, Fukai T, Cutchins A, Harrison DG. Shear stress regulates endothelial nitric-oxide synthase promoter activity through nuclear factor kappaB binding. J Biol Chem 2004;279:163–8.
Geiger B, Spatz JP, Bershadsky AD. Environmental sensing through focal adhesions. Nat Rev Mol Cell Biol 2009;10:21–33.
Gerashchenko MV, Chernoivanenko IS, Moldaver MV, Minin AA. Dynein is a motor for nuclear rotation while vimentin IFs is a "brake". Cell Biol Int 2009;33:1057–64.
Grossi A, Yadav K, Lawson MA. Mechanical stimulation increases proliferation, differentiation and protein expression in culture: stimulation effects are substrate dependent. J Biomech 2007;40:3354–62.
Gruenbaum Y, Margalit A, Goldman RD, Shumaker DK, Wilson KL. The nuclear lamina comes of age. Nat Rev Mol Cell Biol 2005;6:21–31.
Haque F, Lloyd DJ, Smallwood DT, Dent CL, Shanahan CM, Fry AM, et al. SUN1 interacts with nuclear lamin A and cytoplasmic nesprins to provide a physical connection between the nuclear lamina and the cytoskeleton. Mol Cell Biol 2006;26:3738–51.
Huang TT, Kudo N, Yoshida M, Miyamoto S. A nuclear export signal in the N-terminal regulatory domain of IkappaBalpha controls cytoplasmic localization of inactive NF-kappaB/IkappaBalpha complexes. Proc Natl Acad Sci USA 2000;97:1014–9.
Ingber DE. Tensegrity I. Cell structure and hierarchical systems biology. J Cell Sci 2003a;116:1157–73.
Ingber DE. Tensegrity II. How structural networks influence cellular information processing networks. J Cell Sci 2003b;116:1397–408.
Ingber DE. Cellular mechanotransduction: putting all the pieces together again. FASEB J 2006a;20:811–27.
Ingber DE. Mechanical control of tissue morphogenesis during embryological development. Int J Dev Biol 2006b;50:255–66.
Inoh H, Ishiguro N, Sawazaki S, Amma H, Miyazu M, Iwata H, et al. Uni-axial cyclic stretch induces the activation of transcription factor nuclear factor kappaB in human fibroblast cells. FASEB J 2002;16:405–7.
Jaalouk DE, Lammerding J. Mechanotransduction gone awry. Nat Rev Mol Cell Biol 2009;10:63–73.
Ji JY, Lee RT, Vergnes L, Fong LG, Stewart CL, Reue K, et al. Cell nuclei spin in the absence of lamin b1. J Biol Chem 2007;282:20015–26.
Jones JC, Lane K, Hopkinson SB, Lecuona E, Geiger RC, Dean DA, et al. Laminin-6 assembles into multimolecular fibrillar complexes with perlecan and participates in mechanical-signal transduction via a dystroglycan-dependent, integrin-independent mechanism. J Cell Sci 2005;118:2557–66.
Keren A, Tamir Y, Bengal E. The p38 MAPK signaling pathway: a major regulator of skeletal muscle development. Mol Cell Endocrinol 2006;252:224–30.
Kook SH, Lee HJ, Chung WT, Hwang IH, Lee SA, Kim BS, et al. Cyclic mechanical stretch stimulates the proliferation of C2C12 myoblasts and inhibits their differentiation via prolonged activation of p38 MAPK. Mol Cells 2008;25:479–86.
Kumar A, Boriek AM. Mechanical stress activates the nuclear factor-kappaB pathway in skeletal muscle fibers: a possible role in Duchenne muscular dystrophy. FASEB J 2003;17:386–96.
Kumar A, Murphy R, Robinson P, Wei L, Boriek AM. Cyclic mechanical strain inhibits skeletal myogenesis through activation of focal adhesion kinase. Rac-1 GTPase, and NF-kappaB transcription factor. FASEB J 2004;18:1524–35.
Kung C. A possible unifying principle for mechanosensation. Nature 2005;436:647–54.
Lammerding J, Schulze PC, Takahashi T, Kozlov S, Sullivan T, Kamm RD, et al. Lamin A/C deficiency causes defective nuclear mechanics and mechanotransduction. J Clin Invest 2004;113:370–8.
Lei K, Zhang X, Ding X, Guo X, Chen M, Zhu B, et al. SUN1 and SUN2 play critical but partially redundant roles in anchoring nuclei in skeletal muscle cells in mice. Proc Natl Acad Sci USA 2009;106:10207–12.
Levy JR, Holzbaur EL. Dynein drives nuclear rotation during forward progression of motile fibroblasts. J Cell Sci 2008;121:3187–95.
Lu W, Gotzmann J, Sironi L, Jaeger VM, Schneider M, Luke Y, et al. Sun1 forms immobile macromolecular assemblies at the nuclear envelope. Biochim Biophys Acta 2008;1783:2415–26.
Maier S, Lutz R, Gelman L, Sarasa-Renedo A, Schenk S, Grashoff C, et al. Tenascin-C induction by cyclic strain requires integrin-linked kinase. Biochim Biophys Acta 2008;1783:1150–62.
Maniotis AJ, Chen CS, Ingber DE. Demonstration of mechanical connections between integrins, cytoskeletal filaments, and nucleoplasm that stabilize nuclear structure. Proc Natl Acad Sci USA 1997;94:849–54.
Maniotis AJ, Valyi-Nagy K, Karavitis J, Moses J, Boddipali V, Wang Y, et al. Chromatin organization measured by AluI restriction enzyme changes with malignancy and is regulated by the extracellular matrix and the cytoskeleton. Am J Pathol 2005;166:1187–203.
Orr AW, Sanders JM, Bevard M, Coleman E, Sarembock IJ, Schwartz MA. The subendothelial extracellular matrix modulates NF-kappaB activation by flow: a potential role in atherosclerosis. J Cell Biol 2005;169:191–202.
Padmakumar VC, Abraham S, Braune S, Noegel AA, Tunggal B, Karakesisoglou I, et al. Enaptin, a giant actin-binding protein, is an element of the nuclear membrane and the actin cytoskeleton. Exp Cell Res 2004;295:330–9.
Padmakumar VC, Libotte T, Lu W, Zaim H, Abraham S, Noegel AA, et al. The inner nuclear membrane protein Sun1 mediates the anchorage of Nesprin-2 to the nuclear envelope. J Cell Sci 2005;118:3419–30.
Patwari P, Lee RT. Mechanical control of tissue morphogenesis. Circ Res 2008;103:234–43.
Perry RL, Rudnick MA. Molecular mechanisms regulating myogenic determination and differentiation. Front Biosci 2000;5:D750–767.
Pfaffl MW. A new mathematical model for relative quantification in real-time RT-PCR. Nucleic Acids Res 2001;29:e45.
Puckelwartz MJ, Kessler E, Zhang Y, Hodzic D, Randles KN, Morris G, et al. Disruption of nesprin-1 produces an Emery–Dreifuss muscular dystrophy-like phenotype in mice. Hum Mol Genet 2009;18:607–20.
Starr DA, Han M. Role of ANC-1 in tethering nuclei to the actin cytoskeleton. Science 2002;298:406–9.
Stewart-Hutchinson PJ, Hale CM, Wirtz D, Hodzic D. Structural requirements for the assembly of LINC complexes and their function in cellular mechanical stiffness. Exp Cell Res 2008;314:1892–905.
Wallace GQ, McNally EM. Mechanisms of muscle degeneration. Regeneration, and repair in the muscular dystrophies. Annu Rev Physiol 2008.
Wang N, Tytell JD, Ingber DE. Mechanotransduction at a distance: mechanically coupling the extracellular matrix with the nucleus. Nat Rev Mol Cell Biol 2009;10:75–82.
Wilhelmsen K, Ketema M, Truong H, Sonnenberg A. KASH-domain proteins in nuclear migration, anchorage and other processes. J Cell Sci 2006;119:5021–9.
Wilhelmsen K, Litjens SH, Kuikman I, Tshimbalanga N, Janssen H, van den Bout I, et al. Nesprin-3, a novel outer nuclear membrane protein, associates with the cytoskeletal linker protein plectin. J Cell Biol 2005;171:799–810.
Wozniak MA, Chen CS. Mechanotransduction in development: a growing role for contractility. Nat Rev Mol Cell Biol 2009;10:34–43.
Xylourgidis N, Roth P, Sabri N, Tsarouhas V, Samakovlis C. The nucleoporin Nup214 sequesters CRM1 at the nuclear rim and modulates NFkappaB activation in Drosophila. J Cell Sci 2006;119:4409–19.
Zhang J, Felder A, Liu Y, Guo LT, Lange S, Dalton ND, et al. Nesprin 1 is critical for nuclear positioning and anchorage. Hum Mol Genet 2010;19:329–41.
Zhang Q, Bethmann C, Worth NF, Davies JD, Wasner C, Feuer A, et al. Nesprin-1 and -2 are involved in the pathogenesis of Emery–Dreifuss muscular dystrophy and are critical for nuclear envelope integrity. Hum Mol Genet 2007a;16:2816–33.
Zhang Q, Ragnauth C, Greener MJ, Shanahan CM, Roberts RG. The nesprins are giant actin-binding proteins, orthologous to Drosophila melanogaster muscle protein MSP-300. Genomics 2002;80:473–81.
Zhang X, Lei K, Yuan X, Wu X, Zhuang Y, Xu T, et al. SUN1/2 and Syne/Nesprin-1/2 complexes connect centrosome to the nucleus during neurogenesis and neuronal migration in mice. Neuron 2009;64:173–87.
Zhang X, Xu R, Zhu B, Yang X, Ding X, Duan S, et al. Syne-1 and Syne-2 play crucial roles in myonuclear anchorage and motor neuron innervation. Development 2007b;134:901–8.
Zhen YY, Libotte T, Munck M, Noegel AA, Korenbaum E. NUANCE, a giant protein connecting the nucleus and actin cytoskeleton. J Cell Sci 2002;115:3207–22.

III.2 UNPUBLISHED DATA

III.2.1 Investigation of the early response to biaxial cyclic strain

To investigate global cellular responses to biaxial cyclic strain we decided to do transcript profiling by a microarray analysis of stretched primary mouse embryo fibroblasts. Cells were plated on fibronectin-coated silicon membranes and then cyclically (10% elongation, 0.3Hz) stretched for 1 and 6 hours. The gene expression profiles of stretched cells were compared to unstretched cells. After 1 hour of cyclic strain a very distinct group of less than 30 genes was upregulated, none downregulated. However, after 6 hours these genes were back to base level and a large group of other genes was up- or downregulated (see appendix table 5). The group of early response genes includes many transcription factors and immediate early response genes. After 6 hours many different genes are affected, among them also extracellular matrix protein encoding transcripts, for example, tenascin-C. The data obtained from microarray analysis (figure 10 A) was confirmed for a subset of genes by quantitative real-time PCR (figure 10 B).

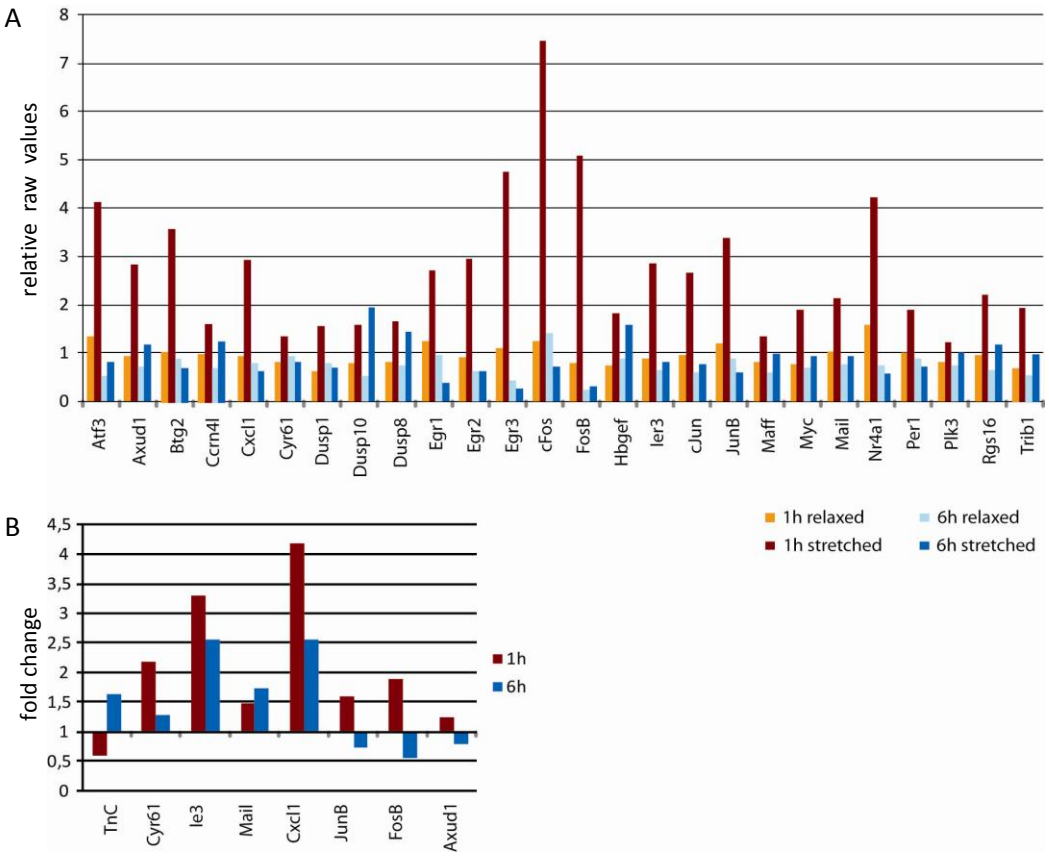

Figure 10 | **Induction of genes in response to 1 and 6 hours of cyclic biaxial strain**. The early stress response leads to an upregulation of about 25 genes **(A)**. This response is transient and diminished after 6 hours. Data from microarray analysis was verified by quantitative realtime PCR **(B)**.

Among the genes upregulated after one hour of biaxial cyclic strain is FosB. Together with JunB, Egr1, Egr2, Egr3 and cFos, which were also shown by gene expression profiling to be upregulated by 1h of biaxial strain, it belongs to the immediate early response genes. FosB exists in 2 isoforms that are a result from alternative splicing (Figure 11B). Delta FosB is the N-terminally truncated version of FosB that results from alternative splicing within the last exon and which is therefore missing the transactivation domain. Only the long FosB form efficiently induces transformation in mouse and rat fibroblast cell lines and trans-represses the cFos promoter. Both of these functions are suppressed by coexpressed ΔFosB. Upon serum stimulation, maximal expression of the oncogenic FosB precedes the expression of the antagonistic ΔFosB [151]. It has been shown, that mechanical stress to bone leads to an upregulation of both splice variants. The increased expression was dependent on Ca^{2+} influx und subsequent activation of Erk1/2 [152]. The question we wanted to address here is whether the 2 isoforms show differences in the stress response.

Therefore, we stretched NIH 3T3 cells for 1h either in the presence or the absence of serum. Then we isolated RNA and used it for reverse transcription and semi-quantitative PCR. We decided to include cFos and JunB in our experiment as well as they have also been shown to respond to 1h of cyclic strain (see figure 10). All of these genes include a serum response element (SRE) in their promoter region, which is necessary for the activation by Erk signaling.

The detection of cFos was very weak whereas the other genes show a significant induction after 30 and 60 minutes of biaxial strain (figure 11A). The induction was also seen in the presence of serum. Both FosB splice variants respond to stretching, although the timing is slightly different.

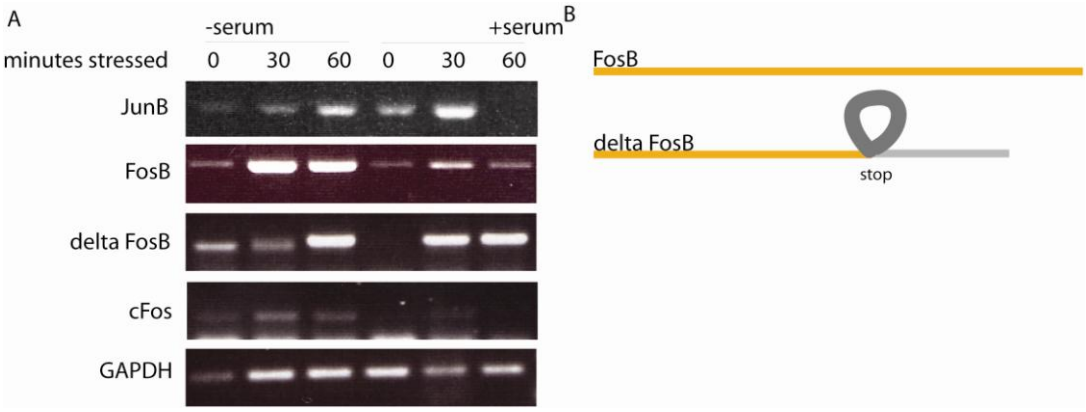

Figure 11 | **Influence of mechanical stress on JunB, FosB, ΔFosB and cFos.** Induction of the genes in response to cyclic strain was observed in the presence and absence of serum **(A)**. cFos was barely detectable whereas the other transcripts are upregulated after 30 to 60 minutes of mechanical stress. ΔFosB results from alternative splicing of FosB within the last exon **(B)**.

To get some more information about the genes responding to 1 and 6 hours of biaxial cyclic strain we did some pathway profiling using Ingenuity Pathways software (Ingenuity® Systems). As input files we took our gene lists generated with Expressionist (Genedata) from our Affymetrix data. The pathway profiling implied that Erk and NfκB pathways are the major pathways involved in activating the 1 hour specific stretch response genes (figure 12) and even after 6 hours of strain the NfκB pathways was one of the major pathways involved in activating the later response genes (figure 13).

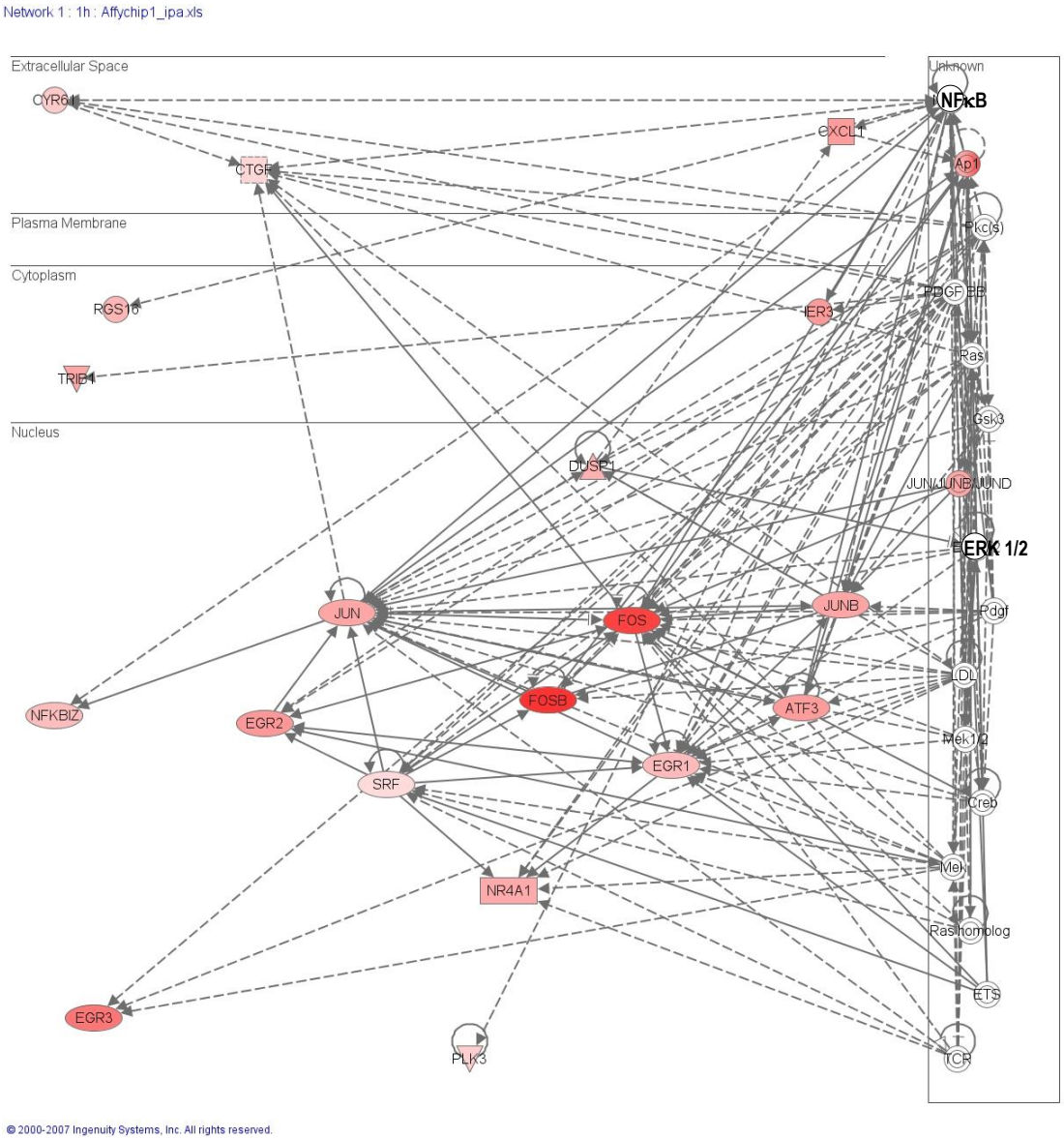

Figure 12 | **Visual display of the relationship of all genes upregulated upon 1 hour of stretching.** Ingenuity Pathways Analysis networks are displayed graphically as nodes (genes/gene products) and edges (the biological relationships between the nodes). The node color represents the fold change (red = upregulation). The higher the fold increase, the more intense the color of red. Solid lines denote direct interactions, while dotted lines represent indirect interactions between the genes. Pathway profiling indicates a central role of NfκB and Erk signaling in the early stress response.

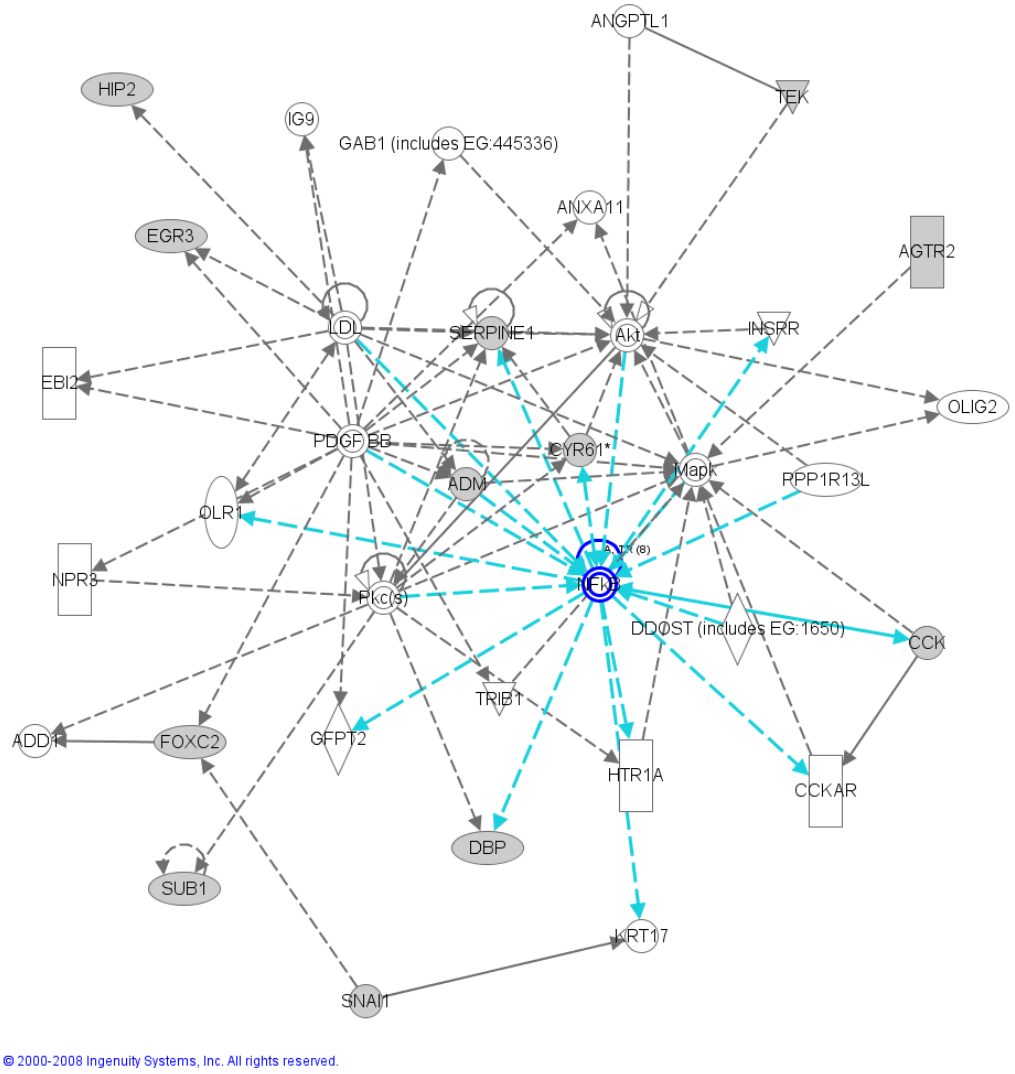

Figure 13 | **Visual display of the relationship of some genes up- or downregulated after 6 hour of stretching.** The length of an edge reflects the evidence supporting that node-to-node relationship, in that edges supported by more articles from the literature are shorter. The blue arrows indicate interaction with NfκB signaling. Even after 6 hours of stress the NfκB pathway is still one of the major pathways involved in activation of the stress response.

As previously shown cyclic strain activates Rho/ROCK signaling and its activation is crucial for the induction of TN-C [30]. Western blot analysis showed that both the Erk and the NfκB pathways are activated by biaxial cyclic strain aswell. This response is already evident within the first 5 to 10 minutes of stretching (figure 14A) and can be inhibited by specific inhibitors (data not shown). As shown by quantitative real-time PCR (figure 14B) inhibition of Erk (PD98059) and Rho/ROCK (Y27632)

signaling did not diminish the induction of those genes previously shown to be induced by stretching except for Nr4a1 and Bcar1. In most cases induction was higher in the presence of PD. However, inhibition of the NfκB pathway by Sulafsalazine blocked the stress response completely. This was confirmed by blocking NfκB signaling with Bay-11-7082 (data not shown).

In the previous chapter we described that stretching leads to nuclear rotation. Neither inhibition of neither Erk nor NfκB signaling had an effect on nuclear rotation indicating that nuclear rotation is independent of the activation of these signaling pathways (figure 14C).

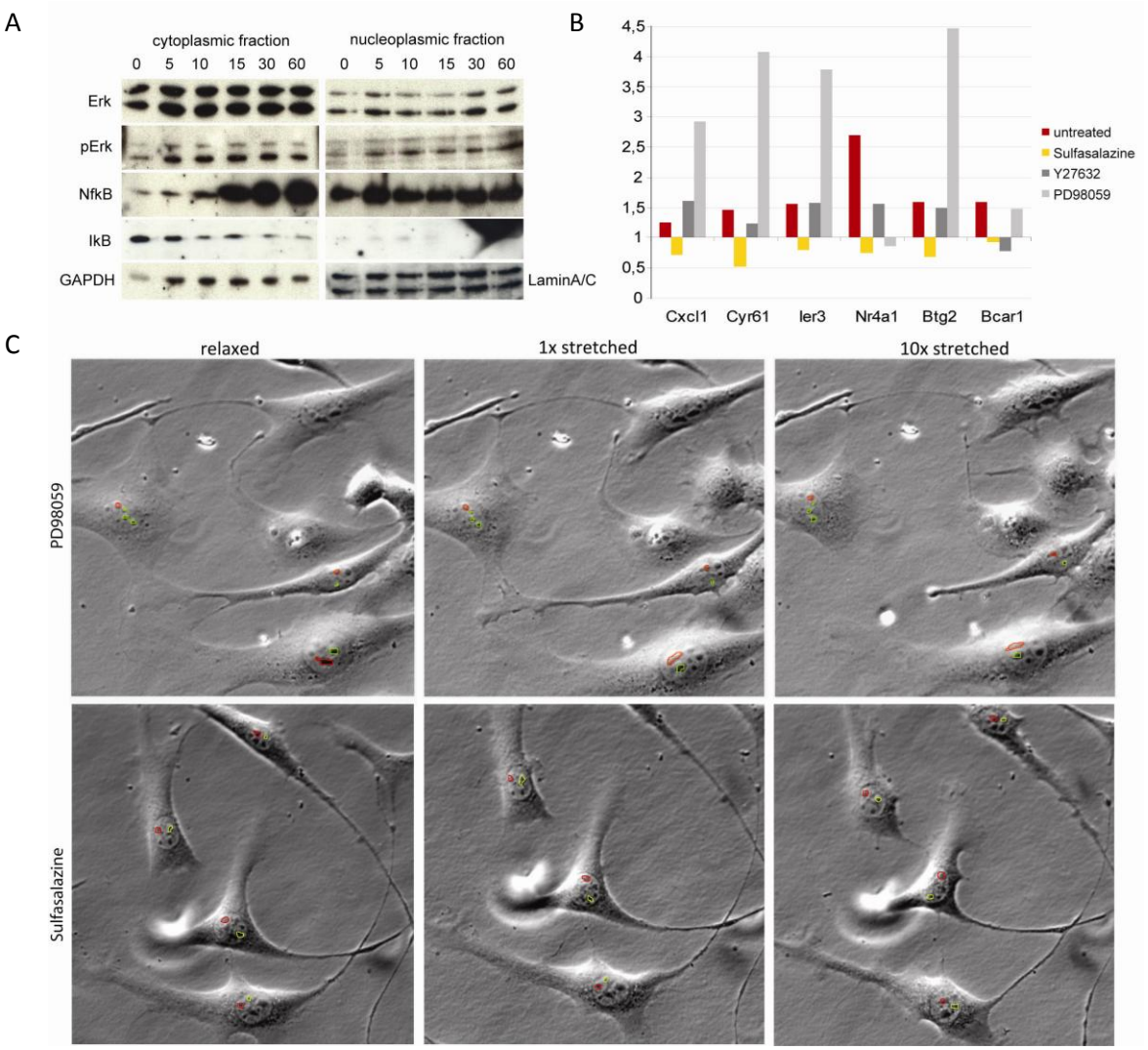

Figure 14 | **Activation of signaling pathways upon stretching.** Although Erk and NfkB pathways both get activated by stretching as shown by western blot **(A)** only NfkB seems responsible for the induction of the early stress response genes **(B)**. QPCR revelaed, that inhibition of NfkB signaling diminishes the early stress response while inhibition of Erk signaling seemed to render cells more responsive to stretching. Inhibition of the Rho/ROCK pathway only inhibited some genes. Inhibition of the Erk and NfκB pathway did not influence nuclear rotation **(C)**.

As shown in the previous chapter and figure 15 NfκB translocates immediately to the nucleus of serum starved NIH 3T3 upon stretching. Already after 15 to 30 minutes it shuttles back to the cytoplasm. However, when Erk signaling is inhibited by PD98059, NfκB remains longer inside the nucleus. The same can be observed in cells lacking functional Sun1 (c.f. previous chapter). Inhibition of Erk signaling and disruption of the LINC complex showed an increased response of genes to cyclic strain (figure 14B and submitted manuscript). This might be due to prolonged presence of NfκB inside the nucleus (figure 15).

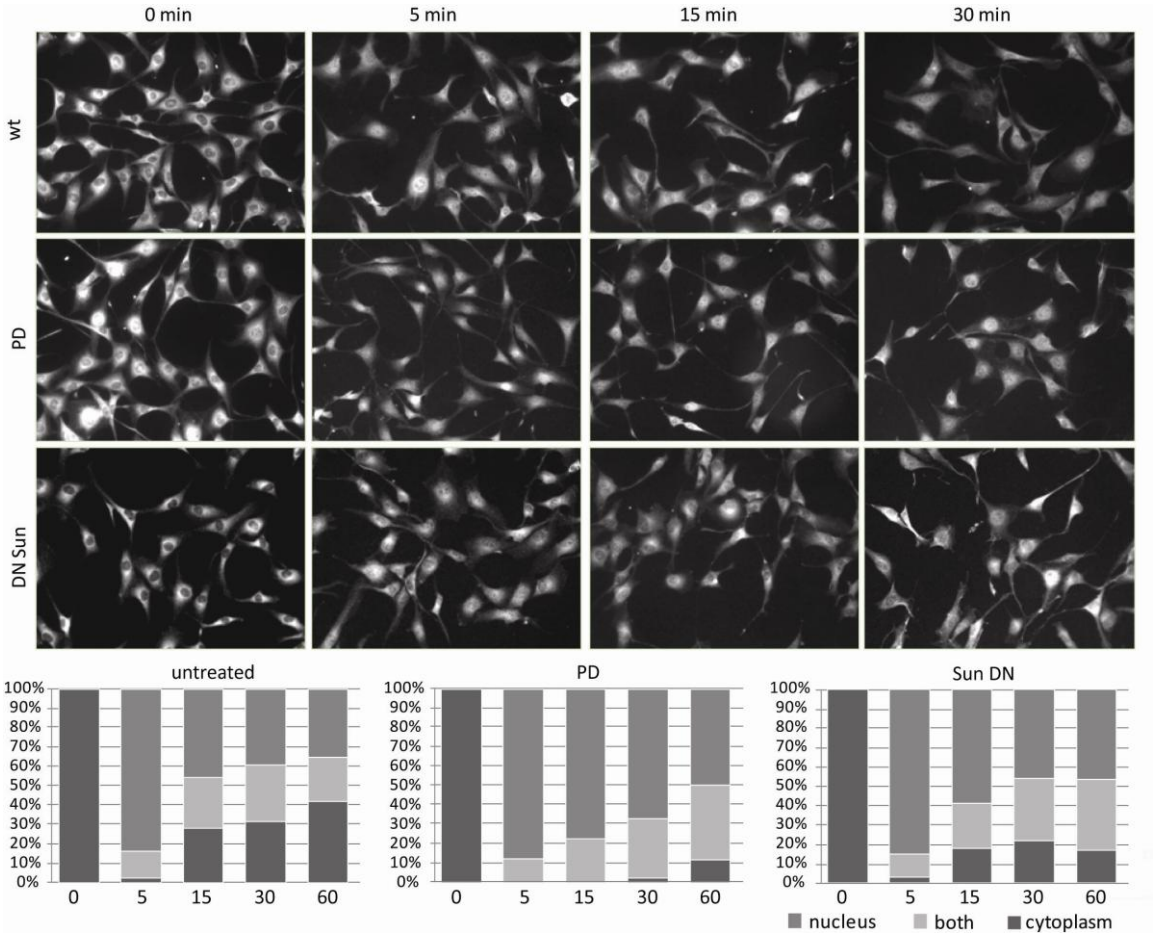

Figure 15 | **Rapid and transient translocation of NfkB into the nucleus upon stretching.** NIH 3T3 were stretched for the time indicated, fixed, permeablized and stained with NfκB antibody. Location of NfkB was investigated using a Zeiss Z1 microscope and quantified by counting the number of cells where NfκB is located in the nucleus, in the cytoplasm or in both. NfκB remains longer in the nucleus upon inhibition of Erk signaling by PD98059. The same has been observed in the absence of functional Sun1.

Nuclear translocation of NFkB was completely abolished by inhibiting NFkB signalling with sulfasalazine (not shown) or by depleting Ca^{2+} from the culture medium (figure 16a, right panels), suggesting an involvement of stretch-activated ion channels in the activation of NFkB. Indeed, we observed a rapid increase in intracellular Ca^{2+} upon stretching as determined by loading the cells with

a Ca^{2+} -indicator (figure 16b). We then tested whether inhibition of NFkB or depletion of calcium also inhibited the stretch-induced transcriptional response. We confirmed by qPCR for a selection of the stretch-induced transcripts that the induction determined by RNA profiling was reproducibly seen in independent experiments and found that for all transcripts tested, omission of Ca^{2+} or inclusion of the NFkB inhibitor sulfasalazine completely blocked their induction by cyclic stretch (figure 16c).

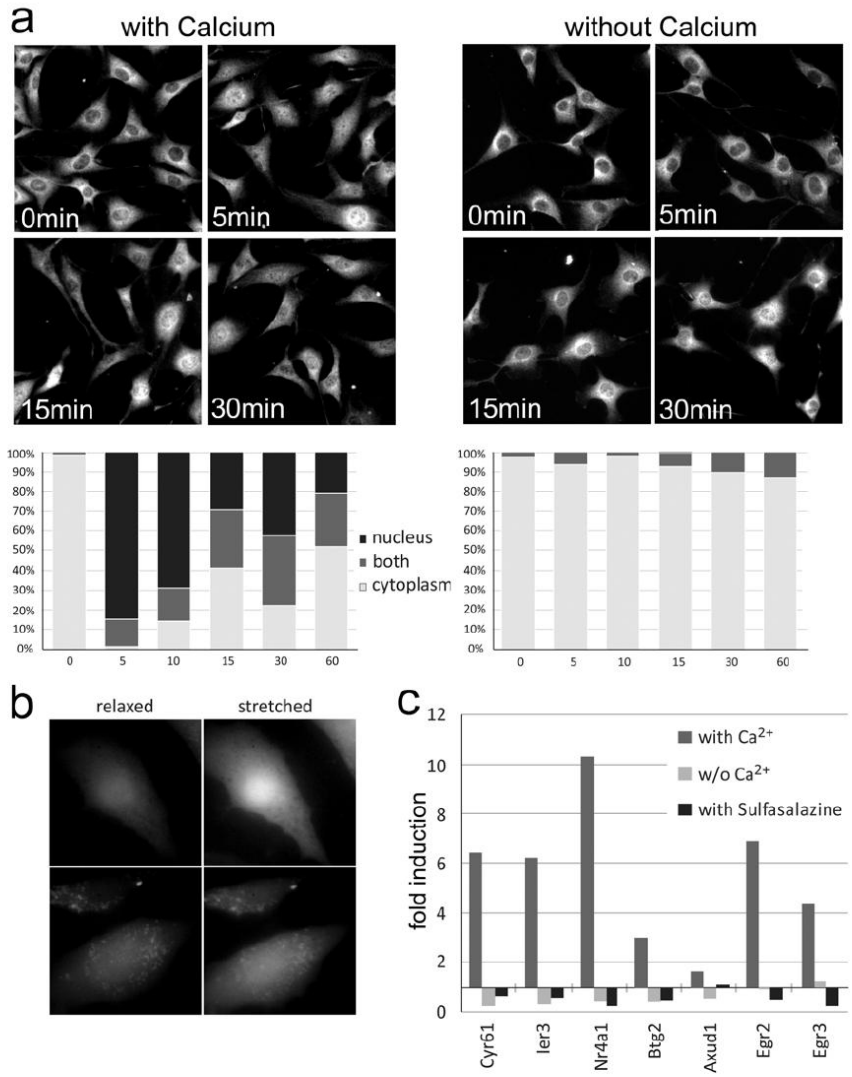

Figure 16 | **Early stretch response depends on calcium influx and subsequent activation of the NfkB pathway.** Immunostaining of NFkB in NIH3T3 cells before and after 5, 15 and 30 minutes of continuous cyclic strain reveals that NFkB translocates into the nucleus already within 5 minutes of continuous cyclic strain. The translocation is transient and does not occur in the absence of Calcium in the medium. Quantification of the predominant localization of NFkB during 0-60 minutes of continuous cyclic strain is shown in the panels below **(A)**. Calcium influx can be observed immediately upon a single stretch of NIH3T3 cells as determined by increased fluorescence in cells loaded with the calcium-sensitive dye Fluo-3 **(B)**. In the absence of Calcium or in the presence of the NFkB inhibitor sulfasalazine the early stress response genes cannot be activated by stretching anymore as shown by quantitative real-time PCR of mRNA isolated from NIH3T3 cells after 1hour of continuous cyclic strain **(C)**.

III.2.2 Activation of tenascin-C by Egr3

Tenascin-C (TN-C) has previously been shown to be activated by mechanical stress in a Rho/ROCK dependent manner. Blockage of actin polymerization by the Rho/ROCK inhibitor Y27632 prevents activation of tenascin-C [30]. Among the genes that respond to 1 hour of cyclic strain is Egr3. As tenascin-C possesses a classical Egr-binding site (5'-GCGGGGCG-3') in its promotor sequence we decided to investigate the role of Egr3 in the stress induced up-regulation of TN-C. Therefore we made promotor studies using the SEAP system that enables measuring alkaline phosphatase secreted into the medium upon promotor induction. We used promotor constructs containing either the 1800bp sequence of the TN-C promotor or a short form of 375bp lacking the Egr-site (see figure 16B). We co-expressed these constructs together with full length eGFP-tagged Egr3 (figure 16A) or an N-terminally truncated inactive version of Egr3 (Egr3s) that is lacking the transactivation domain.

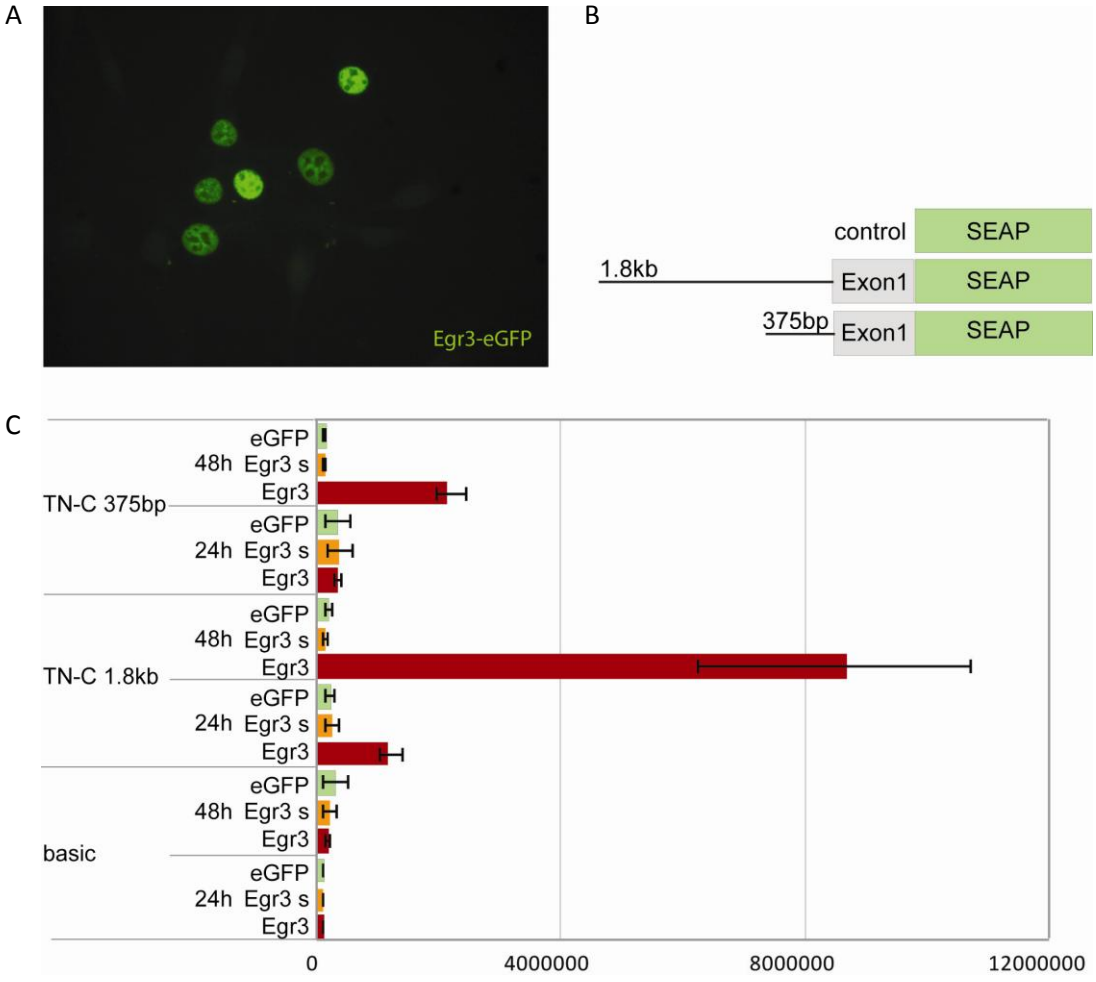

Figure 17 | **Egr3 activates TN-C in promotor studies.** Recombinant Egr3 is expressed in the nucleus of transfected cells **(A)**. In promotor studies using secreted alkaline phosphatase (SEAP) and a long and a short TN-C promotor construct **(B)** recombinant Egr3 was capable of activating the long TN-C promotor construct **(C)** whereas truncated Egr3 was not. Only the long TN-C promotor construct could be activated, not the short one lacking the Egr binding site.

We compared the activation of the promotor constructs to the basic activation caused by co-expressing eGFP and the promotorless basic SEAP vector 24 and 48 hours after transfection (figure 16C). The long TN-C promotor construct is induced by full length Egr3, but not by eGFP or the truncated Egr3. The induction of the promotor construct lacking the Egr motif is much reduced. This leads to the conclusion that Egr3 can indeed activate the TN-C promotor. However, these data need to be confirmed for endogenous TN-C and during stretching. Therefore, we tried to overexpress Egr3 and Egr3s using our retroviral expression system and look for an increase of endogenous TN-C protein upon Egr3 transduction. Unfortunately there was no consistent difference detectable among the three constructs (figure 17A).

Next we stretched NIH 3T3 transduced with Egr3, Egr3s and eGFP and analyzed changes in the TNC mRNA levels after 1 and 6 hours of cyclic strain and compared them to unstretched cells (figure 17B). The induction of TN-C transcripts was very low, but slightly increased in the presence of Egr3 after 6 hours. These experiments are not conclusive and should be repeated with cells that show a better response in TN-C induction by mechanical stress.

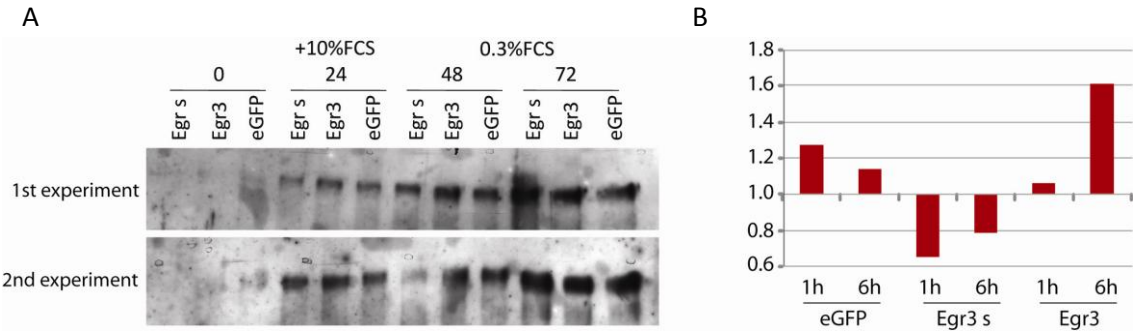

Figure 18 | **Studies with endogenous TN-C activation by Egr3.** There is no consistently detectable difference in TN-C secretion upon overexpression of either inactive or wild type Egr3 (A). Induction of tenascin-C (TN-C) after 1 and 6 hours of cyclic biaxial strain. There is an indication that Egr3 increases the stress response of TN-C, but the basic stress response is too weak for the changes to be significant (B).

III.2.4 Confocal microscopy for detection of changes in nuclear shape and for preparation of FISH

It has been described that lack of laminA/C and emerin lead to changes in the structure of the nuclear lamina [3, 153]. We have also observed changes in the nuclear shape in immunofluorescence microscopy of NIH 3T3 and C2C12 cells overexpressing dominant-negative sun or nesprin (figure 18A). Therefore we decided to have a closer look at the nuclei of NIH 3T3 cells expressing either eGFP or dominant-negative sun or nesprin using confocal laser scanning microscopy and subsequent 3D modeling of the nucleus (figure 18B). First we were interested in imaging the nuclear structure. Then the plan was to establish fluorescence in situ hybridization (FISH) to investigate changes in chromatin structure, chromatin organization and changes in the localization of those genes, up regulated after 1 hour of biaxial strain as it was proposed that the components of the LINC complex directly link the extracellular matrix to the chromosomes [154]. We wanted to analyze whether changes in the stress response seen in expression profiling may be linked to changes in chromatin organization or changes in gene subnuclear location.

Unfortunately, we encountered several problems that prevented us from pursuing this question. One problem was that the stretching device did not fit underneath the objective of the microscope. Thus we were not able to use this method with live cell imaging of stretched cells. The other problem thus was that the nuclei were very flat, too flat for detecting significant changes in the Y-axis.

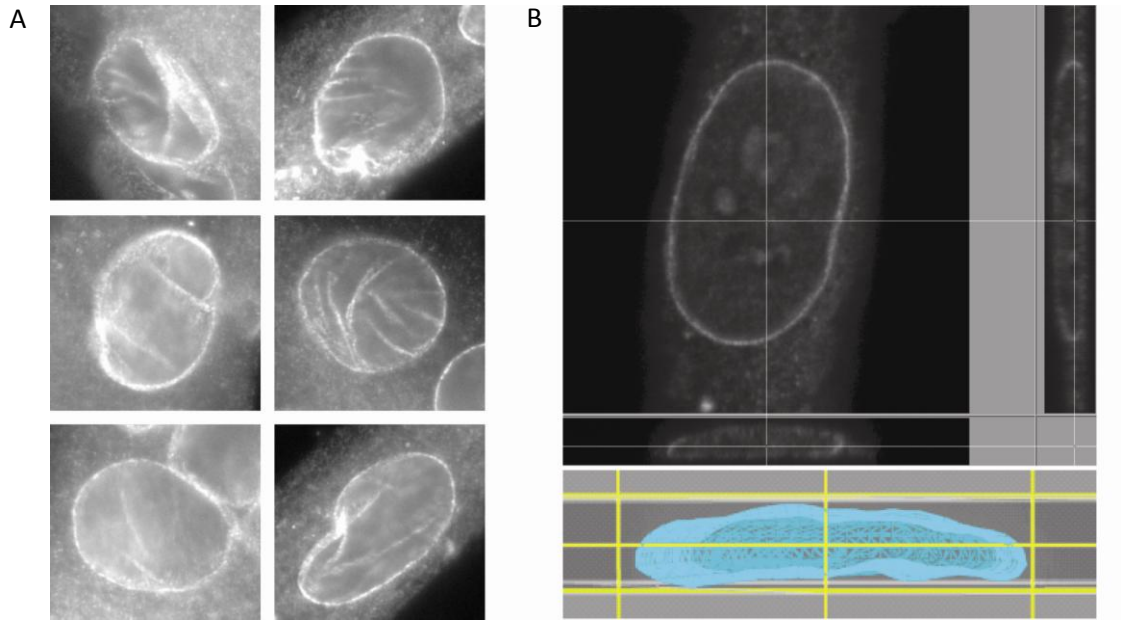

Figure 19 | **Nuclear deformation upon expression of DN nesprin or sun.** Images of nuclei of C2C12 expressing eGFP-tagged dominant-negative sun1 and of NIH 3T3 cells stained with laminA/C antibody. C2C12 cells were transduced with eGFP-tagged DN sun1 and differentiated into myotubes for 5 days (A). NIH 3T3 were cultured on a glass coverslip fixed and stained with laminA/C. The images were acquired at a confocal laser scanning microscope (B).

III.2.5 siRNA-knockdown of sun1 and laminA/C

As previously shown, nuclear rotation in response to biaxial strain depends on the presence of a functional LINC complex. To confirm the data obtained by overexpressing dominant-negative isoforms of nesprin2 and sun1 we decided to transfect NIH 3T3 cells with siRNA against sun1 and laminA/C. LaminA/C was purchased as positive control and was supposed to reduce the levels of an additional protein that is part of the LINC complex. Transfection efficiency was nearly 100% as tested by using Rhodamine-labeled siRNA oligos and testing expression by fluorescence microscopy (see figure 19A). Reduction of the endogenous protein was tested by Western blot (figure 19B).

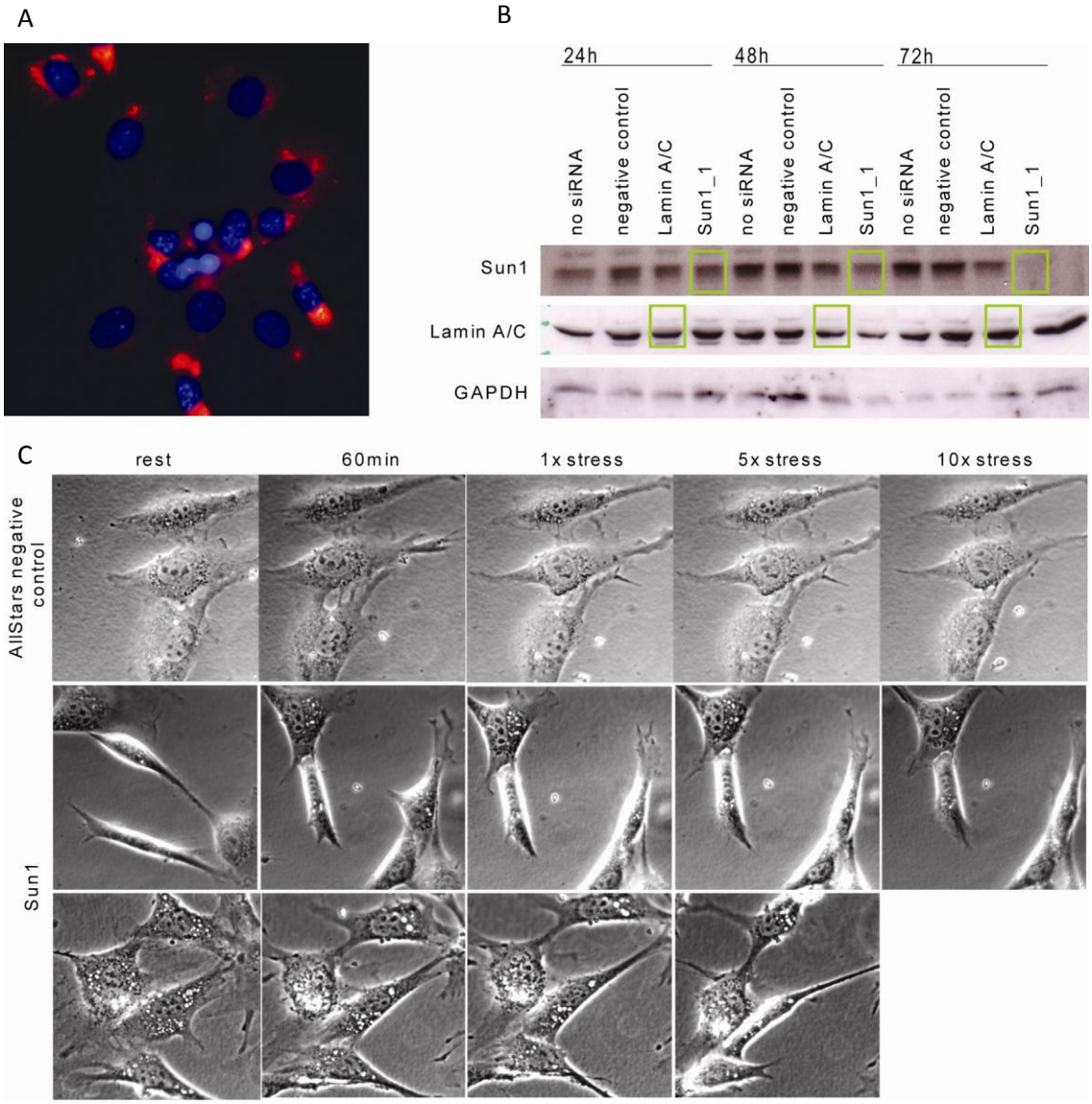

Figure 20 | siRNA experiments for knockdown of sun1 and laminA/C. Transfection efficiency with siRNA was almost 100% even at only 1nM final concentration of siRNA in the well (A). Protein levels of endogenous sun1 was significantly reduced after 72h of incubation with siRNA. LaminA/C however remained present and a higher concentration of laminA/C siRNA was toxic to the cells (B). Even at 1nM final siRNA concentration the cells showed large vacuoles and died upon stretching (C).

Unfortunately the positive control didn't work and the siRNA concentration necessary to reduce laminA/C levels was lethal to the cells. Generally the cells were suffering from the siRNA transfection even after optimizing the concentrations of siRNA and transfection reagent as well as the incubation time after transfection. The cells showed large vacuoles at rest and started detaching and dying as soon as they were stretched (figure 19C).

III.2.6 Scratch assay: wound healing and nuclear rotation

As shown by Levy [155] the nucleus of a cell starts rotating during directed cell migration. Wounding of a monolayer of cells stimulates an induction of nuclear rotation. This rotation is inhibited in cells lacking dynein. As we have observed a similar nuclear rotation in response to stretching and this rotation was inhibited in cells lacking functional sun1 or nesprin2 we were interested in testing rotation behavior in cell migration after wounding. Therefore we used ibidi culture inserts to obtain scratches with smooth edges where we could easily scan the whole rim of the wound and follow nuclear movements. We took pictures every 10 minutes for 2 hours at 20 different positions along the scratch and looked at the nuclear rotation in NIH 3T3 expressing eGFP, dominant-negative sun1 or dominant-negative nesprin2 (see figure 20). Most nuclei of cells transduced with eGFP rotated more than 10° within the first 50 minutes. Nuclear rotation of cells lacking sun or nesprin was reduced but still present (see table 1). Therefore we concluded that functional sun or nesprin are not absolutely required for nuclear rotation in directed cell migration and directed cell migration might be possible without nuclear rotation.

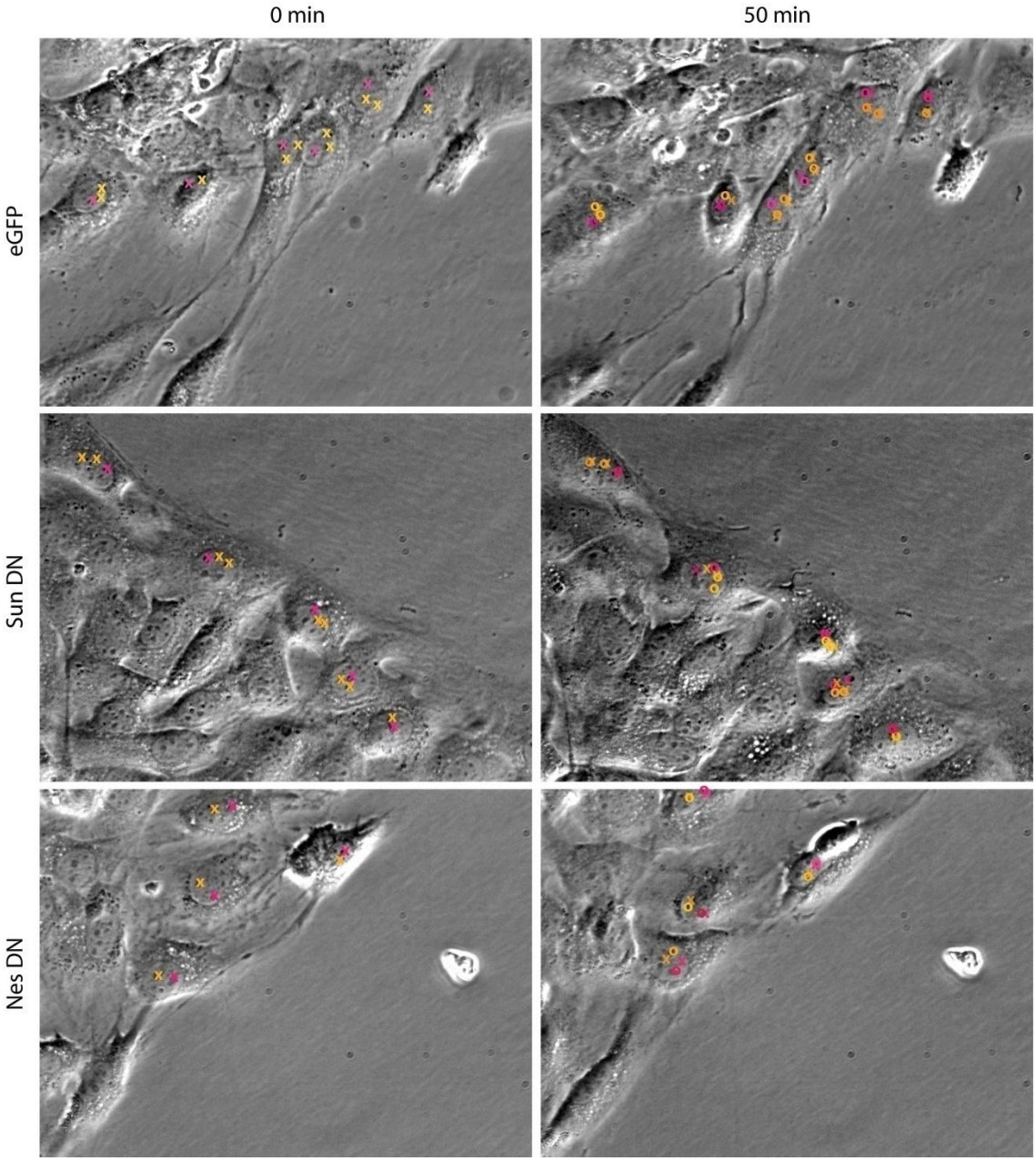

Figure 21 | **Wound healing and nuclear rotation.** In a wound healing assay nuclei rotated in the presence as well as in the absence of a functional LINC complex.

table 1 | number of rotating nuclei

	GFP		Sun		Nes	
	rotation	no rotation	rotation	no rotation	rotation	no rotation
50min	44	16	17	15	13	21

In addition we also observed that there is no difference in the migratory behavior of cells expressing either eGFP or dominant-negative sun or nesprin. Cells do migrate and close the wound at the same speed with or without a functional LINC complex (figure 21).

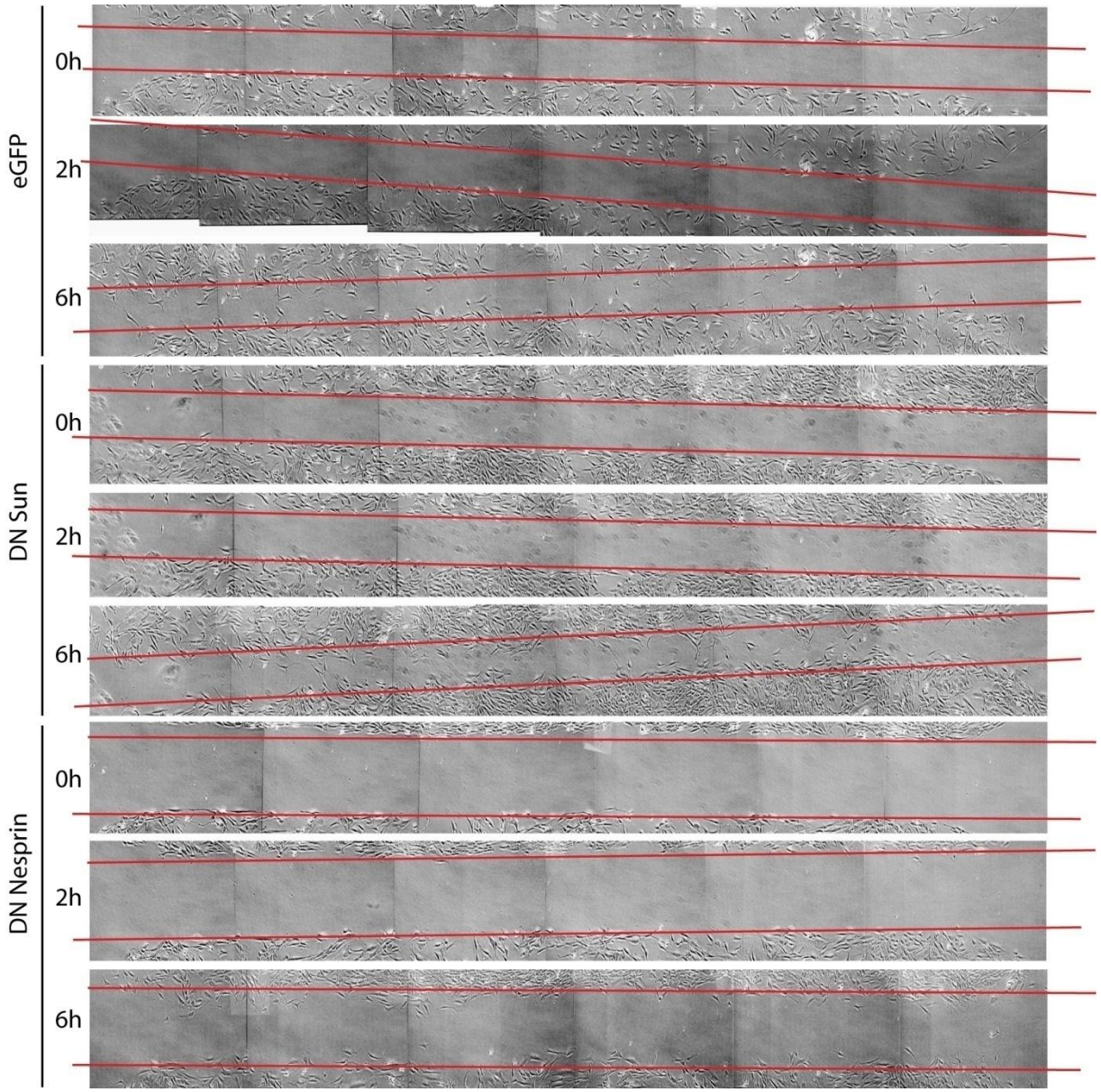

Figure 22 | **Migration behavior after wond healing**. In a wound healing assay there was no significant differences between cells possessing a functional or a dysfunctional LINC complex. NIH 3T3 transduced with eGFP, DN sun1 and DN nesprin2 were plated in ibidi inserts over night. Pictures were acquired 0, 2 and 6 hours after removal of the inserts and wound closure was monitored by counting how many cells cross the lines drawn at the initial edge of the wound. The number of cells crossing these lines of the wound do not differ significantly (eGFP: 182; DN Sun: 197; DN Nes: 104).

III.2.7 Uniaxial strain

It has previously been shown that the actin fibers and even the whole cell is reorienting perpendicular to the direction of applied uniaxial strain [156-158]. So far we did all experiments with biaxial strain where we can detect a thickening of actin fibers and formation of big actin cables as a response to stretching but no reorientation of the cells and actin fibers.

As described in the published results nuclei rotate in response to stretching and this depends on a functional LINC complex and actin polymerization. However, a function of the nuclear rotation is still unclear. It has no or only a small effect on gene regulation as shown by microarray studies. Furthermore it has no influence on cell migration or reorientation of the nuclei in the direction of cell migration as shown in scratch assays.

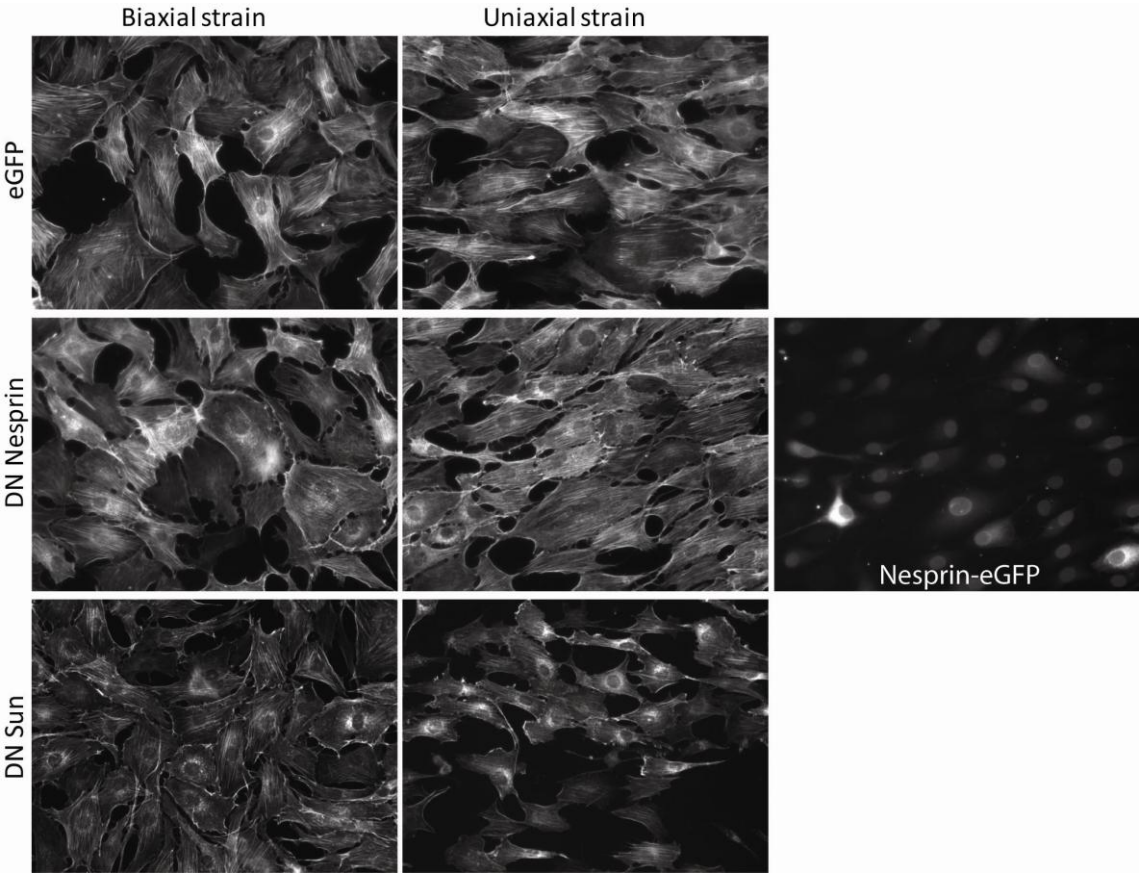

Figure 23 | **NIH 3T3 reorientate perpendicular to the direction of strain.** Cytoskeletal reorientation was observed by phalloidin staining of their actin cytoskeleton. Cells were transduced with eGFP, dominant negative nesprin or sun and stretched for 24hours prior to fixation and staining. The observed cytoskeletal reorientation is independent from a functional LINC complex.

Therefore, we decided to investigate, whether a missing functional direct link has any influence on the reorientation of the stress fibers and the cells in response to uniaxial strain. To investigate this,

we used the Flexercell™ system we previously used for applying biaxial strain to the cells. We used the UniFlex™ plates that are designed especially for the application of uniaxial strain and stretched the cells at 1Hz, 15% elongation for 24 hours. Unfortunately the system is not optimal and uniaxial strain is only applied to the cells at the edges of the stretch area. However, the area of uniaxial strain was wide enough to see a reorientation of all cells perpendicular to the stress axis. This reorientation happened in the presence and the absence of a functional LINC complex and therefore reorientation of the actin cytoskeleton is independent from sun and nesprin (figure 22).

DISCUSSION

IV. DISCUSSION

IV.1 OUR AMBITION

Over the past years it has become more and more evident that mechanical stress is an important factor that contributes to a broad range of cellular functions, not just in a subset of specialized cells and tissues. Response to mechanical stress is needed for cells to adapt to their physical surroundings and is important for tissue homeostasis, tissue architecture and muscle regeneration. Cell differentiation does not only depend on the expression of certain growth factors but also and the mechanical properties of the surrounding microenvironment. Therefore it is necessary that cells can sense mechanical cues, transduce them into biochemical signals and respond to them appropriately [14].

Misregulation of mechanical sensing has been shown to be involved in a series of pathologies. Changes in the matrix stiffness of the tumor surrounding tissue and thereof resulting changes in the forces acting on the cell adhesion molecules lead to altered force transmission to a cell contributing to the development of a metastatic phenotype [13].

Defective mechanotransduction can be observed in laminopathies, a diverse group of diseases that includes Emery-Dreyfuss muscular dystrophy and Hutchinson-Gilford progeria syndrome [1-5]. These diseases develop due to mutations in laminA, emerin or nesprin-1. These proteins are part of a physical link that spans from the nuclear lamina via the cytoskeleton to the extracellular matrix and thus might play a role in a cell's sensation of and response to mechanical stress. Cells lacking either protein display defective nuclear mechanics and mechanotransduction.

Nuclear lamins, the LINC complex, the actin cytoskeleton and cell adhesion molecules act closely together to maintain cell shape and keep the cell in a pre-stressed state. This is required for cells to be able to sense mechanical strain. Thus cell-generated forces and forces from a cell's environment must act together as a mechanosensor to generate a response. The tensegrity model implies that integrins are linked to the nucleus through the cytoskeleton. Thus an applied force is transmitted to the DNA through the cytoskeleton by nuclear lamins and nuclear envelope receptor complexes. This might then directly modulate gene expression by inducing conformational changes in chromatin either by altering the nature of the protein complexes at the telomeres of chromosomes or by changing the activity of DNA remodeling enzymes [59, 60, 70, 71]. Thus, a connection between components of the LINC complex and changes in chromatin structure in response to mechanical cues could dynamically alter gene expression in response to exogenous force [14] [95].

In this study we decided to focus on the early mechanoresponse mechanisms activated within the first hour of biaxial cyclic strain. Initially we focused on gene expression profiling and the activation of signaling pathways and then investigated the role of the LINC complex in response to mechanosensation and muscle cell differentiation.

IV.2 ACTIVATION OF EARLY STRESS RESPONSE GENES BY BIAXIAL CYCLIC STRAIN

From previous studies we know that tenascin-C (TN-C) is heavily induced after sustained periods of mechanical stress. This has been shown in vivo as well as in vitro [18, 138, 150]. It has also been shown, that the activation of TN-C depends on actin polymerization as its inhibition by using the Rho/ROCK inhibitor Y27632 completely blocked TN-C induction [31].
For this reason we decided to analyze in detail the immediate response to biaxial cyclic strain in fibroblasts that leads to the subsequent activation of TN-C.

Our studies with primary as well as immortalized mouse embryo fibroblasts revealed, that biaxial cyclic strain leads to the rapid activation of a very distinct group of genes. This group of genes is relatively small. It comprises about 30 genes that are mainly transcription factors. Interestingly, all genes involved were upregulated, none repressed. This response was only transient and disappeared completely after 6 hours of stress. The later response, after 6 hours of continuous cyclic stretching, included many more genes that were up as well as downregulated. Several of them encode for extracellular matrix proteins including tenascin-C, fibronectin, matrilin-2, nidogen-1 and -2 and laminin.

Consistent with published findings that Erk and NfκB pathways are activated by shear stress and in stretching experiments with smooth muscle cells [48] we found both pathways also activated in fibroblasts already after 5 to 10 minutes of stretching. Whereas inhibition of Erk and Rho/ROCK signaling did not block the activation of the early stretch response genes inhibition of NfκB signaling repressed gene activation. Pathway profiling with the 2 groups of genes, influenced by 1h and 6h of stretching, also implicated, that the NfκB pathway is the major pathway involved in the activation of these genes.

We could show that the activation of NfκB signaling is dependent on the influx of calcium since extracellular calcium was required. Live-imaging experiments showed an increase in cytoplasmic calcium as soon as cells were stretched and at the relaxed state the calcium signal diminished again. A lack of calcium in the medium showed the same blocking effect on the early stress response as inhibition of NfκB signalingby pharmacological inhibitors. Thus, we concluded that stretching opens stretch-gated ion channels in the cell membrane. This leads to a rapid influx of extracellular calcium into the cell and triggers activation of NfκB signaling and subsequent translocation of NfκB into the

nucleus. Inhibition of Erk had an opposite effect. It rendered cells more responsive to stretching. We have preliminary evidence that this is due to a sustained presence of NfκB inside the nucleus.
One of the early stress response genes is Egr3. The Egr-family proteins have already been shown to be activated by stretching [151]. Thus our data confirmed previous observations. TN-C which possesses an Egr binding site in its promotor region can be activated by overexpression of Egr3 but not by expression of an N-terminally truncated dominant negative Egr3. However, we were only able to show this activation in promotor reporter studies and not yet for endogenous TN-C. Therfore, the role of Egr3 in the activation of TN-C in response to stretching needs further investigation.

Taken together, our results imply that the stress reponse seen upon biaxial cyclic strain is very specific as only a relatively small group of genes is affected by it. Stretching triggers influx of intracellular calcium and thus activates NfκB signaling which is responsible for the activation of the early stretch response genes. In addition, how activation of the Erk and Rho/ROCK pathways influences the stress response and how and whether all 3 activated pathways interact with each other needs to be further investigated.

IV.3 THE ROLE OF THE LINC COMPLEX IN STRETCH RESPONSE

In the past couple of years it has become more and more evident that the nucleus is anchored to the actin cytoskeleton via the LINC complex proteins sun and nesprin [75]. We have new esperimental evidence for this, as we see nuclear rotation as an immediate response to cell stretching. As soon as we disrupt this nuclear anchor by overexpression of the dominant-negative isoforms of sun and nesprin there is no rotation detectable upon stretching.

The rotation, however, is not a prerequisite for gene activation upon stretching. Cells lacking a functional LINC complex still respond to stretch by upregulation of the same set of genes and the response is even better. This observation is similar to what we observed after blocking Erk signaling. However, inhibition of Erk did not influence nuclear rotation and neither did inhibition of NfκB signaling which is responsible for the activation of the early stretch response genes. Thus, we conclude that nuclear rotation is a conspicuous change of the intracellular architecture caused by stretching of the cytoskeleton but it does not influence the early stretch response on a gene regulatory level. However, we observed some connection between the LINC complex and the activation of NfκB. As mentioned before, NfκB transiently translocates into the nucleus upon cell stretching. In the absence of functional sun1 NfκB remains inside the nucleus for a longer period of time. This is the same effect as we have seen when we inhibit Erk signaling. As inhibition of Erk and overexpression of dominant-negative sun also show a tendency towards a higher induction of stretch genes, we postulate that there may be a connection between the LINC complex and the activation of Erk signaling but further details need to be investigated.

Nuclear rotation has been described in cells migrating into the wound after an in vitro scratch assay [155]. We could confirm this but it does not seem to require a functional LINC complex for it. Cells overexpressing dominant-negative sun or nesprin show only slight differences in nuclear rotation compared to cells only expressing eGFP. Moreover, disruption of the LINC complex neither had an influence on migration speed nor on the reorientation of the actin cytoskeleton as it can be seen in response to uniaxial strain. Hence we can only speculate about other possible consequences of the observed rotation. We hypothesize that it might influence cellular polarization. This, however, requires further experiments.

VI.4 EFFECTS OF THE LINC COMPLEX ON MUSCLE CELL DIFFERENTIATION

A special interest in the components of the LINC complex arises through its involvement in the development of laminopathies such as Emery-Dreifuss muscular dystrophy (EDMD). Therefore, we decided to extend our studies to C2C12 myogenic progenitor cells. C2C12 cells can differentiate in vitro into myotubes within a period of 5 days when cultured in differentiation medium. After transduction with dominant-negative sun1 or nesprin1 cells did not show any detectable difference in their differentiation behavior. The number and size of myotubes did not vary between the conditions and the differentiation marker creatine kinase was equally increased in wildtype cells and those lacking sun or nesprin. However, when we applied cyclic biaxial strain we observed that C2C12 cells did not differentiate into myotubes anymore. This is consistent with data from Akimoto, Kook and Kumar [6-8]. When we applied strain to C2C12 cells lacking functional sun or nesprin this arrest in differentiation was not observed anymore. Myotubes were indistinguishable from those formed in the absence of strain. QPCR for the differentiation marker MHC confirmed our findings. Thus we propose that the components of the LINC complex are essential for the sensation of mechanical stress and the coordination of the muscle cell differentiation in response to it. Whether these cell culture findings have implications for the in vivo situation or not remains to be established. The results are consistent with reduced muscle precursor or satellite cell proliferation in the presence of mutations in nuclear lamina proteins and concomitant defects in muscle development and regulation. Certain findings in emerin-null mice support our hypothesis [159, 160]. These mice exhibit a mild dystrophic or cardiomyopathic phenotype and delayed muscle regeneration after myotrauma. Thus, these mice exhibit subtle phenotypes consistent with EDMD.

Kook et al. [7] showed that cyclic stretch induces proliferation of C2C12 myoblasts and inhibits their differentiation. p38 kinase is closely involved in this stretch-mediated inhibition of myogenesis due to prolonged activation of p38 and suppression of ERK phosphorylation. In accordance with those results we also found p38 and NfκB signaling to be involved in the myoblast to myotube differentiation. This again marks the central role of NfκB signaling in mechanotransduction.

IV.4 PERSPECTIVES

In recent years, cell biologists realized that the ability to sense mechanical cues is an important feature of all cells in order to adjust their function, differentiation and behavior and changes in mechanotransduction contribute to a variety of diseases that are not obviously linked to mechanosensation.

Our studies have shown a central role for the NfκB signaling pathway upon stretching of cells. Activation of NfκB is one of the first responses a cell shows upon a change in mechanical stress and this is crucial for the subsequent activation of the early stretch response genes. How NfκB signaling crosstalks with Erk and Rho/ROCK activation upon stretching and how it interacts with the components of the LINC complex are not yet known. These are questions that need to be addressed in the future.

It is known that TN-C is activated by many factors and that its activation upon cyclic strain depends on Rho/ROCK signaling and a prestressed cytoskeleton [18, 138, 150]. We now have some indications that Egr3 which is induced by strain can activate TN-C. These data are preliminary and are based on promotor studies. Thus, this mechanism needs to be investigated more closely in the context of activation of endogenous TN-C upon stretching. Further experiments could also include fibroblasts derived from Egr3 deficient mice. Mice lacking Egr3 show severe ataxia that can partly be compensated by physical exercise [161-163]. Tissue sections from muscle and myotendenous junctions from Egr3 knock-out mice might also give some interesting hints about a functional interaction between TN-C and Egr3, maybe revealing differences in TN-C expression in the presence or absence of Egr3.

The nucleus is often proposed as a mechanosensor that functions by altering chromatin accessibility in response to deformations, but direct evidence is still missing [59, 60, 70, 71]. We envisaged to set up FISH experiments to further address the question whether mechanical stress changes chromatin and gene localizations and whether this is dependent on the LINC complex. Due to technical difficulties and because we did not see an inhibition of the stretch response in the absence of a functional LINC complex we did not persue this any further. Nevertheless, it would definitely be worth doing so.

Here we have presented data giving us more insight into the LINC complex and its role in mediating muscle cell differentiation. We have experimental evidence that sun and nesprins are needed to sense mechanical stress in myogenic progenitor cells and that growth is induced and differentiation is blocked by mechanical stress only in the presence of a functional link between the nucleus and the actin cytoskeleton. Whether this has any importance in vivo and whether this is connected to the severe muscle wasting seen in Emery-Dreifuss patients remains unknown and needs to be addressed in the future. Our in vitro studies are supported by the fact that recently patients have been identified with mutations in nesprin-1 and -2 who suffer from Emery-Dreifuss muscular dystrophy and mice lacking nesprin-1 show an EDMD-like phenotype [123, 124].

APPENDIX

V. APPENDIX

V.1 EXPERIMENTAL PROCEDURES (UNPUBLISHED DATA)

Semiquantitative PCR

RNA was isolated according to the protocol using QiaShredder (Qiagen) and the RNeasy kit (Qiagen). RNA was eluted with 30µl H_2O per column for PCR or 10µl H_2O per column for microarray analysis. Reverse transcription of the isolated RNA was performed with the ThermoScript™ RT-PCR System (Invitrogen) according to the manufacturer's protocol using 1µg RNA in a 20µl setup with Oligo dT primers. The generated cDNA was then used for semi-quantitative PCR using 1µl TaqPolymerase (Roche), 5µl polymerase buffer, 1µl 10mM dNTP Mix (Eppendorf), 1µg cDNA, 0.2mM forward and reverse primer (primer sequences see table 2) per 50µl reaction.

table 2 | primer sequences used for semi-quantitative PCR

gene	sense primer	antisense primer
GAPDH sense	5'-ATGACATCAAGAAGGTGGTG-3'	5'-CATACCAGGAAATGAGCTTG-3'
JunB sense	5'-GATCGCTCGGCTAGAGGAA-3'	5'-CTTAAGCTGTGCCACCTGTTC-3'
cFos sense	5'-GATGTTCTCGGGTTTCAACG-3'	5'-GTCTCCGCTTGGAGTGTATC-3'
FosB sense	5'-TGGGCCGGTCTCGGGGAAATG-3'	5'-CCCTCTTGGTAGGGGATCTT-3'
delta-FosB antisense	see FosB sense	5'-GGACTTGAACTTCAATCGGCCA-3'

RNA isolation, transcript profiling, RT and QPCR

RNA was isolated using QiaShredder (Qiagen) and the RNeasy kit (Qiagen) according to the manufacturer's protocol. RNA was eluted with 30µl H_2O per column for RT and QPCR or 10µl H_2O per column for Microarray analyses. RNA was converted into labelled cRNA and hybridized to Affymetrix mouse 430v2 oligonucleotide arrays and the data analyzed. For quantitative PCR, reverse transcription of the isolated RNA was performed with the ThermoScript™ RT-PCR System (Invitrogen) according to the supplied protocol using 1µg RNA in a 20µl setup with oligo dT primers. The generated cDNA was then used for quantitative real-time PCR using Platinum® SYBR® Green qPCR SuperMix-UDG with ROX (Invitrogen) on an Abi7000 (Applied Biosystems). The primers used for qPCR are listed in Table 2. Values were normalized to GAPDH and fold changes calculated using the efficiency ΔΔct method[164].

table 3 | primer sequences used for semi-quantitative PCR

gene	sense primer	antisense primer
GAPDH sense	5'-ATGACATCAAGAAGGTGGTG-3'	5'-CATACCAGGAAATGAGCTTG-3'
JunB sense	5'-GATCGCTCGGCTAGAGGAA-3'	5'-CTTAAGCTGTGCCACCTGTTC-3'
cFos sense	5'-GATGTTCTCGGGTTTCAACG-3'	5'-GTCTCCGCTTGGAGTGTATC-3'
FosB sense	5'-TGGGCCGGTCTCGGGGAAATG-3'	5'-CCCTCTTGGTAGGGGATCTT-3'
delta-FosB antisense	see FosB sense	5'-GGACTTGAACTTCAATCGGCCA-3'

Cellular fractionation

$1x10^5$ NIH 3T3 cells were plated on fibronectin covered UniFlex™ plates (Dunn Labortechnik) and starved overnight. Cells were stretched for 0-60 minutes and samples of the cytoplasmic and nuclear fraction were prepared using CelLytic™ NuCLEAR™ Extraction Kit (Sigma) according to the manufacturer's protocol. 20µl of the samples were mixed with 7µl sample buffer containing β-mercaptoethanol, cooked at 95°C for 5 minutes and loaded on a 10% SDS gel for western blot analysis. Proteins were resolved by SDS-Page and transferred to Immobilon-P membranes. Proteins of interest were visualized using specific antibodies (NfκB p65 (#4764, Cell Signaling), p-NfκB p65 (#3036,Cell Signaling), IκB-α (#9242, Cell Signaling), p-IκB-α (#2859, Cell Signaling), p44/42 MAP kinase (#9102, Cell Signaling), p-p44/42 Map Kinase (#9101, Cell Signaling), LaminA/C (#2032, Cell Signaling), GAPDH (ab9485, Abcam)) and super signal (Pierce) chemiluminescence reagents according to the manufacturer's recommendations.

siRNA transfection

Lyophylized siRNA oligos were obtained from Qiagen (see table 3 for details) and solubilized according to the manufacturer's instructions to obtain a 20µM stock soluition. $1x10^5$ NIH 3T3 were seeded over night in OptiMEM (Invitrogen) + 5% BS in 6-well plates. For transfection the siRNA stock solution was diluted in 100µl serum free OptiMEM to obtain a final siRNA concentration of 1nM in the well (final volume 2.1ml). 12µl HiPerFect (Qiagen) were added to the diluted siRNA, vortexed and incubated for 5-10minutes at room temperature. The mix was added dropwise to the cells and the cells were incubated with the siRNA for 24, 48 and 72 hours. Transfection efficiency was tested by immunofluorescence as the siRNA oligos were labeled with rhodamine. The efficiency of the siRNA knockdown was tested on the protein level using western blot with specific antibodies against Sun1 (thanks to Sue Shackelton) and LaminA/C (#2032, Cell Signaling Technology).

table 4 | sequences of used siRNA oligos

siRNA	sequence	Catalog no.
Mm_Unc84a_1	GACCTTAAAGGTGGAAATAAA	SI01462363
Mm_Unc84a_2	AAGTCGAGGTTTCCTATATTA	SI01462370
Mm_Unc84a_3	TGGAGATATTTCAAATATTA	SI01462377
Mm_Lmna_5	validated-not disclosed	SI0265550
AllStars Neg. siRNA Rhodamine	N/A	1027283

Confocal laser scanning microscopy

NIH 3T3 cells previously transduced with retrovirus containing either eGFP or the dominant-negative constructs of Sun1 and Nesprin1 were plated on glass cover slips in DMEM + 5% BS to 70% confluency. After an over-night incubation the cells were fixed in 4% paraformaldehyde (PFA) for 15 minutes, washed twice with PBS, permeabilized with 0.1% Triton-X-100 in PBS for 5 minutes and washed again 3 times with PBS. After a 1 hour incubation with the primary antibody against LaminA/C (#2032, Cell Signaling Technology), cells were washed 3 times with PBS and then incubated with the secondary antibody (anti-mouse Alexa 568, Invitrogen) for 1 hour and then washed again 3 times with PBS. All steps of fixation and staining were carried out at room temperature. The cover slips were mounted with Prolong Antifade Gold (Invitrogen) and analysed at the confocal laser scanning microscope LSM510 Meta (Zeiss).

Cloning of Egr3

Egr3 was amplified from cDNA obtained from NIH 3T3 cells using PfuTurbo (Stratagene) using nested PCR and a second specific PCR with the primers listed in table 4. An eGFP derived by PCR from pEGF-1 (Invitrogen) was cloned into the first multiple cloning site of the pQCXIX vector (Clontech) using NotI and PacI. The PCR product of Egr3 was digested and cloned into the vector using PacI and EcoRI (see figure 23).

table 5 | sequences for cloning Egr3 into pQCXIX

gene	sense primer	antisense primer
Egr3 nested	5'-AGAGGATTACCCTCTTTGCC-3'	5'-TCCTAACTGAACAAAGCGGG-3'
Egr3	5'-GCGCTTAATTAAAATGACCGGCAAACTCGCCGAGAA-3'	5'- GCTTGAATTCACCTTTCCGCCCCCACGCCTT-3'
Egr3 DN	see Egr3 sense	5'-GCCTGAATTCTCACTTGCGCTCGTCGCTGCGCGCA-3'
eGFP	5'-CGTTGCGGCCGCAAATGGTGAGCAA-3'	5'-CGGCGTTAATTAACTTGTACAGCTCGTCCATGCCGA-3'

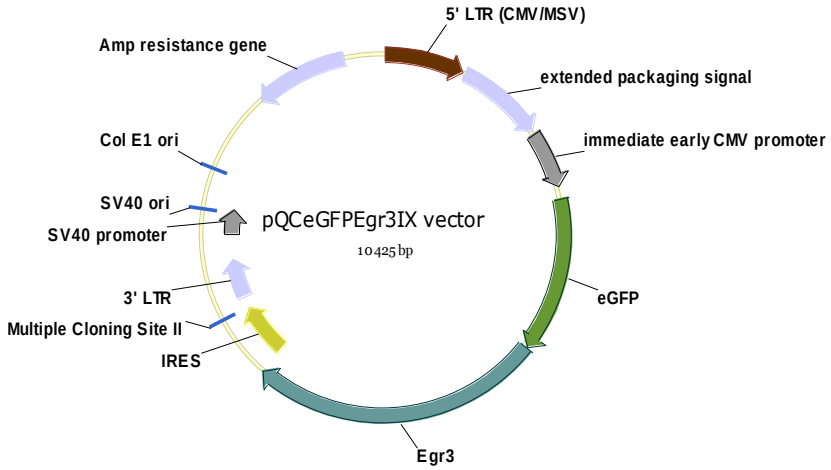

Figure 24 | Vector map of pQCXIX including eGFP-tagged Egr3.

Chemiluminescent SEAP assay

NIH 3T3 cells were cultured in 6-well plates overnight in DMEM +5% BS to 50% confluency. Then they were co-transfected with the Egr constructs and the promoter constructs (1µg DNA each) as indicated in the experiment in DMEM +0.3% BS and incubated for 72 hours. 300µl of the conditioned medium were collected at transfection and 24, 48 and 72 hours after the transfection. The medium was kept at -70°C prior to measuring SEAP activity (Clontech) which was carried out according to the manufacturer's protocol.

Scratch assay

$1x10^5$ NIH 3T3 cells per ml were plated in each well of a culture insert (ibidi, see Figure 24) and incubated overnight. The insert was removed and cells monitored at an Axiovert200 (Zeiss) equipped for live-cell imaging. Pictures of the nuclei were acquired in Z-stacks along the scratch every 10 minutes for 2h. Nuclear rotation was evaluated according to the position of the nucleoli. For the wound healing assay the inserts were removed and pictures were acquired along the whole scratch at 0, 2 and 6 hours after removal.

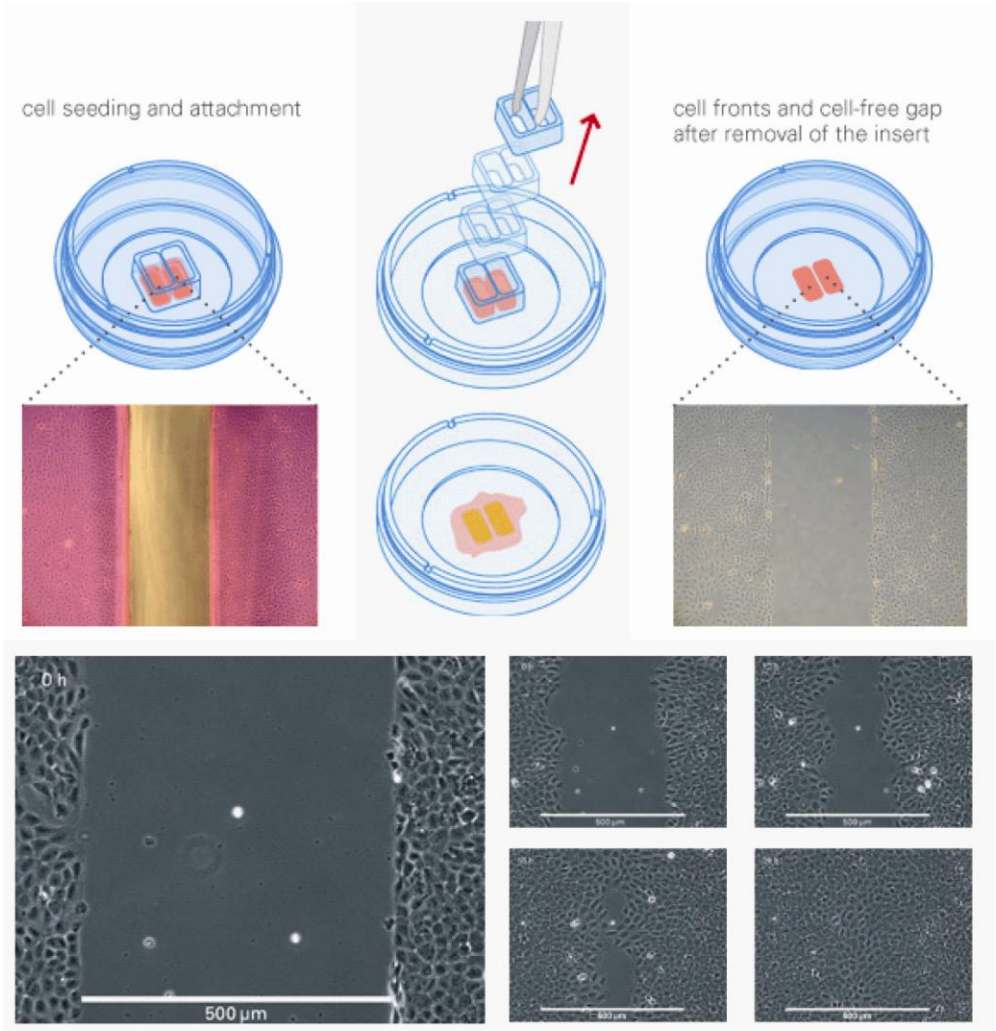

Figure 25 | ibidi culture inserts for scratch assay experiments.

Uniaxial strain

Strain was applied to the cells using the FX-4000T™ Flexercell® Tension Plus™ System (Dunn Labortechnik GmbH, see (Figure 25) $1x10^5$ NIH 3T3 cells were plated in DMEM with 5% bovine serum on UniFlex™ culture plates previously coated for 1h with 100µg/ml fibronectin purified from horse serum. After 4 hours the medium was replaced with DMEM + 0.3% serum and cells were starved over night. Cells were stretched to 15% elongation at 1Hz for 24h.

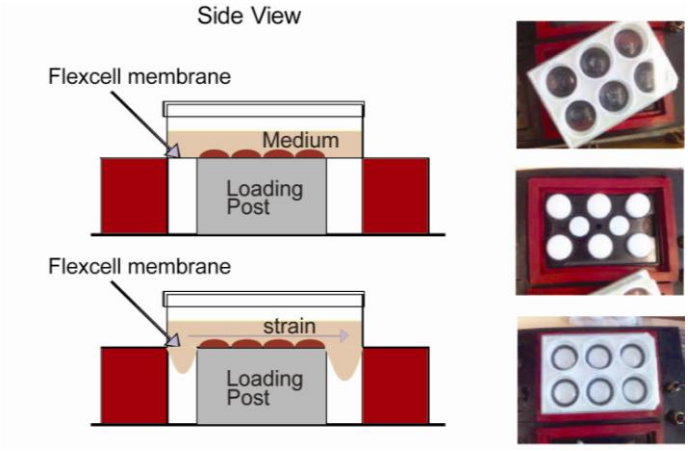

Figure 26 | **Scheme of the Flexercell system used for stretching the cells.** NIH 3T3 were plated on flexible silicon bottom six-well-plates and then stretched to 15% elongation at 1Hz using the Flexercell system (Dunn Labortechnik).

Calcium Imaging

For calcium-imaging lyophilized Fluo-3 (Molecular Probes) was solubilised in DMSO + 20% Pluronic F127 (Sigma Aldrich) to obtain a 1mM stock solution. This stock was diluted 1:1000 in microscopy medium (DMEM w/o Phenolred + 30mM HEPES + 5% BS) and added to NIH 3T3 that were grown to 70% confluency over night in DMEM + 5% BS. Cells were incubated for 30 minutes at 25°C then washed twice with microscopy medium and incubated in that medium for 1h at 37°C. Calcium influx was monitored by acquiring pictures at the relaxed and the stretched state with the same illumination settings.

V.2. MICROARRAY DATA

table 6 | genes upregulated after 6 hours of cyclic strain

Name	Description	Gene Symbol	6h stressed	6h relaxed	fold change
1452941_at	RIKEN cDNA 0610038F07 gene	0610038F07Rik	1.051234	0.4919425	2.136904211
1455040_s_at	RIKEN cDNA 1110062M06 gene	1110062M06Rik	0.9840562	0.4578947	2.149088426
1452584_at	RIKEN cDNA 1500032L24 gene	1500032L24Rik	1.067602	0.4019399	2.656123465
1428705_at	RIKEN cDNA 1700007K13 gene	1700007K13Rik	1.070847	0.4720883	2.268319295
1453008_at	RIKEN cDNA 2300002D11 gene	2300002D11Rik	0.971353	0.3709438	2.618598828
1452130_at	RIKEN cDNA 2310042M24 gene	2310042M24Rik	1.02746	0.3634875	2.826672169
1428450_at	RIKEN cDNA 2610034B18 gene	2610034B18Rik	0.916789	0.3227929	2.840177092
1453000_at	RIKEN cDNA 4930541M15 gene	4930541M15Rik	0.9628085	0.4507424	2.136050436
1450967_at	RIKEN cDNA 4933428I03 gene	4933428I03Rik	0.8971924	0.2804722	3.198863916
1436426_at	RIKEN cDNA 5730509K17 gene	5730509K17Rik	0.9811715	0.4903431	2.000989715
1441972_at	RIKEN cDNA 6230424C14 gene	6230424C14Rik	1.01485	0.4434635	2.288463425
1453188_at	RIKEN cDNA 6230424C14 gene	6230424C14Rik	1.040433	0.5134264	2.02645014
1456765_at	hypothetical protein 6430511F03	6430511F03	0.8532945	0.2712052	3.146305823
1436353_at	RIKEN cDNA A230046K03 gene	A230046K03Rik	1.01503	0.415826	2.440996955
1433939_at	hypothetical protein A730046J16	A730046J16	1.098816	0.5386282	2.040026868
1454708_at	actin-binding LIM protein 1	Ablim1	1.088398	0.3430768	3.172461676
1421171_at	a disintegrin and metalloproteinase domain 12 (meltrin alpha)	Adam12	0.9071339	0.3249393	2.791702635
1421172_at	a disintegrin and metalloproteinase domain 12 (meltrin alpha)	Adam12	0.9540699	0.3241167	2.943599944
1450716_at	a disintegrin-like and metalloprotease with thrombospondin type 1 motif, 1	Adamts1	0.9929238	0.193611	5.128447247
1435990_at	a disintegrin-like and metalloprotease with thrombospondin type 1 motif, 2	Adamts2	0.7403128	0.311693	2.375134507
1422561_at	a disintegrin-like and metalloprotease with thrombospondin type 1 motif, 5	Adamts5	0.9029292	0.1114889	8.098825982
1450658_at	a disintegrin-like and metalloprotease with thrombospondin type 1 motif, 5	Adamts5	0.9590903	0.2450998	3.913060313
1456404_at	a disintegrin-like and metalloprotease with thrombospondin type 1 motif, 5	Adamts5	0.9642131	0.1959534	4.920624495
1437785_at	a disintegrin-like and metalloprotease with thrombospondin type 1 motif, 9	Adamts9	0.9707536	0.4842508	2.004650483
1416225_at	alcohol dehydrogenase 1 (class I)	Adh1	1.184388	0.1674868	7.071530413
1450110_at	alcohol dehydrogenase 7 (class IV), mu or sigma polypeptide	Adh7	1.022426	0.2778318	3.68001791
1436999_at	expressed sequence AL024069	AL024069	0.9409593	0.1905797	4.937353244
1434662_at	APG4 (ATG4) autophagy-related homolog A (S. cerevisiae)	Apg4a	0.979515	0.2720764	3.600146871
1416458_at	ADP-ribosylation factor 2	Arf2	1.112221	0.4666669	2.383329523
1416459_at	ADP-ribosylation factor 2	Arf2	1.099474	0.4252071	2.585737632
1422525_at	ATP synthase, H+ transporting, mitochondrial F1F0 complex, subunit e	Atp5k	1.02839	0.4990335	2.060763456
1426966_at	axin 1	Axin1	0.939466	0.3666782	2.56209941
1455033_at	RIKEN cDNA B430201A12 gene	B430201A12Rik	0.9422849	0.452374	2.08297758
1451398_at	cDNA sequence BC009118	BC009118	0.9440668	0.400142	2.359329438
1451344_at	cDNA sequence BC025600	BC025600	1.117717	0.2865421	3.900707784
1426880_at	CDNA sequence BC026657	BC026657	1.170283	0.3171654	3.689819255
1434621_at	cDNA sequence BC054438	BC054438	1.152027	0.3486534	3.304218459
1428512_at	basic helix-loop-helix domain containing, class B9	Bhlhb9	1.0311	0.3038535	3.393411628
1425491_at	bone morphogenetic protein receptor, type 1A	Bmpr1a	0.9599003	0.4798	2.000625886
1425492_at	bone morphogenetic protein receptor, type 1A	Bmpr1a	0.9937879	0.48353	2.055276612
1425494_s_at	bone morphogenetic protein receptor, type 1A	Bmpr1a	0.9981121	0.3500906	2.851010853
1417365_a_at	calmodulin 1	Calm1	1.108567	0.4709427	2.353931805
1417366_s_at	calmodulin 1	Calm1	1.052683	0.2478991	4.246417192
1417606_a_at	calreticulin	Calr	0.930138	0.1534843	6.060150778
1417604_at	calcium/calmodulin-dependent protein kinase I	Camk1	1.080995	0.4410782	2.450801241
1422519_at	calcium/calmodulin-dependent serine protein kinase	Cask	1.01479	0.4707546	2.155666668
1428064_at	centaurin, delta 2	Centd2	1.055368	0.3361318	3.139744588
1455138_x_at	cofilin 1, non-muscle	Cfl1	1.033643	0.1510336	6.843795023
1418067_at	cofilin 2, muscle	Cfl2	0.9085796	0.3905212	2.326582014
1451440_at	chondrolectin	Chodl	1.140565	0.3355903	3.398682858
1422505_at	chromatin accessibility complex 1	Chrac1	0.9364898	0.388014	2.413546418
1448564_at	calcium and integrin binding 1 (calmyrin)	Cib1	1.034857	0.4629312	2.235444489
1434748_at	cytoskeleton associated protein 2	Ckap2	1.076953	0.3990494	2.698796189
1423641_s_at	CCR4-NOT transcription complex, subunit 7	Cnot7	1.094431	0.3710001	2.949947992
1430519_a_at	CCR4-NOT transcription complex, subunit 7	Cnot7	1.062296	0.4734636	2.243669841
1451102_at	CCR4-NOT transcription complex, subunit 8	Cnot8	1.101376	0.37218	2.959256274
1418237_s_at	procollagen, type XVIII, alpha 1	Col18a1	0.9619222	0.3351552	2.870079891
1424051_at	procollagen, type IV, alpha 2	Col4a2	0.9848874	0.2057911	4.78586003
1433439_at	copine I	Cpne1	0.9619208	0.3424417	2.809006029
1435450_at	Copine III	Cpne3	1.023199	0.3409221	3.001269205
1416612_at	cytochrome P450, family 1, subfamily b, polypeptide 1	Cyp1b1	1.021682	0.1399337	7.301186205
1416613_at	cytochrome P450, family 1, subfamily b, polypeptide 1	Cyp1b1	1.016074	0.18137	5.602216464
1444704_at	DNA segment, Chr 5, ERATO Doi 606, expressed	D5Ertd606e	1.02981	0.4270741	2.41131457
1449368_at	decorin	Dcn	0.7612604	0.1913533	3.978297735
1420862_at	dynactin 4	Dctn4	1.019443	0.488893	2.085206783

1436562_at	DEAD (Asp-Glu-Ala-Asp) box polypeptide 58	Ddx58	0.8006424	0.2987965	2.679557491
1433525_at	endothelin receptor type A	Ednra	0.8246733	0.2523062	3.268541558
1451691_at	endothelin receptor type A	Ednra	0.8195181	0.3013067	2.719880109
1424932_at	epidermal growth factor receptor	Egfr	0.8855363	0.3392426	2.610333431
1417065_at	early growth response 1	Egr1	0.922717	0.246856	3.737875523
1424586_at	EH domain binding protein 1	Ehbp1	0.9094618	0.2023943	4.493514887
1416414_at	elastin microfibril interfacer 1	Emilin1	0.9240808	0.2486734	3.716042005
1456220_at	F-box and leucine-rich repeat protein 7	Fbxl7	0.8690512	0.2759643	3.149143567
1418497_at	fibroblast growth factor 13	Fgf13	1.296519	0.5682711	2.281514932
1449545_at	fibroblast growth factor 18	Fgf18	1.067881	0.3432534	3.111057312
1424050_s_at	Fibroblast growth factor receptor 1	Fgfr1	0.9149137	0.4234388	2.160675167
1425911_a_at	fibroblast growth factor receptor 1	Fgfr1	0.8225867	0.4061734	2.025210661
1449528_at	c-fos induced growth factor	Figf	1.235695	0.389593	3.171758733
1423042_at	fibroblast growth factor inducible 14	Fin14	0.8996018	0.2925388	3.075153792
1426642_at	fibronectin 1	Fn1	0.9574847	0.1604921	5.96593041
1438231_at	forkhead box P2	Foxp2	0.9799325	0.4793507	2.044291372
1438232_at	forkhead box P2	Foxp2	0.9244315	0.2219433	4.165169663
1440108_at	forkhead box P2	Foxp2	1.058734	0.426537	2.482162157
1455604_at	Frizzled homolog 5 (Drosophila)	Fzd5	1.176562	0.5672703	2.074076503
1435606_at	galactose-3-O-sulfotransferase 4	Gal3st4	1.024456	0.4946246	2.071178829
1450112_a_at	growth arrest specific 2	Gas2	0.9581513	0.354652	2.70166614
1459522_s_at	glycogenin 1	Gyg1	0.9439939	0.212795	4.436165793
1423702_at	H1 histone family, member 0	H1f0	1.146271	0.1861997	6.156137738
1428630_x_at	hydroxyacylglutathione hydrolase-like	Haghl	0.8230269	0.4072315	2.021029562
1434557_at	huntingtin interacting protein 1	Hip1	1.143083	0.4625715	2.471148785
1451162_at	heat shock factor binding protein 1	Hsbp1	1.037937	0.5012262	2.070795581
1427489_at	integrin alpha 8	Itga8	1.336024	0.4516708	2.957959647
1421198_at	integrin alpha V	Itgav	1.003848	0.4341791	2.312059701
1417533_a_at	integrin beta 5	Itgb5	0.9778277	0.2077604	4.706516256
1456133_x_at	integrin beta 5	Itgb5	0.9871508	0.2482244	3.976848368
1417279_at	inositol 1,4,5-triphosphate receptor 1	Itpr1	0.9735037	0.328671	2.961939751
1415899_at	Jun-B oncogene	Junb	0.8727928	0.4363727	2.000108623
1423885_at	laminin, gamma 1	Lamc1	0.867676	0.3321745	2.612108997
1417780_at	longevity assurance homolog 4 (S. cerevisiae)	Lass4	1.0047	0.2979713	3.371801244
1421101_a_at	LIM domain binding 2	Ldb2	0.7523468	0.1608826	4.676371466
1439557_s_at	RIKEN cDNA E030026E10 gene	Ldb2	0.7515056	0.1113013	6.751993014
1456786_at	RIKEN cDNA E030026E10 gene	Ldb2	0.7205933	0.2296157	3.138257968
1421654_a_at	lamin A	Lmna	1.030132	0.3812888	2.701710619
1417110_at	mannosidase 1, alpha	Man1a	0.7636498	0.1685967	4.529446899
1417111_at	mannosidase 1, alpha	Man1a	0.8450791	0.1563294	5.405759249
1421877_at	mitogen activated protein kinase 9	Mapk9	1.005952	0.4586843	2.193124988
1415971_at	myristoylated alanine rich protein kinase C substrate	Marcks	0.9407477	0.09336516	10.07600373
1415972_at	myristoylated alanine rich protein kinase C substrate	Marcks	0.952706	0.1317875	7.229107465
1415973_at	Myristoylated alanine rich protein kinase C substrate	Marcks	0.9276785	0.1250944	7.415827567
1456700_x_at	Myristoylated alanine rich protein kinase C substrate	Marcks	0.9810954	0.1512101	6.488292779
1419442_at	matrilin 2	Matn2	1.03756	0.3004851	3.452949913
1455827_at	muscleblind-like 2	Mbnl2	1.020431	0.3226093	3.163055126
1451507_at	myocyte enhancer factor 2C	Mef2c	1.134179	0.4954147	2.289352738
1417359_at	microfibrillar-associated protein 2	Mfap2	0.8787729	0.3007206	2.922223818
1450350_a_at	Jun dimerization protein 2	MGI:1932093	1.126492	0.4513732	2.495699789
1418300_a_at	MAP kinase-interacting serine/threonine kinase 2	Mknk2	1.10875	0.3541275	3.13093448
1439108_at	myeloid/lymphoid or mixed-lineage leukemia 5	Mll5	1.100053	0.3862322	2.848164912
1417256_at	matrix metalloproteinase 13	Mmp13	0.8171688	0.3698941	2.209196632
1417281_a_at	matrix metalloproteinase 23	Mmp23	1.048919	0.4735524	2.215000916
1417282_at	matrix metalloproteinase 23	Mmp23	1.088163	0.3907667	2.784687129
1418945_at	matrix metalloproteinase 3	Mmp3	0.3410464	0.1434311	2.377771627
1418990_at	membrane-spanning 4-domains, subfamily A, member 4D	Ms4a4d	0.9724506	0.2386041	4.075582104
1420473_at	myotrophin	Mtpn	1.02324	0.3028487	3.378716831
1420474_at	myotrophin	Mtpn	1.038558	0.3388958	3.064534881
1420475_at	myotrophin	Mtpn	1.056783	0.4977286	2.123211324
1423321_at	myeloid-associated differentiation marker	Myadm	1.039947	0.2399183	4.334588066
1420171_s_at	myosin, heavy polypeptide 9, non-muscle	Myh9	1.017974	0.3382316	3.009695132
1452651_a_at	myosin, light polypeptide 1	Myl1	1.130953	0.5497431	2.057239099
1424988_at	myosin regulatory light chain interacting protein	Mylip	1.031057	0.2321062	4.442177762
1425505_at	myosin, light polypeptide kinase	Mylk	1.630733	0.5007548	3.256549912
1425506_at	myosin, light polypeptide kinase	Mylk	1.504305	0.4549609	3.306448972

1459679_s_at	myosin IB	Myo1b	1.005427	0.4829841	2.081697928
1419649_s_at	myosin IC	Myo1c	1.145266	0.4590664	2.494771998
1422818_at	neural precursor cell expressed, developmentally down-regulated gene 9	Nedd9	0.9427579	0.2189983	4.30486401
1427680_a_at	nuclear factor I/B	Nfib	0.935845	0.2224962	4.206116779
1449376_at	nicolin 1	Nicn1	1.001057	0.3683644	2.717572599
1448469_at	nidogen 1	Nid1	0.9472943	0.3230077	2.932729777
1423516_a_at	nidogen 2	Nid2	1.057573	0.4050012	2.611283621
1452382_at	neoplastic progression 1	Npn1	1.260768	0.2014885	6.257270266
1422890_at	protocadherin 18	Pcdh18	0.9550395	0.3039246	3.14235669
1430427_a_at	protocadherin 18	Pcdh18	0.9947125	0.2366324	4.2036192
1449249_at	protocadherin 7	Pcdh7	0.880001	0.3095034	2.843267635
1423946_at	PDZ and LIM domain 2	Pdlim2	0.8407216	0.2221739	3.784070046
1417355_at	paternally expressed 3	Peg3	0.9690778	0.2146466	4.51475961
1417356_at	paternally expressed 3	Peg3	0.9946302	0.3301361	3.012788362
1433924_at	Paternally expressed 3	Peg3	0.9975489	0.2933265	3.40081411
1440965_at	Phosphatidylinositol glycan, class L	Pigl	1.128888	0.4217855	2.676450471
1456482_at	phosphatidylinositol 3 kinase, regulatory subunit, polypeptide 3 (p55)	Pik3r3	1.109969	0.3956075	2.805732955
1419835_s_at	plectin 1	Plec1	1.111714	0.4852379	2.291070009
1417133_at	peripheral myelin protein	Pmp22	0.9754788	0.2651984	3.67829821
1422620_s_at	phosphatidic acid phosphatase 2a	Ppap2a	1.114866	0.3008901	3.705226593
1452249_at	prickle like 1 (Drosophila)	Prickle1	0.9836732	0.3135516	3.137197195
1448923_at	protein kinase, interferon inducible double stranded RNA dependent activator	Prkra	0.8906173	0.4186342	2.127435599
1432331_a_at	paired related homeobox 2	Prrx2	1.025332	0.255993	4.005312645
1450344_a_at	prostaglandin E receptor 3 (subtype EP3)	Ptger3	1.691684	0.4418177	3.828918579
1418666_at	pentaxin related gene	Ptx3	0.9416249	0.2726827	3.453189
1433504_at	brain glycogen phosphorylase	Pygb	1.21683	0.2368594	5.137351526
1425981_a_at	retinoblastoma-like 2	Rbl2	0.9823284	0.3257477	3.015611162
1428342_at	REST corepressor 3	Rcor3	0.9834195	0.2311056	4.255282001
1417398_at	related RAS viral (r-ras) oncogene homolog 2	Rras2	0.9584077	0.4645553	2.063064828
1415943_at	syndecan 1	Sdc1	0.9891529	0.4930907	2.006026275
1439368_a_at	solute carrier family 9 (sodium/hydrogen exchanger), isoform 3 regulator 2	Slc9a3r2	1.0029	0.325462	3.081465732
1419255_at	spectrin beta 2	Spnb2	0.9587454	0.270197	3.54831993
1419256_at	spectrin beta 2	Spnb2	1.00301	0.3744026	2.678961097
1417644_at	sarcospan	Sspn	0.9099873	0.1933118	4.707355164
1417645_at	sarcospan	Sspn	0.973445	0.4420526	2.202102193
1434089_at	synaptopodin	Synpo	1.131148	0.2401741	4.709700172
1419222_at	thromboxane A2 receptor	Tbxa2r	1.160048	0.5038206	2.302502121
1420123_at	T-cell leukemia translocation altered gene	Tcta	1.350666	0.3752244	3.599621986
1420124_s_at	T-cell leukemia translocation altered gene	Tcta	1.473581	0.3830682	3.846784985
1452264_at	tensin like C1 domain-containing phosphatase	Tenc1	1.02052	0.4492598	2.271558684
1447862_x_at	thrombospondin 2	Thbs2	0.822934	0.3066957	2.683226403
1448402_at	talin 1	Tln1	1.04078	0.3810707	2.731199224
1427178_at	transmembrane channel-like gene family 4	Tmc4	0.9744419	0.417049	2.336516572
1416342_at	tenascin C	Tnc	1.029385	0.2852299	3.60896596
1425028_a_at	tropomyosin 2, beta	Tpm2	1.448677	0.4786059	3.026868244
1427260_a_at	tropomyosin 3, gamma	Tpm3	1.037973	0.2600227	3.991855326
1433883_at	tropomyosin 4	Tpm4	0.9744828	0.1998876	4.875153836
1418884_x_at	tubulin, alpha 1	Tuba1	1.051218	0.3795708	2.769491225
1419417_at	vascular endothelial growth factor C	Vegfc	0.9949627	0.2787518	3.569349866
1439766_x_at	vascular endothelial growth factor C	Vegfc	1.003787	0.2302975	4.358653481
1440739_at	vascular endothelial growth factor C	Vegfc	0.9928586	0.190041	5.224444199
1421433_at	zinc finger homeodomain 4	Zfhx4	0.8848666	0.2799193	3.161148945
1439503_at	zinc finger protein 28	Zfp28	0.9780167	0.4356093	2.245169467
1441727_s_at	zinc finger protein 467	Zfp467	1.313801	0.545218	2.409680165
1451332_at	zinc finger protein 521	Zfp521	0.9459953	0.2777122	3.40638726
1449732_at	zinc finger proliferation 1	Zipro1	1.007825	0.3755597	2.683528078
1417534_at	integrin beta 5		0.9827138	0.3309045	2.969780707
1419821_s_at	isocitrate dehydrogenase 1 (NADP+), soluble		1.065771	0.1743847	6.111608415
1420172_at	Myosin heavy chain IX		1.07811	0.296866	3.631638517
1422433_s_at	isocitrate dehydrogenase 1 (NADP+), soluble		1.017639	0.1484655	6.854380311
1422437_at	Procollagen, type V, alpha 2		1.010339	0.1427277	7.078787089
1422518_at	calcium/calmodulin-dependent serine protein kinase		0.9997052	0.3313944	3.016662925
1422533_at	cytochrome P450, family 51		1.478172	0.6586778	2.244150327
1422619_at	phosphatidic acid phosphatase 2a		1.132388	0.215488	5.254993317
1427250_at	ATPase, Ca++ transporting, cardiac muscle, slow twitch 2		1.036569	0.2855148	3.630526333
1434380_at	Diabetic nephropathy-like protein (Dnr12) mRNA, partial sequence		0.7999971	0.2833473	2.82338
1434856_at	RIKEN cDNA E130014H08 gene [BLAST]		1.176473	0.2207611	5.329168046
1436699_x_at	ribosomal protein L18		1.060791	0.2722629	3.896201062
1437318_at	p21 (CDKN1A)-activated kinase 3 [BLAST]		1.321604	0.5923051	2.231289246
1438953_at			1.039987	0.3095478	3.359697598
1438954_x_at			1.10896	0.3355043	3.305352569
1441389_at	Transcribed locus		0.8743718	0.227116	3.849890805
1457042_at			0.8831247	0.3324246	2.656616568

table 7| genes downregulated after 6 hours of cyclic strain

Name	Description	Gene Symbol	6h stressed	6h relaxed	fold change
1417642_at	aldehyde dehydrogenase family 1, subfamily A3	Aldh1a3	0.276375	1.042324	0.265152678
1427395_a_at	aldehyde dehydrogenase family 1, subfamily A3	Aldh1a3	0.3194725	1.086401	0.294064991
1448789_at	aldehyde dehydrogenase family 1, subfamily A3	Aldh1a3	0.293036	1.19527	0.245163018
1420008_s_at	cDNA sequence BC037006	BC037006	0.7187271	1.523722	0.471691752
1427261_at	cDNA sequence BC037006	BC037006	1.022896	2.064228	0.495534408
1418096_at	docking protein 3	Dok3	0.8904615	2.043275	0.435801104
1425145_at	interleukin 1 receptor-like 1	Il1rl1	1.130348	2.823135	0.400387512
1419082_at	serine (or cysteine) proteinase inhibitor, clade B, member 2	Serpinb2	0.2833816	1.055686	0.268433606
1440527_at	Transcribed locus		0.4745028	1.421887	0.333713439
1450693_at	regulator of G-protein signaling 17		0.6805437	1.7683	0.384857603

V.3 LIST OF ABBREVIATIONS

abbreviation	full name	abbreveation	full name
BMD	Becker muscular dystrophy	MMP	matrix metallo proteinase
BS	bovine calf serum		
cDNA	coding desoxyribonucleic acid	MRI	magnetic resonance imaging
DCM	dilated cardiomyopathy	NfκB	nuclear factor kappa B
DM	differentiation medium		
DMD	Duchenne muscular dystrophy	siRNA	small interfering RNA
DMEM	dublecco's modified eagle medium		
DN	dominant-negative	ROS	reactive oxygen species
DNA	desoxyribonucleic acid	TBS	tris-buffered saline
dNTP	Deoxynucleotide Triphosphate	PAGE	polyacrylamide gel electrophoresis
ECM	extracellular matrix	OptiMEM	optimized modified eagle medium
EDMD	Emery-Dreifuss muscular dystrophy	ONM	outer nuclear membrane
ER	endoplasmic reticulum	Pa	Pascal
ERK	extracellular signal-related kinase	PBS	phosphate-buffered saline
FAK	focal adhesion kinase	PCR	polymerase chain reaction
FCS	fetal calf serum	PD	PD98059
		PNS	perinuclear space
FISH	fluorescent in-situ hybridization	QPCR	quantitative real-time PCR
		RNA	ribonucleic acid
FN	fibronectin		
GFP	green fluorescent protein	ROCK	Rho activated kinase
HGPS	Hutchinson-Gilford progeria syndrome	SDS	sodium dodecyl sulfate
HS	horse serum	SEAP	secreted alkaline phosphatase
Hz	Hertz	SRF	serum response factor
ILK	integrin linked kinase	TBS-T	factor tris-buffered saline with Tween
INM	inner nuclear membrane	TCF	ternary complex
KASH	Klarsicht homology	TGFβ	transforming growth factor beta
kDa	kilo-Dalton	TNFα	tumor necrosis factor alpha
LMNA	lamin A gene	TN-C	tenascin C
MAL	megakaryoblastic leukemia	TN-R	tenascin R
MAPK	mitogen activated protein kinase	TN-W	tenascin W
MEF	mouse embryo fibroblast	TN-X	tenascin X
mRNA	messenger RNA	Y	Y27632

V.4 LIST OF FIGURES

chapter II

chapter III

chapter IV

V.5 REFERENCES

diss

1. Hutchison, C.J., M. Alvarez-Reyes, and O.A. Vaughan, *Lamins in disease: why do ubiquitously expressed nuclear envelope proteins give rise to tissue-specific disease phenotypes?* J Cell Sci, 2001. **114**(Pt 1): p. 9-19.
2. Lammerding, J., et al., *Lamins A and C but not lamin B1 regulate nuclear mechanics.* J Biol Chem, 2006. **281**(35): p. 25768-80.
3. Lammerding, J., et al., *Abnormal nuclear shape and impaired mechanotransduction in emerin-deficient cells.* J Cell Biol, 2005. **170**(5): p. 781-91.
4. Lammerding, J. and R.T. Lee, *Torn apart: membrane rupture in muscular dystrophies and associated cardiomyopathies.* J Clin Invest, 2007. **117**(7): p. 1749-52.
5. Lammerding, J., et al., *Lamin A/C deficiency causes defective nuclear mechanics and mechanotransduction.* J Clin Invest, 2004. **113**(3): p. 370-8.
6. Akimoto, T., et al., *Mechanical stretch inhibits myoblast-to-adipocyte differentiation through Wnt signaling.* Biochem Biophys Res Commun, 2005. **329**(1): p. 381-5.
7. Kook, S.H., et al., *Cyclic mechanical stress suppresses myogenic differentiation of adult bovine satellite cells through activation of extracellular signal-regulated kinase.* Mol Cell Biochem, 2008. **309**(1-2): p. 133-41.
8. Kumar, A., et al., *Cyclic mechanical strain inhibits skeletal myogenesis through activation of focal adhesion kinase, Rac-1 GTPase, and NF-kappaB transcription factor.* FASEB J, 2004. **18**(13): p. 1524-35.
9. Vogel, V., *Mechanotransduction involving multimodular proteins: converting force into biochemical signals.* Annu Rev Biophys Biomol Struct, 2006. **35**: p. 459-88.
10. Vogel, V. and M. Sheetz, *Local force and geometry sensing regulate cell functions.* Nat Rev Mol Cell Biol, 2006. **7**(4): p. 265-75.
11. Paszek, M.J., et al., *Tensional homeostasis and the malignant phenotype.* Cancer Cell, 2005. **8**(3): p. 241-54.
12. Jaalouk, D.E. and J. Lammerding, *Mechanotransduction gone awry.* Nat Rev Mol Cell Biol, 2009. **10**(1): p. 63-73.
13. Butcher, D.T., T. Alliston, and V.M. Weaver, *A tense situation: forcing tumour progression.* Nat Rev Cancer, 2009. **9**(2): p. 108-22.
14. Ingber, D.E., *Cellular mechanotransduction: putting all the pieces together again.* FASEB J, 2006. **20**(7): p. 811-27.
15. Bakker, A.D., J. Klein-Nulend, and E.H. Burger, *Mechanotransduction in bone cells proceeds via activation of COX-2, but not COX-1.* Biochem Biophys Res Commun, 2003. **305**(3): p. 677-83.
16. Burger, E.H. and J. Klein-Nulend, *Mechanotransduction in bone--role of the lacuno-canalicular network.* FASEB J, 1999. **13 Suppl**: p. S101-12.
17. Klein-Nulend, J., et al., *Microgravity and bone cell mechanosensitivity.* Adv Space Res, 2003. **32**(8): p. 1551-9.
18. Fluck, M., et al., *Reloading of atrophied rat soleus muscle induces tenascin-C expression around damaged muscle fibers.* Am J Physiol Regul Integr Comp Physiol, 2003. **284**(3): p. R792-801.
19. Lammerding, J., R.D. Kamm, and R.T. Lee, *Mechanotransduction in cardiac myocytes.* Ann N Y Acad Sci, 2004. **1015**: p. 53-70.
20. Pritchard, W.F., et al., *Effects of wall shear stress and fluid recirculation on the localization of circulating monocytes in a three-dimensional flow model.* J Biomech, 1995. **28**(12): p. 1459-69.

21. Takahashi, M., et al., *Mechanotransduction in endothelial cells: temporal signaling events in response to shear stress.* J Vasc Res, 1997. **34**(3): p. 212-9.
22. Garcia-Cardena, G., et al., *Biomechanical activation of vascular endothelium as a determinant of its functional phenotype.* Proc Natl Acad Sci U S A, 2001. **98**(8): p. 4478-85.
23. Gimbrone, M.A., Jr., et al., *Endothelial dysfunction, hemodynamic forces, and atherogenesis.* Ann N Y Acad Sci, 2000. **902**: p. 230-9; discussion 239-40.
24. Haga, J.H., Y.S. Li, and S. Chien, *Molecular basis of the effects of mechanical stretch on vascular smooth muscle cells.* J Biomech, 2007. **40**(5): p. 947-60.
25. Li, Y.S., J.H. Haga, and S. Chien, *Molecular basis of the effects of shear stress on vascular endothelial cells.* J Biomech, 2005. **38**(10): p. 1949-71.
26. Hammerschmidt, S., et al., *Stretch-induced alveolar type II cell apoptosis: role of endogenous bradykinin and PI3K-Akt signaling.* Am J Respir Cell Mol Biol, 2007. **37**(6): p. 699-705.
27. Wozniak, M.A. and C.S. Chen, *Mechanotransduction in development: a growing role for contractility.* Nat Rev Mol Cell Biol, 2009. **10**(1): p. 34-43.
28. Engler, A.J., et al., *Matrix elasticity directs stem cell lineage specification.* Cell, 2006. **126**(4): p. 677-89.
29. Ingber, D.E., *Mechanical control of tissue morphogenesis during embryological development.* Int J Dev Biol, 2006. **50**(2-3): p. 255-66.
30. Sarasa-Renedo, A., V. Tunc-Civelek, and M. Chiquet, *Role of RhoA/ROCK-dependent actin contractility in the induction of tenascin-C by cyclic tensile strain.* Exp Cell Res, 2006. **312**(8): p. 1361-70.
31. Chiquet, M., A. Sarasa-Renedo, and V. Tunc-Civelek, *Induction of tenascin-C by cyclic tensile strain versus growth factors: distinct contributions by Rho/ROCK and MAPK signaling pathways.* Biochim Biophys Acta, 2004. **1693**(3): p. 193-204.
32. Chiquet, M., et al., *How do fibroblasts translate mechanical signals into changes in extracellular matrix production?* Matrix Biol, 2003. **22**(1): p. 73-80.
33. Clark, E.A., et al., *Integrin-mediated signals regulated by members of the rho family of GTPases.* J Cell Biol, 1998. **142**(2): p. 573-86.
34. Cox, E.A., S.K. Sastry, and A. Huttenlocher, *Integrin-mediated adhesion regulates cell polarity and membrane protrusion through the Rho family of GTPases.* Mol Biol Cell, 2001. **12**(2): p. 265-77.
35. Chess, P.R., L. Toia, and J.N. Finkelstein, *Mechanical strain-induced proliferation and signaling in pulmonary epithelial H441 cells.* Am J Physiol Lung Cell Mol Physiol, 2000. **279**(1): p. L43-51.
36. Milkiewicz, M., et al., *Static strain stimulates expression of matrix metalloproteinase-2 and VEGF in microvascular endothelium via JNK- and ERK-dependent pathways.* J Cell Biochem, 2007. **100**(3): p. 750-61.
37. Chaturvedi, L.S., et al., *Repetitive deformation activates focal adhesion kinase and ERK mitogenic signals in human Caco-2 intestinal epithelial cells through Src and Rac1.* J Biol Chem, 2007. **282**(1): p. 14-28.
38. Ahn, K.S., et al., *Deficiency of NRH:quinone oxidoreductase 2 differentially regulates TNF signaling in keratinocytes: up-regulation of apoptosis correlates with down-regulation of cell survival kinases.* Cancer Res, 2007. **67**(20): p. 10004-11.
39. Kippenberger, S., et al., *Signaling of mechanical stretch in human keratinocytes via MAP kinases.* J Invest Dermatol, 2000. **114**(3): p. 408-12.
40. Kippenberger, S., et al., *Melanocytes respond to mechanical stretch by activation of mitogen-activated protein kinases (MAPK).* Pigment Cell Res, 2000. **13**(4): p. 278-80.
41. Plotkin, L.I., et al., *Mechanical stimulation prevents osteocyte apoptosis: requirement of integrins, Src kinases, and ERKs.* Am J Physiol Cell Physiol, 2005. **289**(3): p. C633-43.
42. Sawada, Y., et al., *Force sensing by mechanical extension of the Src family kinase substrate p130Cas.* Cell, 2006. **127**(5): p. 1015-26.

43. Tamada, M., M.P. Sheetz, and Y. Sawada, *Activation of a signaling cascade by cytoskeleton stretch.* Dev Cell, 2004. **7**(5): p. 709-18.
44. Lee, J.G. and E.P. Kay, *Cross-talk among Rho GTPases acting downstream of PI 3-kinase induces mesenchymal transformation of corneal endothelial cells mediated by FGF-2.* Invest Ophthalmol Vis Sci, 2006. **47**(6): p. 2358-68.
45. Lin, G., et al., *Acute inhibition of Rho-kinase improves cardiac contractile function in streptozotocin-diabetic rats.* Cardiovasc Res, 2007. **75**(1): p. 51-8.
46. Geiger, B., et al., *Transmembrane crosstalk between the extracellular matrix--cytoskeleton crosstalk.* Nat Rev Mol Cell Biol, 2001. **2**(11): p. 793-805.
47. Geiger, B. and A. Bershadsky, *Assembly and mechanosensory function of focal contacts.* Curr Opin Cell Biol, 2001. **13**(5): p. 584-92.
48. Kumar, A. and A.M. Boriek, *Mechanical stress activates the nuclear factor-kappaB pathway in skeletal muscle fibers: a possible role in Duchenne muscular dystrophy.* FASEB J, 2003. **17**(3): p. 386-96.
49. Creton, R., J.A. Kreiling, and L.F. Jaffe, *Calcium imaging with chemiluminescence.* Microsc Res Tech, 1999. **46**(6): p. 390-7.
50. Rohatgi, R., et al., *Mechanoregulation of intracellular Ca2+ in human autosomal recessive polycystic kidney disease cyst-lining renal epithelial cells.* Am J Physiol Renal Physiol, 2008. **294**(4): p. F890-9.
51. Guharay, F. and F. Sachs, *Stretch-activated single ion channel currents in tissue-cultured embryonic chick skeletal muscle.* J Physiol, 1984. **352**: p. 685-701.
52. Brehm, P., R. Kullberg, and F. Moody-Corbett, *Properties of non-junctional acetylcholine receptor channels on innervated muscle of Xenopus laevis.* J Physiol, 1984. **350**: p. 631-48.
53. Sukharev, S.I., et al., *Two types of mechanosensitive channels in the Escherichia coli cell envelope: solubilization and functional reconstitution.* Biophys J, 1993. **65**(1): p. 177-83.
54. Kubalski, A., et al., *Activities of a mechanosensitive ion channel in an E. coli mutant lacking the major lipoprotein.* J Membr Biol, 1993. **131**(3): p. 151-60.
55. Morris, A.P., K.L. Kirk, and R.A. Frizzell, *Simultaneous analysis of cell Ca2+ and Ca2(+)-stimulated chloride conductance in colonic epithelial cells (HT-29).* Cell Regul, 1990. **1**(12): p. 951-63.
56. Ingber, D.E., *Integrins, tensegrity, and mechanotransduction.* Gravit Space Biol Bull, 1997. **10**(2): p. 49-55.
57. Ingber, D.E., *Tensegrity: the architectural basis of cellular mechanotransduction.* Annu Rev Physiol, 1997. **59**: p. 575-99.
58. Ingber, D.E., *Opposing views on tensegrity as a structural framework for understanding cell mechanics.* J Appl Physiol, 2000. **89**(4): p. 1663-70.
59. Ingber, D.E., *Tensegrity II. How structural networks influence cellular information processing networks.* J Cell Sci, 2003. **116**(Pt 8): p. 1397-408.
60. Ingber, D.E., *Tensegrity I. Cell structure and hierarchical systems biology.* J Cell Sci, 2003. **116**(Pt 7): p. 1157-73.
61. Bresnick, A.R., *Molecular mechanisms of nonmuscle myosin-II regulation.* Curr Opin Cell Biol, 1999. **11**(1): p. 26-33.
62. Mogilner, A. and G. Oster, *Force generation by actin polymerization II: the elastic ratchet and tethered filaments.* Biophys J, 2003. **84**(3): p. 1591-605.
63. Beningo, K.A., C.M. Lo, and Y.L. Wang, *Flexible polyacrylamide substrata for the analysis of mechanical interactions at cell-substratum adhesions.* Methods Cell Biol, 2002. **69**: p. 325-39.
64. Ingber, D.E., *Tensegrity and mechanotransduction.* J Bodyw Mov Ther, 2008. **12**(3): p. 198-200.
65. Wang, N., J.P. Butler, and D.E. Ingber, *Mechanotransduction across the cell surface and through the cytoskeleton.* Science, 1993. **260**(5111): p. 1124-7.
66. Wang, N., et al., *Mechanical behavior in living cells consistent with the tensegrity model.* Proc Natl Acad Sci U S A, 2001. **98**(14): p. 7765-70.

67. Zhao, X.H., et al., *Force activates smooth muscle alpha-actin promoter activity through the Rho signaling pathway.* J Cell Sci, 2007. **120**(Pt 10): p. 1801-9.
68. Galbraith, C.G., K.M. Yamada, and M.P. Sheetz, *The relationship between force and focal complex development.* J Cell Biol, 2002. **159**(4): p. 695-705.
69. Choquet, D., D.P. Felsenfeld, and M.P. Sheetz, *Extracellular matrix rigidity causes strengthening of integrin-cytoskeleton linkages.* Cell, 1997. **88**(1): p. 39-48.
70. Bloom, S., V.G. Lockard, and M. Bloom, *Intermediate filament-mediated stretch-induced changes in chromatin: a hypothesis for growth initiation in cardiac myocytes.* J Mol Cell Cardiol, 1996. **28**(10): p. 2123-7.
71. Bustamante, C., Z. Bryant, and S.B. Smith, *Ten years of tension: single-molecule DNA mechanics.* Nature, 2003. **421**(6921): p. 423-7.
72. Maniotis, A.J., C.S. Chen, and D.E. Ingber, *Demonstration of mechanical connections between integrins, cytoskeletal filaments, and nucleoplasm that stabilize nuclear structure.* Proc Natl Acad Sci U S A, 1997. **94**(3): p. 849-54.
73. Knight, M.M., et al., *Chondrocyte deformation induces mitochondrial distortion and heterogeneous intracellular strain fields.* Biomech Model Mechanobiol, 2006. **5**(2-3): p. 180-91.
74. Silberberg, Y.R., et al., *Mitochondrial displacements in response to nanomechanical forces.* J Mol Recognit, 2008. **21**(1): p. 30-6.
75. Crisp, M., et al., *Coupling of the nucleus and cytoplasm: role of the LINC complex.* J Cell Biol, 2006. **172**(1): p. 41-53.
76. Mislow, J.M., et al., *Nesprin-1alpha self-associates and binds directly to emerin and lamin A in vitro.* FEBS Lett, 2002. **525**(1-3): p. 135-40.
77. Mislow, J.M., et al., *Myne-1, a spectrin repeat transmembrane protein of the myocyte inner nuclear membrane, interacts with lamin A/C.* J Cell Sci, 2002. **115**(Pt 1): p. 61-70.
78. Zhang, Q., et al., *The nesprins are giant actin-binding proteins, orthologous to Drosophila melanogaster muscle protein MSP-300.* Genomics, 2002. **80**(5): p. 473-81.
79. Padmakumar, V.C., et al., *Enaptin, a giant actin-binding protein, is an element of the nuclear membrane and the actin cytoskeleton.* Exp Cell Res, 2004. **295**(2): p. 330-9.
80. Starr, D.A. and M. Han, *Role of ANC-1 in tethering nuclei to the actin cytoskeleton.* Science, 2002. **298**(5592): p. 406-9.
81. Patterson, K., et al., *The functions of Klarsicht and nuclear lamin in developmentally regulated nuclear migrations of photoreceptor cells in the Drosophila eye.* Mol Biol Cell, 2004. **15**(2): p. 600-10.
82. Wilhelmsen, K., et al., *Nesprin-3, a novel outer nuclear membrane protein, associates with the cytoskeletal linker protein plectin.* J Cell Biol, 2005. **171**(5): p. 799-810.
83. Luke, Y., et al., *Nesprin-2 Giant (NUANCE) maintains nuclear envelope architecture and composition in skin.* J Cell Sci, 2008. **121**(Pt 11): p. 1887-98.
84. Haque, F., et al., *SUN1 interacts with nuclear lamin A and cytoplasmic nesprins to provide a physical connection between the nuclear lamina and the cytoskeleton.* Mol Cell Biol, 2006. **26**(10): p. 3738-51.
85. Liu, J., et al., *Essential roles for Caenorhabditis elegans lamin gene in nuclear organization, cell cycle progression, and spatial organization of nuclear pore complexes.* Mol Biol Cell, 2000. **11**(11): p. 3937-47.
86. Holt, I., et al., *The R482Q lamin A/C mutation that causes lipodystrophy does not prevent nuclear targeting of lamin A in adipocytes or its interaction with emerin.* Eur J Hum Genet, 2001. **9**(3): p. 204-8.
87. Sullivan, T., et al., *Loss of A-type lamin expression compromises nuclear envelope integrity leading to muscular dystrophy.* J Cell Biol, 1999. **147**(5): p. 913-20.
88. Biamonti, G., et al., *The gene for a novel human lamin maps at a highly transcribed locus of chromosome 19 which replicates at the onset of S-phase.* Mol Cell Biol, 1992. **12**(8): p. 3499-506.

89. Lin, F. and H.J. Worman, *Structural organization of the human gene encoding nuclear lamin A and nuclear lamin C.* J Biol Chem, 1993. **268**(22): p. 16321-6.
90. Lin, F. and H.J. Worman, *Structural organization of the human gene (LMNB1) encoding nuclear lamin B1.* Genomics, 1995. **27**(2): p. 230-6.
91. Furukawa, K., H. Inagaki, and Y. Hotta, *Identification and cloning of an mRNA coding for a germ cell-specific A-type lamin in mice.* Exp Cell Res, 1994. **212**(2): p. 426-30.
92. Machiels, B.M., et al., *An alternative splicing product of the lamin A/C gene lacks exon 10.* J Biol Chem, 1996. **271**(16): p. 9249-53.
93. Harborth, J., et al., *Identification of essential genes in cultured mammalian cells using small interfering RNAs.* J Cell Sci, 2001. **114**(Pt 24): p. 4557-65.
94. Gruenbaum, Y., et al., *Review: nuclear lamins--structural proteins with fundamental functions.* J Struct Biol, 2000. **129**(2-3): p. 313-23.
95. Moore, K.A., et al., *Control of basement membrane remodeling and epithelial branching morphogenesis in embryonic lung by Rho and cytoskeletal tension.* Dev Dyn, 2005. **232**(2): p. 268-81.
96. Le Beyec, J., et al., *Cell shape regulates global histone acetylation in human mammary epithelial cells.* Exp Cell Res, 2007. **313**(14): p. 3066-75.
97. Chiquet, M., et al., *From mechanotransduction to extracellular matrix gene expression in fibroblasts.* Biochim Biophys Acta, 2009.
98. Degen, M., et al., *Tenascin-W is a novel marker for activated tumor stroma in low-grade human breast cancer and influences cell behavior.* Cancer Res, 2007. **67**(19): p. 9169-79.
99. Fluck, M., et al., *Tensile stress-dependent collagen XII and fibronectin production by fibroblasts requires separate pathways.* Biochim Biophys Acta, 2003. **1593**(2-3): p. 239-48.
100. Huang, S. and D.E. Ingber, *Cell tension, matrix mechanics, and cancer development.* Cancer Cell, 2005. **8**(3): p. 175-6.
101. Paszek, M.J. and V.M. Weaver, *The tension mounts: mechanics meets morphogenesis and malignancy.* J Mammary Gland Biol Neoplasia, 2004. **9**(4): p. 325-42.
102. Zahir, N. and V.M. Weaver, *Death in the third dimension: apoptosis regulation and tissue architecture.* Curr Opin Genet Dev, 2004. **14**(1): p. 71-80.
103. Weaver, V.M. and P. Gilbert, *Watch thy neighbor: cancer is a communal affair.* J Cell Sci, 2004. **117**(Pt 8): p. 1287-90.
104. Weaver, V.M., et al., *The importance of the microenvironment in breast cancer progression: recapitulation of mammary tumorigenesis using a unique human mammary epithelial cell model and a three-dimensional culture assay.* Biochem Cell Biol, 1996. **74**(6): p. 833-51.
105. Huang, S. and D.E. Ingber, *The structural and mechanical complexity of cell-growth control.* Nat Cell Biol, 1999. **1**(5): p. E131-8.
106. Yee, K.L., V.M. Weaver, and D.A. Hammer, *Integrin-mediated signalling through the MAP-kinase pathway.* IET Syst Biol, 2008. **2**(1): p. 8-15.
107. Lopez, J.I., J.K. Mouw, and V.M. Weaver, *Biomechanical regulation of cell orientation and fate.* Oncogene, 2008. **27**(55): p. 6981-93.
108. Hebner, C., V.M. Weaver, and J. Debnath, *Modeling morphogenesis and oncogenesis in three-dimensional breast epithelial cultures.* Annu Rev Pathol, 2008. **3**: p. 313-39.
109. Barry, S.P., et al., *Role of the JAK-STAT pathway in myocardial injury.* Trends Mol Med, 2007. **13**(2): p. 82-9.
110. Kumar, A., et al., *Loss of dystrophin causes aberrant mechanotransduction in skeletal muscle fibers.* FASEB J, 2004. **18**(1): p. 102-13.
111. Hoshijima, M., *Mechanical stress-strain sensors embedded in cardiac cytoskeleton: Z disk, titin, and associated structures.* Am J Physiol Heart Circ Physiol, 2006. **290**(4): p. H1313-25.
112. Emery, A.E., *The muscular dystrophies.* Lancet, 2002. **359**(9307): p. 687-95.
113. Blake, D.J., et al., *Function and genetics of dystrophin and dystrophin-related proteins in muscle.* Physiol Rev, 2002. **82**(2): p. 291-329.

114. Durbeej, M. and K.P. Campbell, *Muscular dystrophies involving the dystrophin-glycoprotein complex: an overview of current mouse models.* Curr Opin Genet Dev, 2002. **12**(3): p. 349-61.
115. Lapidos, K.A., R. Kakkar, and E.M. McNally, *The dystrophin glycoprotein complex: signaling strength and integrity for the sarcolemma.* Circ Res, 2004. **94**(8): p. 1023-31.
116. Heydemann, A. and E.M. McNally, *Consequences of disrupting the dystrophin-sarcoglycan complex in cardiac and skeletal myopathy.* Trends Cardiovasc Med, 2007. **17**(2): p. 55-9.
117. Heydemann, A., K.R. Doherty, and E.M. McNally, *Genetic modifiers of muscular dystrophy: implications for therapy.* Biochim Biophys Acta, 2007. **1772**(2): p. 216-28.
118. Claflin, D.R. and S.V. Brooks, *Direct observation of failing fibers in muscles of dystrophic mice provides mechanistic insight into muscular dystrophy.* Am J Physiol Cell Physiol, 2008. **294**(2): p. C651-8.
119. Jimenez-Mallebrera, C., et al., *Congenital muscular dystrophy: molecular and cellular aspects.* Cell Mol Life Sci, 2005. **62**(7-8): p. 809-23.
120. Roux, K.J., et al., *Nesprin 4 is an outer nuclear membrane protein that can induce kinesin-mediated cell polarization.* Proc Natl Acad Sci U S A, 2009.
121. Wheeler, M.A., et al., *Distinct functional domains in nesprin-1[alpha] and nesprin-2[beta] bind directly to emerin and both interactions are disrupted in X-linked Emery-Dreifuss muscular dystrophy.* Experimental Cell Research, 2007. **313**(13): p. 2845-2857.
122. Ji, J.Y., et al., *Cell nuclei spin in the absence of lamin b1.* J Biol Chem, 2007. **282**(27): p. 20015-26.
123. Zhang, Q., et al., *Nesprin-1 and -2 are involved in the pathogenesis of Emery Dreifuss muscular dystrophy and are critical for nuclear envelope integrity.* Hum. Mol. Genet., 2007. **16**(23): p. 2816-2833.
124. Puckelwartz, M.J., et al., *Disruption of nesprin-1 produces an Emery Dreifuss muscular dystrophy-like phenotype in mice.* Hum. Mol. Genet., 2009. **18**(4): p. 607-620.
125. Starr, D.A., et al., *unc-83 encodes a novel component of the nuclear envelope and is essential for proper nuclear migration.* Development, 2001. **128**(24): p. 5039-50.
126. Malone, C.J., et al., *UNC-84 localizes to the nuclear envelope and is required for nuclear migration and anchoring during C. elegans development.* Development, 1999. **126**(14): p. 3171-81.
127. Capell, B.C., F.S. Collins, and E.G. Nabel, *Mechanisms of cardiovascular disease in accelerated aging syndromes.* Circ Res, 2007. **101**(1): p. 13-26.
128. Cao, K., et al., *A lamin A protein isoform overexpressed in Hutchinson-Gilford progeria syndrome interferes with mitosis in progeria and normal cells.* Proc Natl Acad Sci U S A, 2007. **104**(12): p. 4949-54.
129. Verstraeten, V.L., et al., *Increased mechanosensitivity and nuclear stiffness in Hutchinson-Gilford progeria cells: effects of farnesyltransferase inhibitors.* Aging Cell, 2008. **7**(3): p. 383-93.
130. Raharjo, W.H., et al., *Nuclear envelope defects associated with LMNA mutations cause dilated cardiomyopathy and Emery-Dreifuss muscular dystrophy.* J Cell Sci, 2001. **114**(Pt 24): p. 4447-57.
131. Cockell, M. and S.M. Gasser, *Nuclear compartments and gene regulation.* Curr Opin Genet Dev, 1999. **9**(2): p. 199-205.
132. Cockell, M.M. and S.M. Gasser, *The nucleolus: nucleolar space for RENT.* Curr Biol, 1999. **9**(15): p. R575-6.
133. De Keulenaer, G.W., et al., *Identification of IEX-1 as a biomechanically controlled nuclear factor-kappaB target gene that inhibits cardiomyocyte hypertrophy.* Circ Res, 2002. **90**(6): p. 690-6.
134. Dhe-Paganon, S., et al., *Structure of the globular tail of nuclear lamin.* J Biol Chem, 2002. **277**(20): p. 17381-4.

135. Krimm, I., et al., *The Ig-like structure of the C-terminal domain of lamin A/C, mutated in muscular dystrophies, cardiomyopathy, and partial lipodystrophy.* Structure, 2002. **10**(6): p. 811-23.
136. Lloyd, D.J., R.C. Trembath, and S. Shackleton, *A novel interaction between lamin A and SREBP1: implications for partial lipodystrophy and other laminopathies.* Hum Mol Genet, 2002. **11**(7): p. 769-77.
137. Ostlund, C., et al., *Properties of lamin A mutants found in Emery-Dreifuss muscular dystrophy, cardiomyopathy and Dunnigan-type partial lipodystrophy.* J Cell Sci, 2001. **114**(Pt 24): p. 4435-45.
138. Mounkes, L., et al., *The laminopathies: nuclear structure meets disease.* Curr Opin Genet Dev, 2003. **13**(3): p. 223-30.
139. Tan, J.C., F.B. Kalapesi, and M.T. Coroneo, *Mechanosensitivity and the eye: cells coping with the pressure.* Br J Ophthalmol, 2006. **90**(3): p. 383-8.
140. Cui, W., et al., *Changes in gene expression in response to mechanical strain in human scleral fibroblasts.* Exp Eye Res, 2004. **78**(2): p. 275-84.
141. Chiquet-Ehrismann, R., *Tenascins.* Int J Biochem Cell Biol, 2004. **36**(6): p. 986-90.
142. Chiquet-Ehrismann, R. and M. Chiquet, *Tenascins: regulation and putative functions during pathological stress.* J Pathol, 2003. **200**(4): p. 488-99.
143. Scherberich, A., et al., *Murine tenascin-W: a novel mammalian tenascin expressed in kidney and at sites of bone and smooth muscle development.* J Cell Sci, 2004. **117**(Pt 4): p. 571-81.
144. Jones, F.S. and P.L. Jones, *The tenascin family of ECM glycoproteins: structure, function, and regulation during embryonic development and tissue remodeling.* Dev Dyn, 2000. **218**(2): p. 235-59.
145. Jones, P.L. and F.S. Jones, *Tenascin-C in development and disease: gene regulation and cell function.* Matrix Biol, 2000. **19**(7): p. 581-96.
146. Chiquet, M. and M. Fluck, *Ectopic expression of tenascin-C.* J Cell Sci, 2003. **116**(Pt 19): p. 3851; author reply 3851-3; discussion 3853.
147. Bourdon, M.A., et al., *Human glioma-mesenchymal extracellular matrix antigen defined by monoclonal antibody.* Cancer Res, 1983. **43**(6): p. 2796-805.
148. Chiquet, M. and D.M. Fambrough, *Chick myotendinous antigen. I. A monoclonal antibody as a marker for tendon and muscle morphogenesis.* J Cell Biol, 1984. **98**(6): p. 1926-36.
149. Chiquet, M. and D.M. Fambrough, *Chick myotendinous antigen. II. A novel extracellular glycoprotein complex consisting of large disulfide-linked subunits.* J Cell Biol, 1984. **98**(6): p. 1937-46.
150. Fluck, M., V. Tunc-Civelek, and M. Chiquet, *Rapid and reciprocal regulation of tenascin-C and tenascin-Y expression by loading of skeletal muscle.* J Cell Sci, 2000. **113 (Pt 20)**: p. 3583-91.
151. Mumberg, D., et al., *Alternative splicing of fosB transcripts results in differentially expressed mRNAs encoding functionally antagonistic proteins.* Genes Dev, 1991. **5**(7): p. 1212-23.
152. Inoue, D., S. Kido, and T. Matsumoto, *Transcriptional induction of FosB/DeltaFosB gene by mechanical stress in osteoblasts.* J Biol Chem, 2004. **279**(48): p. 49795-803.
153. Lammerding, J. and R.T. Lee, *The nuclear membrane and mechanotransduction: impaired nuclear mechanics and mechanotransduction in lamin A/C deficient cells.* Novartis Found Symp, 2005. **264**: p. 264-73; discussion 273-8.
154. Kim, Y.B., et al., *Cell adhesion status-dependent histone acetylation is regulated through intracellular contractility-related signaling activities.* J Biol Chem, 2005. **280**(31): p. 28357-64.
155. Levy, J.R. and E.L. Holzbaur, *Dynein drives nuclear rotation during forward progression of motile fibroblasts.* J Cell Sci, 2008. **121**(Pt 19): p. 3187-95.
156. Takemasa, T., K. Sugimoto, and K. Yamashita, *Amplitude-dependent stress fiber reorientation in early response to cyclic strain.* Exp Cell Res, 1997. **230**(2): p. 407-10.
157. Ingber, D.E., *Mechanobiology and diseases of mechanotransduction.* Ann Med, 2003. **35**(8): p. 564-77.

158. Mack, P.J., et al., *Force-induced focal adhesion translocation: effects of force amplitude and frequency.* Am J Physiol Cell Physiol, 2004. **287**(4): p. C954-62.
159. Ozawa, R., et al., *Emerin-Lacking Mice Show Minimal Motor and Cardiac Dysfunctions with Nuclear-Associated Vacuoles.* Am J Pathol, 2006. **168**(3): p. 907-917.
160. Melcon, G., et al., *Loss of emerin at the nuclear envelope disrupts the Rb1/E2F and MyoD pathways during muscle regeneration.* Hum. Mol. Genet., 2006. **15**(4): p. 637-651.
161. Gallitano-Mendel, A., et al., *Mice lacking the immediate early gene Egr3 respond to the anti-aggressive effects of clozapine yet are relatively resistant to its sedating effects.* Neuropsychopharmacology, 2008. **33**(6): p. 1266-75.
162. Tourtellotte, W.G., et al., *The transcription factor Egr3 modulates sensory axon-myotube interactions during muscle spindle morphogenesis.* Dev Biol, 2001. **232**(2): p. 388-99.
163. Tourtellotte, W.G. and J. Milbrandt, *Sensory ataxia and muscle spindle agenesis in mice lacking the transcription factor Egr3.* Nat Genet, 1998. **20**(1): p. 87-91.
164. Pfaffl, M.W., *A new mathematical model for relative quantification in real-time RT-PCR.* Nucleic Acids Res, 2001. **29**(9): p. e45.

V.6 CURRICULUM VITAE

PERSONAL INFORMATION

First Name:	Michaela
Middle Name:	Inge
Family Name:	Brosig
Title:	Dr. Phil II
Address:	Spalentorweg 42
	4051 Basel, Switzerland
Nationality:	German
Place of Birth:	Munich, Germany
Date of Birth:	December 20th 1977
Marital Status:	Unmarried

EDUCATION AND WORK

EDUCATIONAL BACKGROUND

Jan 2005 – Oct 2009	**PhD thesis** in the lab of **Dr. Ruth Chiquet-Ehrismann** at the Friedrich Miescher Institute, Basel, Switzerland Mechanotransduction in Fibroblasts
July 2003 – July 2004	**Diploma thesis** In the lab of Prof. Dr. Dieter Marmé and Dr. Ralph Graeser at ProQinase GmbH, Freiburg, Germany Functional characterization of p21-activated kinases (PAK) 1, 2, and 4
Oct 2000 – June 2003	**Diploma** at the Albert-Ludwig-University, Freiburg, Germany Cell Biology and Bioinformatics
Oct 1998 – Oct 2000	**Bachelor** at the Technical University, Munich, Germany General Biology
Sep 1988 – July 1997	**High School** Gymnasium Kirchheim, Munich, Germany

INTERNATIONAL EXPERIENCE

Aug 2002 – Dec 2002	**Toronto, Canada** Internship in the lab of Prof. Dr. Emil Pai, Ontario Cancer Institute
Sep 1997 – Oct 1998	**Palo Alto, CA, USA** Language stay as an Au Pair

WORK EXPERIENCE

Sep 2004 – Dec 2004	**ATG Biosynthetics**, Freiburg, Germany Database programming
Jan 2003 – Jul 2003	**Max Planck Institute for Immunobiology**, Freiburg, Germany Internship in the lab of Dr. Ursula Klingmüller General methods of cell biology and biochemistry
Aug 2002 – Dec 2002	**Ontario Cancer Institute**, Toronto, Canada Internship in the lab of Prof. Dr. Emil Pai Protein purification and X-ray crystallography

SPECIAL SKILLS AND EXPERIENCES

Professional	**Student representative** at the Friedrich Miescher Institute, Basel, Switzerland (organized seminars, meetings and other events for the institute) Various times **tutor** for medical and biology students
Computer skills	Profound IT-knowledge, familiar with **Windows, MacOS and Linux** Excellent knowledge of Office, Adobe Creative Suite Programming in Java, HTML and use of R (for statistics)
Languages	**German:** native language **English:** excellent (written and spoken) **French:** basic (written and spoken)

HOBBIES

Music	Playing and teaching Basel piccolo in a carnival clique (Opti-Mischte) Flute, concert piccolo, piano Fife in an American fife and drum corps (Grey Coats)
Sports	Running, rock climbing, skiing
Other	Travelling, Photography

PUBLICATIONS & SCIENTIFIC CONTRIBUTIONS

POSTERS

EACR Meeting (cancer research)
July 3 – July 6, 2004, Innsbruck, Austria
Functional Characterization of p21-activated kinases (PAK) 1, 2, and 4
Michaela Brosig, Sarah Umber, Michael H. G. Kubbutat, and Ralph Graeser
ELSO Meeting (cell signaling)

FECTS Meeting (cell signaling)
July 1-5, 2006, Oulu, Finland
Regulation of gene expression by mechanical stimulation of fibroblasts
Michaela Brosig, Matthias Chiquet, and Ruth Chiquet-Ehrismann

USGEB Meeting (cell biology)
February 6-7, 2008, Lausanne, Switzerland
The role of the nuclear membrane proteins Sun1 and Nesprins in mechanotransduction
Michaela Brosig, Jacqueline Ferralli, Matthias Chiquet, and Ruth Chiquet-Ehrismann

ELSO Meeting (cell signaling)
August 30 – September 2, 2008, Nice, France
Turning on the stress-response in fibroblasts: stretching leads to nuclear rotation and activation of NfκB signaling
Michaela Brosig, Jacqueline Ferralli, Matthias Chiquet, and Ruth Chiquet-Ehrismann

PUBLICATIONS

Graeser, R., Umber, S., **Brosig, M**., and Kubbutat, M.H.G.,
Highly efficient gene silencing using 2-for-Silencing siRNA Duplexes targeting protein kinase genes
Qiagen News 2004, e32

Graeser, R., Umber, S., **Brosig, M.,** and Kubbutat, M.H.G.,
The HiPerformance algorithm designs highly potent and specific siRNA
Qiagen News 2004, Technical Information

Brosig, M., Ferralli, J., Gelman, L., Chiquet, M., and Chiquet-Ehrismann, R., **Interfering with the connection between the nucleus and the cytoskeleton affects nuclear rotation, mechanotransduction and myogenesis**
Int J Biochem Cell Biol. 2010 Oct:42(10):1717-28. Epub 2010 Jul 17

V.7 ACKNOWLEDGEMENTS

First I would like to thank **Dr. Ruth Chiquet-Ehrismann** for giving me the opportunity of writing my thesis in her lab and for her support and patience during the past 4 years.

I would also like to thank **Dr. Susan Gasser**, **Dr. Matthias Chiquet** and **Dr. Markus Rüegg** for being part of my thesis committee and for helpful discussions and suggestions.

Many thanks go to **Jacqueline Ferralli** for all her support. Mentioning everything in detail would probably be even longer than her tally of my mistakes. Although that's not that easy ;)

Thanks very much to all the current and former **lab members** for a nice working atmosphere and their willingness to taste my baking experiments.

Very special thanks to the people at the FMI, especially the **facilities (FAIM, microarray)** for helpful discussions and support in realizing my projects.

To **my friends:** thank you very much for cheering me up when things didn't work out that well and for your patience with me when I was telling the same thing again and again.

And most importantly to **my parents** and **my sister:** thank you so much for always being there for me and for your endless support during my university time and my PhD.